

vertical in the order of 1.2 m. These results validate our clock estimation process and show that we are able to estimate the position of any user everywhere at any time with an accuracy of about 1m.

CONCLUSION

ESOC has been producing high rate GPS satellite clock bias estimates from January 1994. The motivation for estimating them is to be able to use them for point positioning and navigation of spacecraft. The results that we have obtained show that is possible to obtain positions with about 1m error using only pseudo-ranges. We intend to further improve our estimation process in order to make it more robust against changes in Anti Spoofing tracking.

THE PERTURBATION OF THE ORBITAL ELEMENTS OF GPS SATELLITES THROUGH DIRECT RADIATION PRESSURE AND Y-BIAS

Markus Rothacher, Gerhard Beutler, Leoš Mervart
Astronomical Institute, University of Berne
CJI-3012 Bern, Switzerland

ABSTRACT

A direct radiation pressure p_0 and a constant p_2 , so-called *y-bias*, are estimated for each GPS satellite and each arc of one to three days on top of the a priori radiation pressure model defined by the *IERS Standards* in the daily analyses performed at the *CODE Analysis Center of the IGS*.

In this article we are analyzing the influence of the two estimated parameters on the orbital elements using the methods of special perturbations. We develop approximated expressions for the perturbations in the Keplerian elements which allow us to study the perturbations analytically. We are in particular interested in the correlations of these parameters with the length of day (*UT1-UTC drift*) estimates and the so-called *pseudo-stochastic parameters* which are also solved for routinely at *CODE*. Using the IGS data stemming from a time interval of 46 days in 1994 we show that the theoretical results are confirmed in practice.

INTRODUCTION

CODE, Center for Orbit Determination in Europe, is one of at present seven Analysis Centers of the *IGS, the international GPS Service for Geodynamics*. *CODE* is formed as a joint venture of the Astronomical Institute of the University of Bern (AIUB), the Swiss Federal Office of Topography (L+T), the German Institute for Applied Geodesy (IfAG), and the French Institut Géographique National (IGN). *CODE* is located at the AIUB in Bern.

Since 21 June 1992 ephemerides for all GPS satellites are available and daily values for the earth orientation parameters (x and y of the pole position, and drift values for *UT1-UTC*) are solved for and made available to the scientific community by *CODE*. For test purposes the drifts $\Delta\dot{\psi}$ and $\Delta\dot{\epsilon}$ in the nutation corrections are determined for test purposes. These values are *not (yet)* made available to the community.

Other parameters like station coordinates and their velocities are estimated by combining the daily solutions. So far, they were produced for the annual solutions of the *IERS, the international Earth Rotation Service*.

The *CODE* products are analysed and compared to other solutions stemming from *GPS* or from other space techniques like *VLBI* and *SLR*. Whereas in general the *CODE* results compare well to all the other results there is a slight problem in the *UT1-UTC* drift rates as determined by *CODE*. This problem is not obvious if we just compare our length-of-day estimates to those established by *VLBI* - there clearly all the signatures of a physical nature are present. Figure 1 shows our length-of-day estimates (after removal of the tidal terms up to 35 days).

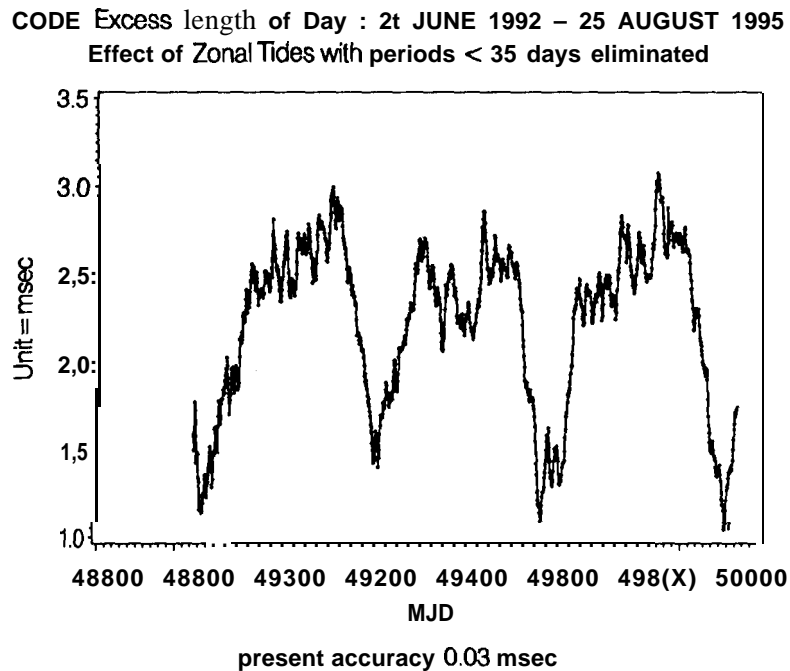


Figure 1. *CODE* length-of-day estimates after removal of tidal terms.

That there is a small bias with respect to the *VLBI* becomes obvious if we sum up our daily *UT1-UTC* drifts and subtract the corresponding *VLBI UT1-UTC* series from our series. Figure 2 shows the result. There is a net drift between the two series, There also seems to be a net change of the drift around May 1995.

CENTER FOR ORBIT DETERMINATION IN EUROPE: DAYS200/1993 - 238/1995
UT1 - UTC

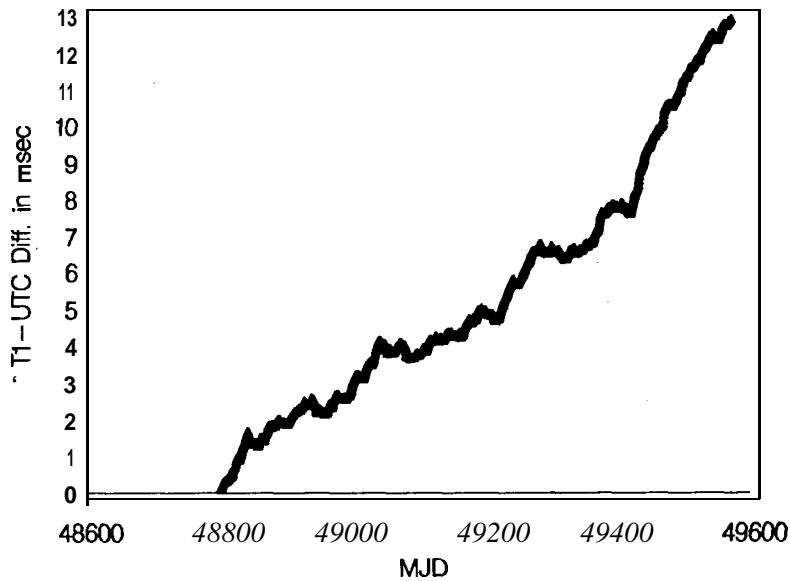


Figure 2. *CODE UT1-UTC* series minus corresponding *VLBI* series (actually the IERS Bulletin A series).

It is well known that satellite geodesy *not having direct access to direction observations in the celestial reference frame* is not able to determine *UT1-UTC* itself because of the correlation with the right ascensions of the ascending nodes of the GPS satellites which have to be solved for in each arc.

Could we assume that the force field acting on GPS satellites is completely known, we would be in a perfect position to solve for the *UT1-UTC drift*, however. This statement is *almost true* in the case of GPS satellites: The earth's gravity field may be assumed known for these high orbiting satellites, third body perturbations and tidal effects do not pose problems. On the other hand, we have to solve for radiation pressure parameters for each arc and each satellite. Should these parameters generate (among other effects) a net rotation of the orbital system, a correlation with the *UT1-UTC drift estimates* would be possible. This aspect is studied on a theoretical basis in the next section, empirical evidence is presented in the subsequent section.

PERTURBATIONS DUE TO RADIATION PRESSURE: ORDERS OF MAGNITUDE

in this section we study the influence of the radiation pressure model used at CODE on the estimated orbits using the method of special perturbations. For that purpose we first have to develop analytical expressions for the perturbing forces, then we have to present (simplified) perturbation equations. We assume in particular that GPS orbits are almost

circular. Finally we will develop and discuss the effects and possible correlations of radiation pressure estimates with earth rotation parameters.

Analytical Expressions for the Radiation Pressure

Figure 3 shows the projection on a unit sphere of the geocentric positions of the satellite and the sun at a particular instant of time t . For the description of the positions of satellite and sun we introduce two coordinate systems, one which is described by the axes x_1, x_2 and x_3 in Figure 3 and the other which is described by the axes y_1, y_2 and y_3 . The latter system is rotating with the satellite, it may be generated from the first coordinate system by a rotation around the $x_3 = y_3$ axis with the argument of latitude u of the satellite as the rotation angle.

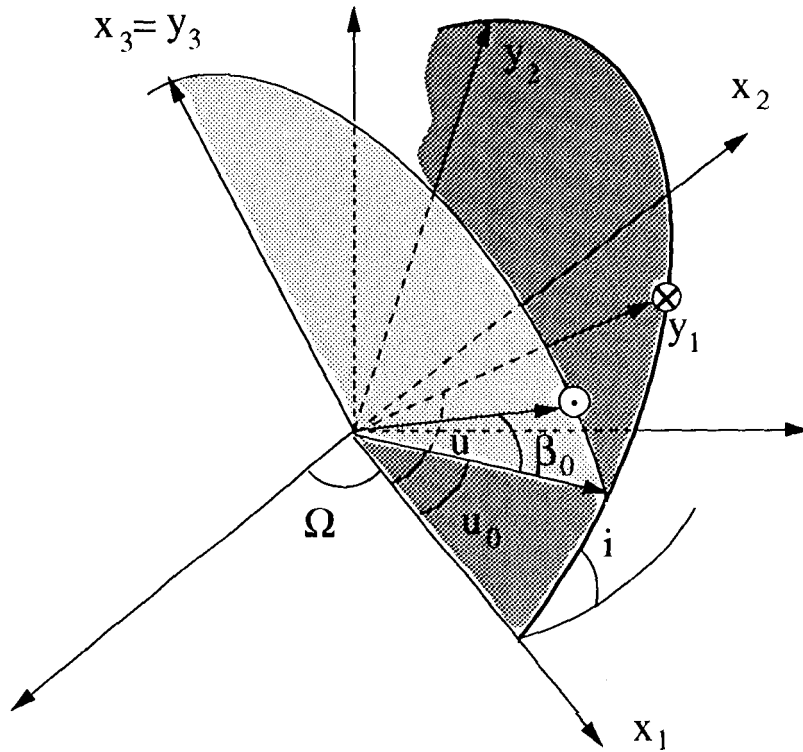


Figure 3. Positions of satellite and sun. u and u_0 are the arguments of latitude of satellite and sun, β_0 is the elevation of the sun above the orbital plane; Ω is the right ascension of the ascending node of the satellite's orbital plane.

The coordinates r_x of the satellite position r and the coordinates $e_{s,x}$ of the unit vector e pointing from the satellite to the sun may be expressed as follows in the coordinate system

$\{x_1, x_2, x_3\}$:

$$\mathbf{r}_x = r \cdot \begin{pmatrix} \cos u \\ \sin u \\ 0 \end{pmatrix} \quad (1)$$

$$\mathbf{e}_{s,x} = \begin{pmatrix} \cos u_0 \cdot \cos \beta_0 \\ \sin u_0 \cdot \cos \beta_0 \\ \sin \beta_0 \end{pmatrix} \quad (2)$$

where we assume that the direction *satellite - sun* may be approximated by the direction *center of earth - sun*.

The perturbation equations given in the next section ask for the radial, the tangential, and the out of plane components \mathbf{R} , \mathbf{S} , and \mathbf{W} of the perturbing forces. We thus have to express the two position vectors in the coordinate system $\{y_1, y_2, y_3\}$:

$$\mathbf{r}_y = \mathbf{R}_3(u) \cdot \mathbf{r}_x = r \cdot \begin{pmatrix} 1 \\ 0 \\ 0 \end{pmatrix} \quad (3)$$

$$\mathbf{e}_{s,y} = \mathbf{R}_3(u) \cdot \mathbf{e}_{s,x} = \begin{pmatrix} \cos(u - u_0) \cdot \cos \beta_0 \\ -\sin(u - u_0) \cdot \cos \beta_0 \\ \sin \beta_0 \end{pmatrix} \quad (4)$$

where $\mathbf{R}_3(u)$ stands for a rotation matrix describing a particular rotation around axis 3 and angle u .

At CODE the acceleration \mathbf{a}_{drp} due to the solar radiation pressure is modeled as (Beutler et al., 1994):

$$\mathbf{a}_{drp} = \mathbf{a}_{Rock} \cdot p_0 \cdot \mathbf{e}_s + p_2 \cdot \mathbf{e}_y \quad (5)$$

where

\mathbf{a}_{Rock} is the standard model Rock4 for Block I, the standard model Rock42 for Block II satellites (Fliegel et al., 1992),

\mathbf{e}_s is the unit vector *satellite - sun*, in our approximation the unit vector *center of earth - sun*,

\mathbf{e}_y is the unit vector pointing along the spacecraft's solar panels axis (Fliegel et al., 1992):

$$\mathbf{e}_y = \frac{\mathbf{e}_s \times \mathbf{r}}{|\mathbf{e}_s \times \mathbf{r}|} \quad (6)$$

p_0 and p_2 are the direct radiation pressure parameters estimated for each satellite and each arc.

It should be pointed out that - in a first approximation - the vector \mathbf{a}_{Rock} is parallel to the vector $p_0 \cdot \mathbf{e}_y$. We therefore do *not* analyse the term stemming from the Rock4/42 models separately. By forming the vector product in the coordinate system $\{y_1, y_2, y_3\}$ we obtain:

$$\begin{aligned} \mathbf{a}_{drp,y} &= \mathbf{a}_{Rock,y} + \mathbf{a}_{0,y} + \mathbf{a}_{2,y} \\ &= \mathbf{a}_{Rock,y} + p_0 \cdot \begin{pmatrix} -\cos(u - u_0) \cdot \cos \beta_0 \\ \sin(u - u_0) \cdot \cos \beta_0 \\ -\sin \beta_0 \end{pmatrix} - \\ &\quad \frac{p_2}{\sqrt{\sin^2 \beta_0 + \cos^2 \beta_0 \cdot \sin^2(u - u_0)}} \begin{pmatrix} 0 \\ \sin \beta_0 \\ \cos \beta_0 \cdot \sin(u - u_0) \end{pmatrix} \end{aligned} \quad (7)$$

It is of interest to write down the equation (7) for the cases $\beta_0 \rightarrow \frac{\pi}{2}$ (corresponding to the case when the sun is in the zenith of the orbital plane) and $\beta_0 \rightarrow 0$ (corresponding to the case where the sun lies in the orbital plane). In the subsequent expressions we neglect all terms of first or higher order in the small angle β_0 resp. $\beta_0 - \frac{\pi}{2}$.

(a) $\beta_0 \rightarrow \frac{\pi}{2}$:

$$\begin{aligned} \mathbf{a}_{drp,y} &\doteq \mathbf{a}_{Rock,y} + \mathbf{a}_{0,y} + \mathbf{a}_{2,y} \\ &= \mathbf{a}_{Rock,y} + p_0 \cdot \begin{pmatrix} 0 \\ 1 \\ -\text{sign}(\beta_0) \end{pmatrix} - \\ &\quad \frac{p_2}{\sqrt{\beta_0^2 + \sin^2(u - u_0)}} \begin{pmatrix} 0 \\ \text{sign}(\beta_0) \\ 0 \end{pmatrix} \end{aligned} \quad (8)$$

(b) $\beta_0 \rightarrow 0$:

$$\begin{aligned} \mathbf{a}_{drp,y} &\doteq \mathbf{a}_{Rock,y} + \mathbf{a}_{0,y} + \mathbf{a}_{2,y} \\ &= \mathbf{a}_{Rock,y} + p_0 \cdot \begin{pmatrix} -\cos(u - u_0) \\ \sin(u - u_0) \\ 0 \end{pmatrix} - \\ &\quad \frac{p_2}{\sqrt{\beta_0^2 + \sin^2(u - u_0)}} \begin{pmatrix} 0 \\ \beta_0 \\ \sin(u - u_0) \end{pmatrix} \end{aligned} \quad (9)$$

In the first case ($\beta_0 \rightarrow \frac{\pi}{2}$) the perturbation parallel to the direction *sun-satellite* is a *constant* out of plane acceleration. in the second case ($\beta_0 \rightarrow 0$) this perturbation lies in the orbital plane and oscillates. Both, the *R* and *S* components oscillate with a period equal to the revolution period of the satellite.

In the first case ($\beta_0 \rightarrow \frac{\pi}{2}$) the perturbation due to the *y-bias* is a constant along-track acceleration (the sign depending on the position of the sun). In the second case ($\beta_0 \rightarrow 0$) this perturbation consists of an *along-track* and an *out-of-plane* component. The out-of-plane component is constant in absolute value, but changes sign for $u = u_0$ and $u = u_0 + \pi$. The along-track component is zero everywhere *except* near $u = u_0$ and $u = u_0 + \pi$, where the acceleration reaches p_2 in absolute value. Obviously we have in this case a strong correlation with the pseudo-stochastic pulses.

Approximate Perturbation Equations for Almost Circular Orbits

in (Beutler,1991) we find the perturbation equations for the Keplerian elements semimajor axis a , numerical eccentricity e , inclination i , right ascension of the ascending node Ω , argument of perigee ω , and mean anomaly σ at time t_0 :

$$\dot{a} = \frac{2}{n \cdot \sqrt{1-e^2}} \cdot (e \cdot \sin v \cdot \mathbf{R} + \frac{p}{r} \cdot \mathbf{S}) \quad (10)$$

$$\dot{e} = \frac{\sqrt{1-e^2}}{n a} (\sin v \cdot \mathbf{R} + (\cos v + \cos E) \cdot \mathbf{S}) \quad (11)$$

$$i^{(\cdot)} = \frac{r \cdot \cos(\omega + v)}{n \cdot a^2 \cdot \sqrt{1-e^2}} \cdot \mathbf{W} \quad (12)$$

$$\dot{\Omega} = \frac{r \cdot \sin(\omega + v)}{n \cdot a^2 \cdot \sqrt{1-e^2} \cdot \sin i} \cdot \mathbf{W} \quad (13)$$

$$\dot{\omega} = \frac{\sqrt{1-e^2}}{e \cdot n \cdot a} \left(-\cos v \cdot \mathbf{R} + \left(1 + \frac{r}{p}\right) \cdot \sin v \cdot \mathbf{S} \right) - \cos i \cdot \dot{\Omega} \quad (14)$$

$$\dot{\sigma} = \frac{1-e^2}{e \cdot n \cdot a} \cdot \left(\left(\cos v - 2 \cdot e \cdot \frac{r}{p} \right) \cdot \mathbf{R} - \left(1 + \frac{r}{p}\right) \cdot \sin v \cdot \mathbf{S} \right) + \frac{3}{2} \cdot \frac{n}{a} \cdot (t - t_0) \cdot \dot{a} \quad (15)$$

where r is the length of the radius vector at time t , n is the mean motion of the satellite, E is the eccentric anomaly, v the true anomaly, and $p = a \cdot (1 - e^2)$ the parameter of the ellipse. \mathbf{R} , \mathbf{S} , and \mathbf{W} are the accelerations in radial, tangential (actually normal to \mathbf{R} in the orbital plane), and out-of-plane directions.

GPS orbits are low eccentricity orbits. If we neglect all terms of the first and higher orders in the eccentricity e (circular orbit), these equations may be considerably simplified. We may formally assume the perigee to coincide with the ascending node at time t_0 , which allows us to use the approximation $v \approx E = u$, where $u = n \cdot (t - t_0)$. Moreover we do not need to consider the equation for the argument of perigee, in this case. We include, instead, an equation for the argument of perigee u_0 at time t_0 by adding the equations for the argument of perigee w and for the mean anomaly σ at time t_0 . The resulting perturbation equations are:

$$\dot{a} = \frac{2}{n} \cdot \mathbf{S} \quad (16)$$

$$\dot{e} = \frac{1}{n \cdot a} \cdot (\sin u \cdot \mathbf{R} + 2 \cdot \cos u \cdot \mathbf{S}) \quad (17)$$

$$i^{(\cdot)} = \frac{\cos u}{n \cdot a} \cdot \mathbf{W} \quad (18)$$

$$\dot{\Omega} = \frac{\sin u}{n \cdot a \cdot \sin i} \cdot \mathbf{W} \quad (19)$$

$$\dot{u}_0 = -\frac{2}{n \cdot a} \cdot \mathbf{R} - \cos i \cdot \dot{\Omega} + \frac{3}{2} \cdot \frac{n}{a} \cdot (t - t_0) \cdot \dot{a} \quad (20)$$

Let us assume that the initial values for these elements at time t_0 are a_0, e_0, i_0, Ω_0 , and u_{00} . The influence of the perturbation terms due to radiation pressure at, time t are computed

by the equations $\delta a \doteq a(t) - a_0$, $\delta e \doteq e(t) - CO$, $\delta i \doteq i(t) - i_0$, $\delta \Omega \doteq \Omega(t) - \Omega_0$, and $\delta u_0 \doteq u_0(t) - u_{00}$. Usually the dominant perturbation term is that in along track direction, i.e. the error in the argument of latitude $u(t)$ at time t :

$$\delta u(t) = \delta u_0(t) + \delta n \cdot (t - t_0) \quad (21)$$

where, using Kepler's third law, we have

$$\delta n = -\frac{3}{2} \cdot \frac{n}{a} \cdot \delta a \quad (22)$$

The solutions of the above simplified perturbation equations formally may be written as follows:

$$\delta a(t) = \frac{2}{n} \cdot \int_{t_0}^t \mathbf{S} \cdot dt' \quad (23)$$

$$\delta e(t) = \frac{1}{n \cdot a} \cdot \int_{t_0}^t (\sin u \cdot \mathbf{R} + 2 \cdot \cos u \cdot \mathbf{S}) \cdot dt' \quad (24)$$

$$\delta i(t) = \frac{1}{n \cdot a} \cdot \int_{t_0}^t \cos u \cdot \mathbf{W} \cdot dt' \quad (25)$$

$$\delta \Omega(t) = \frac{1}{n \cdot a \cdot \sin i} \cdot \int_{t_0}^t \sin u \cdot \mathbf{W} \cdot dt' \quad (26)$$

$$\begin{aligned} \delta u_0(t) = & -\frac{2}{n \cdot a} \cdot \int_{t_0}^t \mathbf{R} \cdot dt' - \cos i \cdot \delta \Omega(t) \\ & + \frac{3}{2} \cdot \frac{n}{a} \cdot (t - t_0) \cdot \delta a - \frac{3}{2} \cdot \frac{n}{a} \cdot \int_{t_0}^t \delta a(t') \cdot dt' \end{aligned} \quad (X')$$

This last equation allows us to write the equation for the argument of latitude in the more explicit form

$$\delta u(t) = -\frac{2}{n \cdot a} \cdot \int_{t_0}^t \mathbf{R} \cdot dt' - \cos i \cdot \delta \Omega(t) - \frac{3}{2} \cdot \frac{n}{a} \cdot \int_{t_0}^t \delta a(t') \cdot dt' \quad (2s)$$

Solution of the Perturbation Equations for Radiation Pressure Terms

Let us deal separately with the terms p_0 and p_2 , and with the cases when the sun lies in the orbital plane ($\beta_0 = 0$) resp. when the sun is in the zenith of the orbital plane ($\beta_0 = \frac{\pi}{2}$).

Perturbations due to p_0 , Sun in Zenith of Orbital Plane ($\beta_0 = \frac{\pi}{2}$)

The perturbing acceleration reads as

$$\mathbf{a}_{0,y} = \begin{pmatrix} \mathbf{R} \\ \mathbf{S} \\ \mathbf{W} \end{pmatrix} = p_0 \cdot \begin{pmatrix} 0 \\ 0 \\ -\text{sign}(\beta_0) \end{pmatrix} \quad (29)$$

We easily see that there are only short period perturbations in the orbital elements i and Ω . The result of the integration is easily verified to be:

$$\begin{aligned}\delta\Omega(t) &= \frac{p_0 \cdot \text{sign}(\beta_0)}{n^2 \cdot a \cdot \sin i} \cdot [\text{Cos } u - 1] \\ \delta i(t) &= - \frac{p_0 \cdot \text{sign}(\beta_0)}{n^2 \cdot a} \cdot \sin u\end{aligned}\tag{30}$$

The perturbations are purely periodical where the period is equal to the revolution period of the satellite. Obviously, a small error in the parameters p will *not* contaminate the estimation of earth rotation parameters, This statement is no longer valid if we are looking for a sub-diurnal resolution of these terms. In this case, a correlation of the perturbation in Ω with length-of-day estimates is very well possible. For GPS satellites (semimajor axis $a \approx 26500 \text{ km}$, revolution period $U \approx 43'200 \text{ s}$, $p \approx 10^{-6} \text{ m/s}^2$) we have:

$$\begin{aligned}\delta\Omega(t) &\approx 449 \text{ mas} \cdot \text{sign}(\beta_0) \cdot [\cos u - 1] \\ \delta i(t) &\approx -368 \text{ mas} \cdot \text{sign}(\beta_0) \cdot \sin u\end{aligned}\tag{31}$$

or, in meters:

$$\begin{aligned}a \cdot \delta\Omega(t) &\approx 58 \text{ m} \cdot \text{sign}(\beta_0) \cdot [\cos u - 1] \\ a \cdot \delta i(t) &\approx -47 \text{ m} \cdot \text{sign}(\beta_0) \cdot \sin u\end{aligned}\tag{32}$$

The periodic variations thus are of a considerable size.

Perturbations due to p_0 , Sun in Orbital Plane ($\beta_0 = 0$)

The perturbing acceleration reads as

$$\mathbf{a}_{0,y} = \begin{pmatrix} \mathbf{R} \\ \mathbf{S} \\ \mathbf{W} \end{pmatrix} = p_0 \cdot \begin{pmatrix} -\cos(u - u_0) \\ \sin(u - u_0) \\ 0 \end{pmatrix}\tag{33}$$

in this case there obviously is *no* out-of-plane component, and no correlation with earth rotation parameters has to be expected. On the other hand there are strong \mathbf{R} and \mathbf{S} components. One easily verifies that these accelerations generate periodic *perturbations* (period equal to orbital period, amplitudes comparable to those in the previous section) in a , u_0 , and $u(t)$. The prominent perturbation feature, however, is the perturbation in the eccentricity e , where we have perturbations proportional to $\sin u_0$. Because u_0 has an annual period (revolution of the sun around the earth (or vice-versa)) the period of this perturbation will be roughly one year, too. Its amplitude is of the order of a few kilometers (Beutler, 1992).

Perturbations due to p_2 , Sun in Zenith of Orbital Plane ($\beta_0 = \frac{\pi}{2}$)

The perturbing acceleration reads as

$$\mathbf{a}_{2,y} = \begin{pmatrix} \mathbf{R} \\ \mathbf{S} \\ \mathbf{W} \end{pmatrix} = -p_2 \cdot \begin{pmatrix} 0 \\ \text{sign } (\beta_0) \\ 0 \end{pmatrix}\tag{34}$$

We merely have a constant along-track-component S of the perturbing acceleration. Periodic variations (period =revolution period, amplitudes comparable to those in Ω and i given above) in e will be one consequence.

The prominent perturbation will be that in a and in $u(t)$, however. We include these results *although a correlation with UT1-UTC is not expected in this case*. The quadrature of the perturbation equation in the semi-major axis a may be performed without problems:

$$\delta a(t) = -\frac{2}{n} \cdot p_2 \cdot (t - t_0) \cdot \text{sign}(\beta_0) \quad (35)$$

This perturbation in a produces a very pronounced perturbation in along-track direction:

$$a \cdot \delta u(t) \approx \frac{3}{2} \cdot p_2 \cdot (t - t_0) \cdot \text{sign}(\beta_0) \quad (36)$$

where we have left out all periodic perturbations.

Typically the y-bias p_2 is of the order of a few 10^{-10} m/s^2 . Assuming a value of $p_2 \approx .5 \cdot 10^{-10} \text{ m/s}^2$ this gives rise to an along-track-effect of about 6 meters in along-track-direction. Theoretically there might be a correlation of an orbit error in along-track direction S with the UT1-UTC drift. This correlation would be for low inclination satellites. Because GPS satellites have inclination of 55° and because with 3 days our arc-length is usually quite long we do *not* expect a significant contribution in this case.

Perturbations due to p_2 , **Sun in Orbital Plane** ($\beta_0 = 0$)

The perturbing acceleration reads as

$$\mathbf{a}_{2,y} = \begin{pmatrix} R \\ s \\ \mathbf{W} \end{pmatrix} = -p_2 \cdot \begin{pmatrix} 0 \\ \beta_0 / (\beta_0^2 + \sin^2(u - u_0)) \\ \text{sign}(\sin(u - u_0)) \end{pmatrix} \quad (37)$$

Let us start our considerations by looking at the along-track component S . This component is very small everywhere but in the immediate vicinity of these instants of time where $u(t) \approx U$ and $u(t) \approx u_0 + \pi$. For $u = u_0$ and $u = u_0 + \pi$ the S -component reaches its maximum value (which is equal to $|p_2|$). The total effect thus actually corresponds to a velocity change at the time when $u = u_0$ resp. $u = u_0 + \pi$. Keeping in mind that p_2 is of the order of a few 10^{-10} m/s^2 which acts only for a very short period of time, we conclude that the along track effect is very small when compared to the same effect when the sun is in the zenith of the orbital plane (compare previous section). We will not further consider this effect.

The out-of-plane component, *will* in general produce a net rotation of the orbital plane! This becomes apparent if we introduce the above R acceleration into the perturbation equation for Ω :

$$\mathbf{m}(i) = \frac{2}{n \cdot a \cdot \sin i} \int_{t_0}^t \sin u \cdot \text{sign}(\sin(u - u_0)) \cdot dt' \quad (38)$$

The worst case obviously results for $u_0 = 0$ or $u_0 = \pi$ (which will be the case in spring and fall). Let us give the result for $u_0 = 0$:

$$\delta\Omega(t) = -\frac{p_2}{n \cdot a \cdot \sin i} \cdot \int_{t_0}^t |\sin u| \cdot dt' \quad (39)$$

It is thus easy to verify that the net rotation after one revolution is:

$$\delta\Omega(t_0 + U) = -\frac{4 \cdot p_2}{n^2 \cdot a \cdot \sin i} \quad (40)$$

For a **typical y-bias** of $p_2 \approx 5 \cdot 10^{-10} \text{ m/s}^2$ a rotation about 1.8 mas per day is the result. This seems to be a very small value, but it is not negligible. From Figure 2 we conclude that we are looking for an effect of about **0.22 mas/day!** The conclusion is thus clear: a correlation of the *y--biases* with the drift parameter in *UT1-UTC* cannot be excluded. Let us look for empirical evidence in the next section.

RESULTS FROM GLOBAL IGS DATA PROCESSING USING DIFFERENT ORBIT STRATEGIES

The IGS Data and Orbit Strategies Used

To study the correlation between the y-bias and the *UT1-UTC drift* **46 days of data** from the global IGS network were processed using different options (see below). The time period from day **245 to day 290 in 1994** was selected because **it contains both**, a period where *no* satellites were eclipsed (at the beginning of the series) and a period with 8 satellites (PRN 1, 6, 7, 18, 26, 28, 29, and 31) going through the earth shadow once per revolution (from the middle to the end of the series). The data from about **40 IGS sites** were included. Overlapping 3-days solutions as in the routine *CODE* analysis were produced for the period mentioned above using the following orbit estimation strategies:

Strategy A: No pseudo-stochastic pulses were set up, one y-bias and one direct radiation pressure parameter estimated on top of the Rock 4/42 models.

Strategy B: Pseudo-stochastic pulses were set up in R and S direction for the eclipsing satellites only. The two pulses per revolution were set up about 45 minutes after the shadow exit of the satellite. Y-bias and direct pressure parameters as in the strategy A.

Strategy C: Pseudo-stochastic pulses were set up in the R and S direction for *all* satellites once per revolution (at 0:00 h and 12:00 h).

Strategy D: Pulses were set up as in solution C, but for all the three components (**R, S, W**).

Strategy E: Same solution as C, but the y-bias parameters were *constrained* using an a priori sigma of 10^{-10} m/s^2 to the values determined from 2 years of y-bias results.

Strategy F: Same solution as C, but instead of estimating a y-bias for each satellite (and arc) a constant along track acceleration was determined. The same constraints were applied to the along-track acceleration as in the strategy E to the y-bias.

In all these solutions 12 troposphere parameters per day and site were set up and 8 orbital elements (6 Keplerian elements and the parameters p_0 and p_2 (see eqn. (5)) or, for solution of type F, a constant along-track acceleration) were determined. The x- and y-pole coordinates, and UT1-UTC were estimated exactly in the same way as in the routine processing CODE (Rothacher et al., 1995).

UT1-UTC Results and Comparison to the Rotation of the Satellite Nodes

The UT1-UTC drifts of the middle days of the 3-days solutions were summed up to give GPS-derived UT1-UTC series. The series resulting from strategies A through F are shown in Figure 4. The figure clearly indicates that the orbit estimation strategy has an important impact on the UT1-UTC drift. Strategies E and F exhibit the smallest drifts, at least for this time period.

UT1 - UTC FROM 3 - DAY SOLUTIONS USING DIFFERENT ORBIT MODELS
Differences to Bulletin B Values

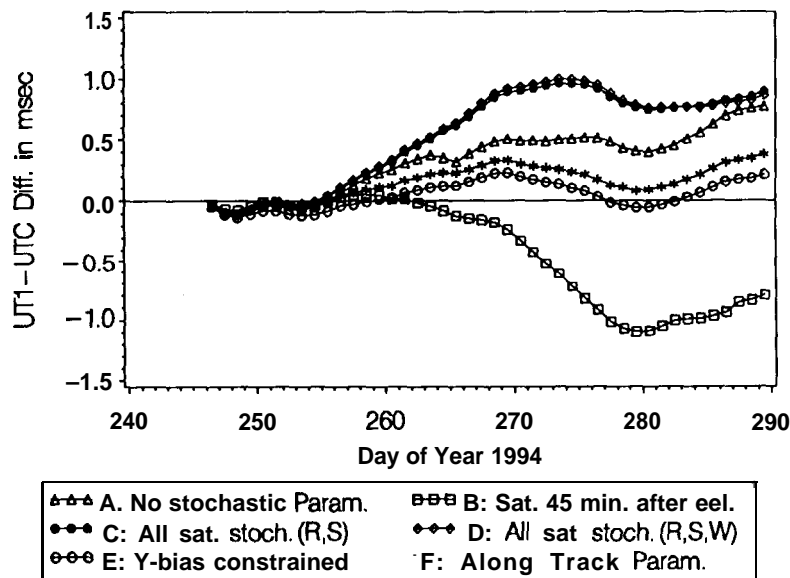


Figure 4. UT1-UTC series estimated from global 3-days solutions using different orbit estimation strategies

To see whether the perturbations due to p_2 may explain the UT1-UTC series in Figure -1), the perturbation eqn. (27) was used to compute the rotation of the ascending node Ω due to p_2 for each individual satellite. The mean value of these daily rotations over all satellites

should then reflect a mean rotation of the reference frame that may be absorbed by a drift in $UT1-UTC$. The actual computation was performed by numerically integrating eqn. (27) using eqn. (7) for the out-of-plane perturbing force \mathbf{W} and the y -bias values that were saved for each individual solution. The resulting mean rotation of the nodes is shown in Figure 5 for all strategies except F. Because the y -bias was fixed to the same a priori values as in solution E, the rotation of the nodes would be very similar to the ones of type E.

MEAN ROTATION OF NODES COMPUTED FROM THE y -BIAS PARAMETERS
For Different Orbit Models

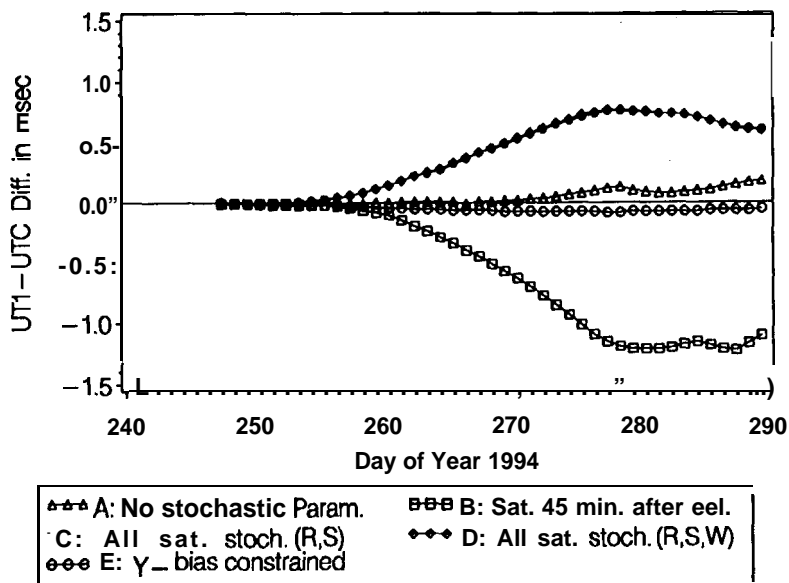


Figure 5. Mean rotation of the nodes computed from the y -bias parameters estimated using different orbit strategies

Comparing Figures 4 and 5 we see the high correlation between the $UT1-UTC$ series and the mean rotations of the nodes. This shows that the estimated y -bias plays indeed a key role in the $UT1-UTC$ series originating from GPS. Although most of the features visible in the $UT1-UTC$ series may be explained by the correlation with the y -bias estimate discussed above, there still remain residual drifts in $UT1-UTC$ when compared to VLBI. The remaining drift will have to be studied in future.

Orbit Quality of the Strategies Used

From Figures 4 and 5 we see that constraining the y -biases (solution type E) or estimating a constant along-track acceleration (solution type F) instead of a y -bias improves the stability of the $UT1-UTC$ estimates. It is therefore important to check whether the orbit quality is the same in these two cases compared to e.g. solution type C. Figure 6 summarizes the rms errors obtained by fitting a 7-days arc through the 7 daily solutions of GPS week 765 using the radiation pressure model described in (Beutler et al., 1994).

COMPARISON OF ORBIT ESTIMATION STRATEGIES (WEEK 765)

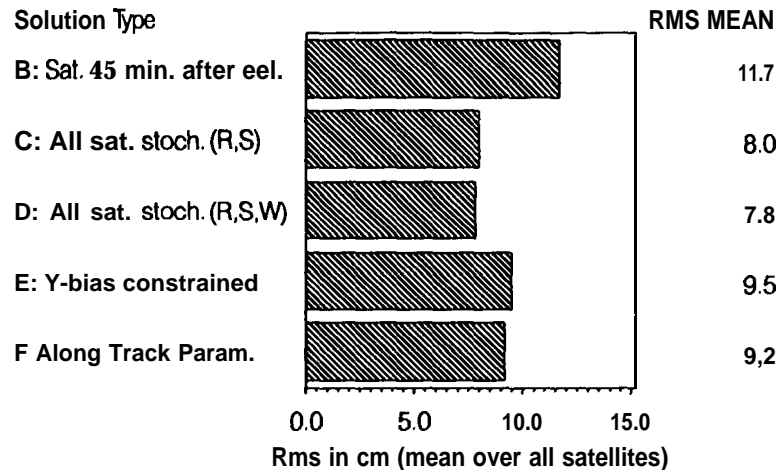


Figure 6. Orbit quality assessment by fitting a 7-days arc through the 7 daily solutions

The small degradation of the orbit quality for solutions E and F with respect to solutions types C and D indicates that there remain some unmodeled biases in the orbits if the y-biases are heavily constrained or not estimated at all. The estimation of a constant along-track acceleration is *not* sufficient to get, down to the consistency level obtained with strategies C and D. It is interesting to note that the estimation of pseudo-stochastic pulses in the *W* direction does not significantly change the *UT1-UTC* behaviour.

SUMMARY AND CONCLUSIONS

In the first part of this article we developed the perturbations due to the radiation pressure parameters p_0 and p_2 using special perturbation theory. We showed that the nature for these perturbations is quite different for the cases when the sun is in the zenith of the orbital plane resp. lies in the orbital plane. We have shown in particular that a net rotation of the orbital plane around the axis pointing to the celestial pole will result due to a constant y-bias p_2 in the case where the sun lies in the orbital plane. Such rotations are *potentially dangerous* because they are very closely correlated with the estimates for the *drifts in UT1-UTC*.

We found evidence that our theoretical considerations are relevant in practice: Figures 4 and 5 underline this statement. Since June 1995 solution of Type C is the official solution of the *CODE Analysis Center*. We are in the process of studying solutions of type E in order to reduce the bias in our *UT1-UTC drift* estimates. Our concern at present is a degradation of the orbit quality as seen in Figure 6.

An alternative which is believed to be superior consists of removing the Rock models completely and to replace them by the new radiation pressure model developed in (Beutler

et al., 1994). An analysis of the kind presented in this paper will have to be performed for this new model, too.

We should state in conclusion, however, that length-of-day estimates made by GPS will always suffer from potential correlations with orbit parameters which have to be estimated. This situation could be changed radically if direction observations of highest quality (of the order of a few mas) were available for GPS satellites.

REFERENCES

- Beutler, G. (1991). *Himmelsmechanik II: Der erdnahe Raum*. Mitteilungen der Satelliten-Beobachtungsstation Zimmerwald, No. 28, Druckerei der Universität Dem.
- Beutler, G., E. Brockmann, W. Gurtner, U. Hugentobler, I. Mervart, M. Rothacher (1994). *Extended Orbit Modeling Techniques at the CODE Processing Center of the International GPS Service for Geodynamics (IGS): Theory and Initial Results.*, Manuscript Geodaetica, Vol. 19, pp. **367-386**.
- Fliegel, H. F., T. F. Gallini, E. R. Swift (1992). *Global Positioning System Radiation Force Model for Geodetic Applications*. Journal of Geophysical Research, Vol. 97, No. B1, pp. 559-568.
- Rothacher, M., R. Weber, U. Wild, A. Wiget, C. Boucher, S. Botton, H. Seeger, 1995, *Annual Report 1994 of the CODE Processing Center of the IGS*, International GPS Service for Geodynamics, Annual Report 1994, ed. J. Z. Zumberge, R. Liu, and R. Neilan, JPL, California, in preparation.

An Estimate of Ocean-Loading Effects on Baseline Repeatability from GPS Observations

M. S. Schenewerk, G. L. Mader,
NOAA, SSMC4, 1305 East-West Highway
Silver Spring, MD 20910
301-7 13-2854; e-mail: mark @tony.grdl.noaa.gov

T. M. vanDam
NOAA, CIRES/University of Colorado
Boulder CO 80309
303-492-5670; e-mail: tonie@roberson.colorado.edu

ABSTRACT

The proliferation of continuously operating GPS tracking sites and improvements in the vertical accuracy of GPS measurements present a unique opportunity to directly observe the effects of ocean-loading on the Earth's crust. A technique in which GPS observations are coherently accumulated with respect to a tidal component may make possible subdaily estimates of the effects from that tidal component. Techniques like this minimize atmospheric, geometrical, and multipathing effects which can have comparable magnitudes to, but different characteristic periods from the tidal signals. Initial results from 16 IGS sites around North America look promising. Good agreement with existing models was found for the magnitude of height variations at many sites. Significant differences with the phase of these variations were seen at several sites. This presentation will describe the technique used, results and the feasibility of extending this processing globally. The significance of these results for local, regional, and global GPS data processing will be discussed.

INTRODUCTION

Ocean-loading of the Earth's crust from tides (OLT) is one of the most poorly modeled phenomena remaining in GPS processing. Ocean-loading models are primarily limited by the ocean tidal model employed. Tidal models are accurate to better than 10% in the open ocean, but suffer near coastlines where loading effects are the greatest. Other independent geodetic techniques such as gravimeters, SLR, and VLBI can be used to measure OLT effects, but practically, can not keep up with the anticipated explosion of GPS sites. GPS itself suffers from limited vertical accuracy, a problem exacerbated by the longer ties from stable inland to coastal sites required to measure these tidal effects.

This is not to question the ability of GPS to detect OLT but rather how best to use these data to measure OLT variations with the highest accuracy in shortest time.

These questions are particularly timely for NOAA. Its participation in the U.S. Coast Guard's GPS network will make available data from many permanent coastal sites. The current generation of NOAA's GPS processing software, called *page3* (Schenewerk, et al., 1994), does not include an OLT model. The intent is to rectify this shortcoming in the next software generation; however, the previous discussion begs the question of how best to implement such a model. Furthermore, it seemed reasonable to test our ability to detect OLT in our vertical solutions as a first step prior to selecting and incorporating one of the available models. We would then be able to discriminate between or improve existing models. We suspected that this might be done by coherently averaging the GPS observations, a technique in common use in astronomical spectroscopy, seismology, and even GPS studies of *multipath*. Coherently combining observations in phase with the period of a tidal component should constructively reinforce the effects of that tidal component while destructively interfering with (averaging out) all random and out-of-phase periodic contributions.

For example, the white circles in Figure 1 show the times when the Moon crosses the meridian (highest elevation angle; 0 hour angle) as seen from Potsdam. The daily shift in the time of the meridian crossing is caused by the Moon's orbital motion. Figure 1 also represents the apparent shift in the Moon's position with respect to the Sun and the lunar tide with respect to the solar.

Figure 2 shows the idealized case of semidiurnal solar and lunar tides again for Potsdam. The combined OLT height variation from these two tides is shown as a bold, solid line, the lunar component as a bold, dotted line, and the solar component as a thin, solid line. The gray vertical bars indicate when the Moon is at the meridian. The values of the lunar, solar, and combined OLT height variations at those times are given at the bottom of the figure. In two weeks (half the lunar orbital period), a complete solar tidal cycle has been sampled and, being cyclic, approximately equals zero leaving the lunar component. Of course, the actual observed variations in a site's height are more complex but the potential advantages of coherent averaging outweigh this disadvantage. Diurnal, sidereal, weather, and seasonal effects, which contaminate the GPS measurements, would be minimized because their characteristic time scales are different. Difficulties do persist, particularly with the number of physical

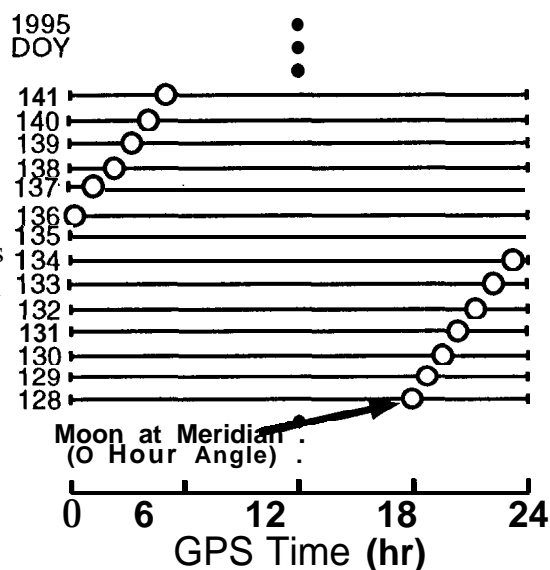


Figure 1: Times when the Moon crosses the meridian as seen from Potsdam

phenomena which have a diurnal signature. However, the use of longer averaging times and the possibility of physically eliminating or modeling some site specific phenomena should mitigate these difficulties. In total, the potential advantages seemed to warrant an investigation of this technique.

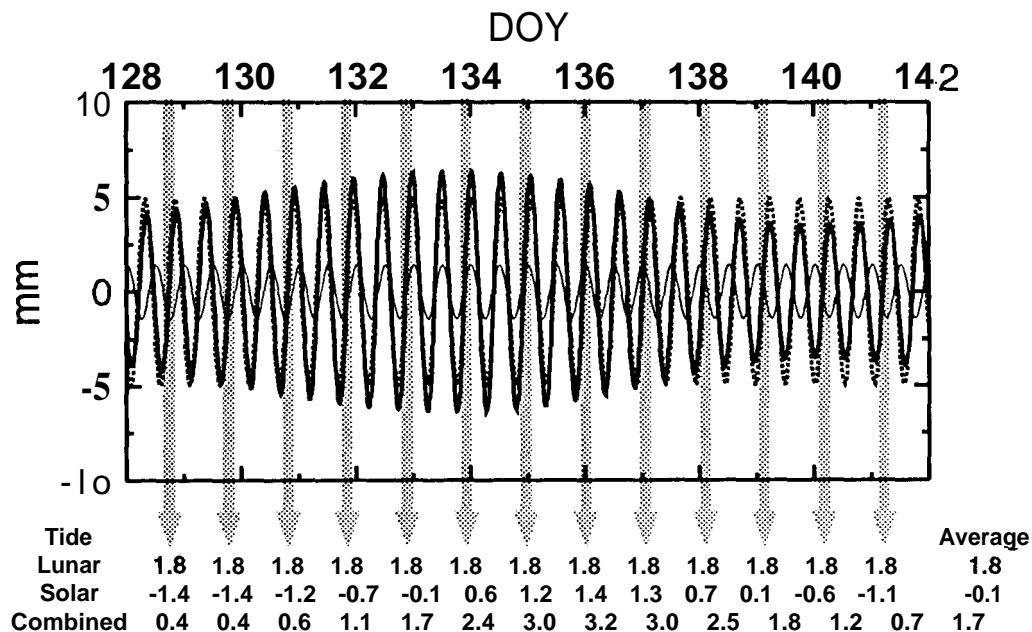


Figure 2: Simplified OLT variations in height at Potsdam

PROCESSING

A modified version of the *page4* program is being used for this project. *page4* is the newest generation orbit adjustment software and will soon be operational at NOAA. Differences from the *page3* software pertinent to this project are:

- 1) an updated solid Earth tide model using Shida and Love numbers which better account for the mantle inelasticity and free core nutation frequency (Mathews. et al., 1995), and
- 2) NMF mapping functions for the troposphere model (Neill, 1993).

Special variants of *page4* were created permitting the estimation of time-dependent height variations in the site coordinates.

Two strategies for estimating OLT variations were used. One strategy was to estimate two horizontal plus 24 vertical site adjustments. Each vertical estimate is derived from coherently accumulating observations in phase with one of 24 sub-intervals of the tidal

cycle of interest. Hereafter, estimates made using this technique will be called “hourly” estimates. The other, more conventional strategy was to estimate a mean position plus an amplitude and phase offset for a sinusoidal variation in height with the period of the tidal component of interest. Hereafter these will be called “sinusoid” estimates. Site velocities were estimated in both cases,

The IGS combined orbits were used with no additional orbit adjustment. *page4* uses double-differenced, ionosphere-free, phase as the observable. The tracking interval was 30 seconds and a 15° elevation cutoff imposed. Three hour, piece-wise, linear, continuous tropo scaling factors were estimated at all sites. Other intervals for the tropo models were tried, but seemed to yield less consistent results.

Table 1: Site names, ID’s, and baseline lengths

Algonquin, Canada	algo	Reference
Bermuda, UK	brmu	1887.740 km
Greenbelt, MD, USA	gode	776.525 km
North Liberty, IA, USA	nlib	1177.319 km
Richmond, FL, USA	rcm5	2254.576 km
St. John’s, Canada	Stjo	1931.826 km
Westford, MA, USA	wes2	642.544 km
Yellowknife, Canada	yell	2912.779 km
Goldstone, CA, USA	gold	Reference
Albert Head, Canada	albh	1535.468 km
Penticton, Canada	drao	1556.108 km
Fairbanks, AK, USA	fair	3807.036 km
Kokee Park, HI, USA	kokb	4304.765 km
Ft. Davis, TX, USA	mdo1	1309.116 km
Pietown, NM, USA	pie1	810.970 km
Quincy, CA, USA	quin	618.446 km

The sites used in this project are listed in Table 1. Figure 3 shows the location of these sites and the resulting baselines. Algonquin and Goldstone are two of the thirteen fundamental tracking sites agreed to by the IGS analysis centers. As such, their GPS monuments have well determined coordinates and velocities in the International Terrestrial Reference Frame (ITRF). Changes in the antennas were taken from the site logs on-line at the IGS Central Bureau. Examination of the mutual visibility from possible networks indicated that these two sites were also adequate as references for all double-differenced station pairs. Therefore, Algonquin or Goldstone was used in each baseline and their coordinates and velocities tightly constrained to their ITRF93 values (Altimimi and Boucher, 1994). 24 hour data sets containing a single baseline pair were created at five

day intervals for the period March 11, 1994 through March 11, 1995. The intent in using one year's data was to average over a sidereal year, and many solar and lunar cycles. In addition, the effects of satellite geometry, multipath, seasonal, weather, and other tidal effects would be minimized (averaged out). All data sets were manually edited.

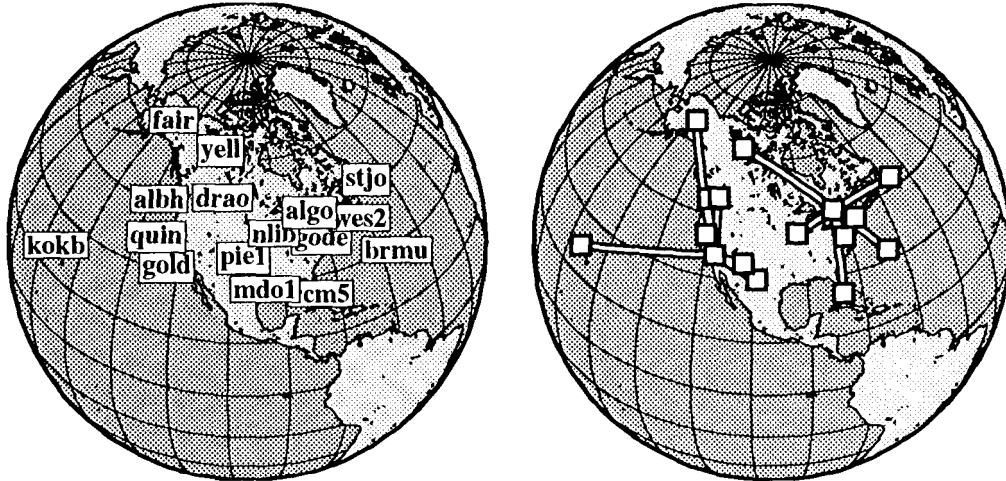


Figure 3: Sites used in the project

DISCUSSION

Estimates of the vertical site displacements were made for each of the fourteen baselines, however, only three sites will be discussed in detail. The three sites represent examples of a good match to the model, an unanticipated result, and a null detection. A summary of the results for all sites is given at the end of this section. A number of conventions will be used in the following discussion. All values are in centimeters. A simple mean was removed from all data sets plotted. The associated figures show the variations in height relative to the reference site and are plotted versus the lunar or solar hour angle as seen from the non-reference site. In all figures, the thin, solid curve is created using the hourly estimates (strategy 1); the bold, solid curve is created using the sinusoid amplitude and phase estimate (strategy 2); and the dashed curve is the model. The error bars shown for the hourly estimates are the formal errors from the solution. The formal errors from the sinusoid are, much to our surprise, so small as to be effectively concealed by the bold line.

The ocean-loading model used for comparison with the GPS results is derived by including a recent TOPEX/POSEIDON tidal analysis (Schrama and Ray, 1994) into the load-tide formalism described by Ray and Sanchez (1989). The model curves were created by coherently accumulating the predicted hourly variations as similarly as possible as the GPS data, i.e. at tidal frequencies, over the same period and using the same five day interval as the data. A sine function was then fit to those results.

Penticton is representative of sites in good agreement with the model. The estimated variations in height are shown in Figure 4. An excellent match to the amplitude and phase of the lunar semidiurnal tidal, signal is seen in the upper panel of Figure 4. The amplitude of the solar semidiurnal tidal, lower panel, exceeds the model and a slight phase shift is apparent. This situation is not unexpected and probably represents small model errors plus other diurnal signals in the GPS data,

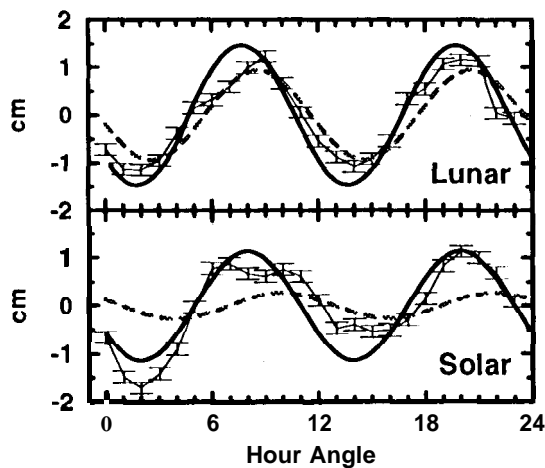


Figure 4: drao-gold

In contrast, Albert Head, only 300 km west of Penticton, represents a significant departure from the model. Figure 5 shows the lunar semidiurnal tidal signal to be two times the amplitude of the model with a 2.3 hour phase shift. The solar tide is virtually identical to Penticton. A reasonable assumption might be that the source of this signal is the reference site, Goldstone, which is common to both baselines. However, remember that the abscissa is the hour angle of the Sun as seen from the non-reference site. The difference in longitude between the sites would amount to a 15.5 minute shift if this signal originated solely at Goldstone. Although a shift of this size is only marginally detectable, none is evident.

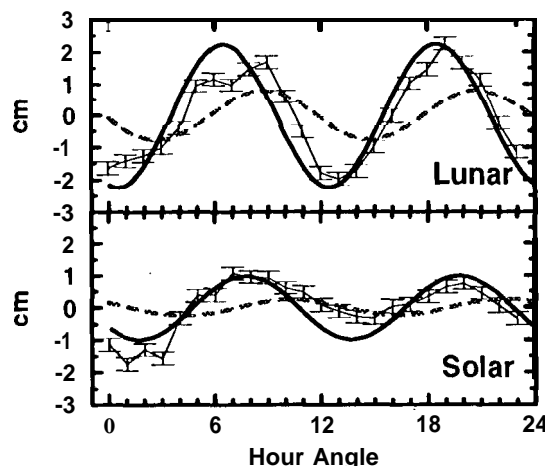


Figure 5: albh-gold

Kokee Park, Figure 6, represents an apparent non-detection. The RMS scatter of the 24 height estimates is 1.01 cm. Therefore, a signal with the amplitude of the model should be easily detectable. The Kokee Park - Goldstone line is the longest of these baselines, 4300 km, and may represent an upper limit for these techniques. Certainly the longer baseline results in diminishing mutual visibility, poorer satellite geometry, greater difficulty in editing, and growing susceptibility to

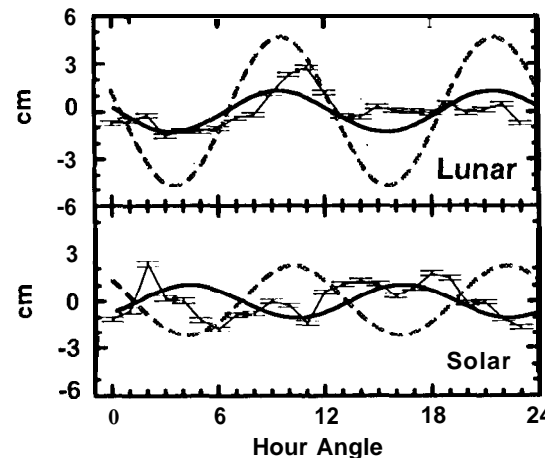


Figure 6: kokb-gold

model errors. However, loading model errors caused by the presence of the Hawaiian Hot Spots could account for some of the discrepancy. If the non-detection withstands further investigation and comparison to other techniques, this result may be one of the more interesting.

Figure 7 shows the lunar results for all the North American baselines used in this study. All panels in the figure are forced to have the same vertical scale for ease of comparison. Broadly, the amplitude estimates match expectations. The most notable exception, the null detection from Kokee Park, has already been discussed. The magnitude of the lunar semidiurnal variation for Bermuda, the other deep-ocean site in this study, also appears smaller than the model would imply. The Richmond hourly estimates show no clear signal and the sinusoid differs at the few sigma level from both the hourly estimates and the model. Other, routine processing for Richmond yields poorer than anticipated results. The source of these problems is being investigated at NOAA.

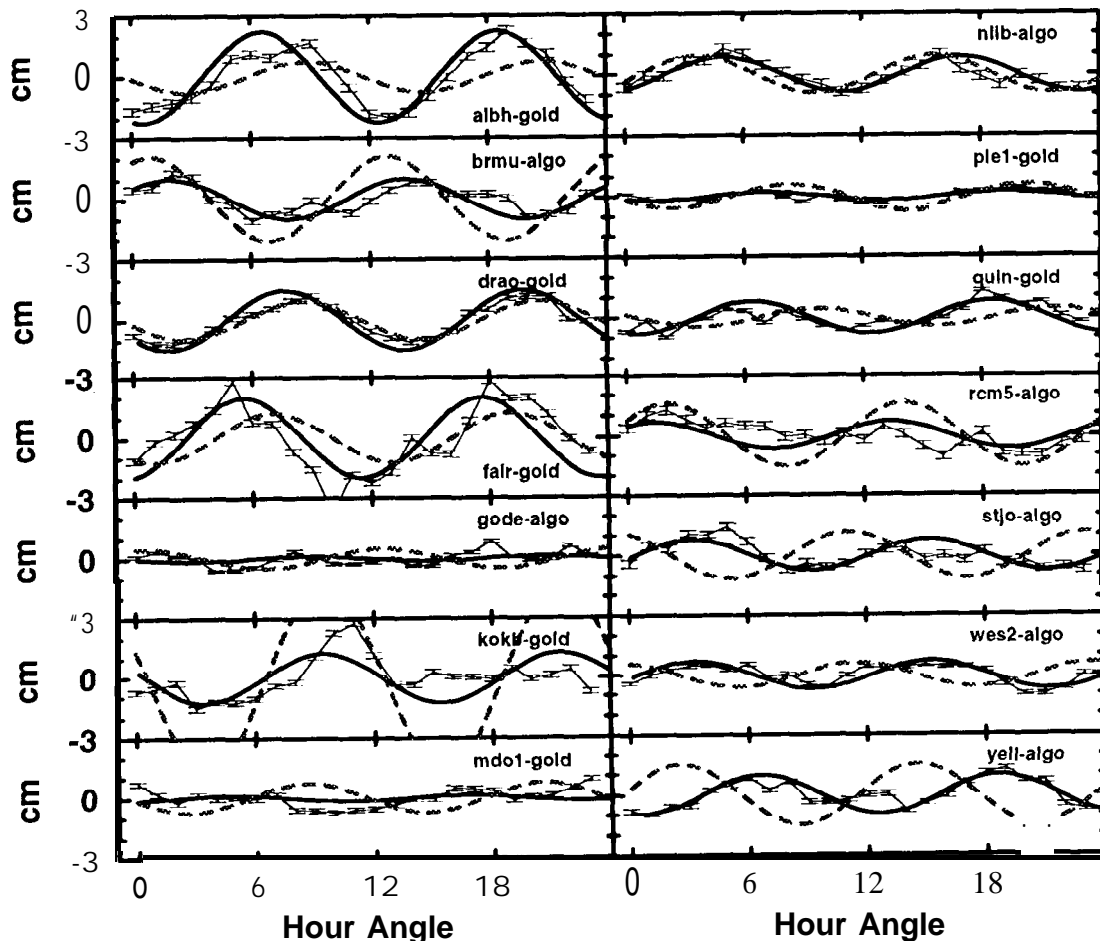


Figure 7: Summary of lunar OLT results

The phases shown in Figure 7 are intriguing, particularly for those sites tied to Algonquin. North Liberty shows an excellent match both in amplitude and phase. Given that this site is far inland, the implication is an excellent match between the actual and modeled OLT variations at Algonquin. Sites closer to the load (ocean) in ocean loading models, are more sensitive to errors in the loading calculations. Thus errors in the load model resulting from poor altimetric determination of near coastal tides or mismodeling the shape of the coast have a relatively larger effect at coastal versus inland sites. This would explain the superior agreement between the model and the measurements at sites such as Algonquin and North Liberty. The discrepancy between the model and the GPS measurements at St. John 's, Westford and Yellowknife can most likely be attributed to shortcomings in the load tide model. As yet, there is still no tide model for the Gulf of Maine/Bay of Fundy. In addition, the tide model only extends to 65 degrees north which may account for the disagreement at Yellowknife.

The results for the semidiurnal solar tide are summarized in Figure 8. As with the lunar OLT results, the amplitude estimates generally seem to match expectations. This resulted in fewer convincing detections because the solar OLT effects are approximately 40%

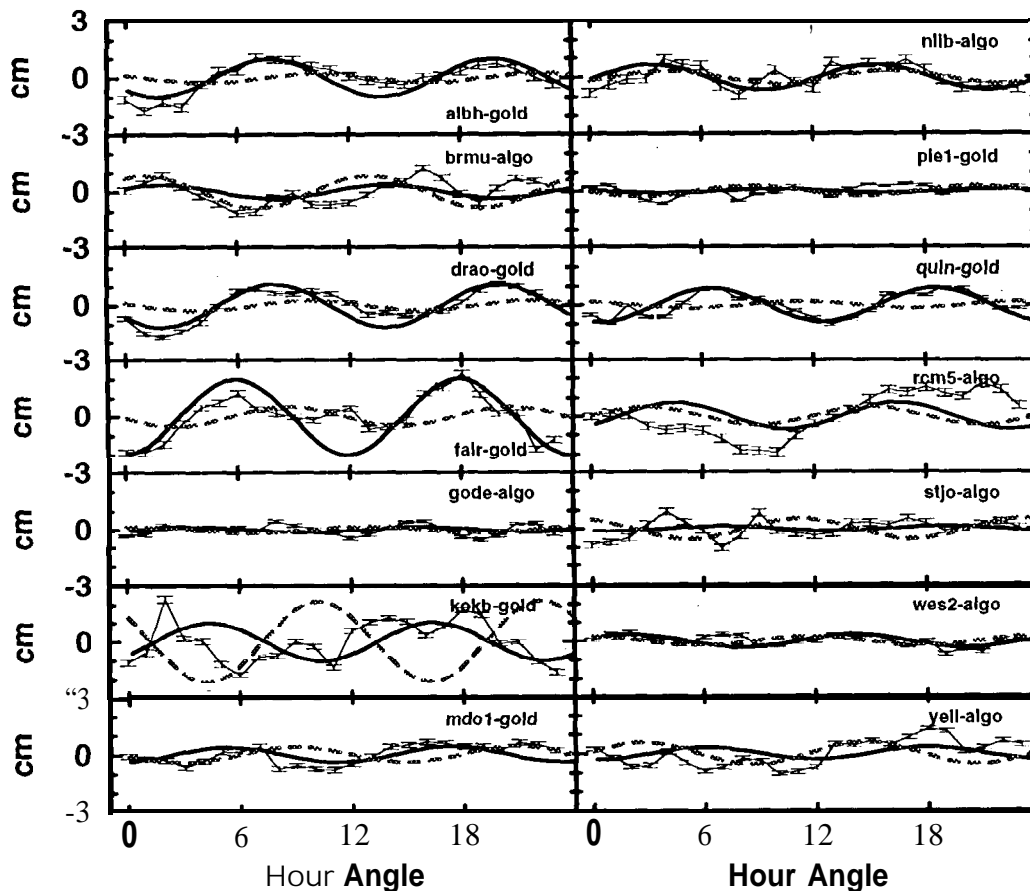


Figure 8: Summary of solar OLT results

those of the Moon. Nevertheless, signals do seem evident from Albert Head, Penticton, Fairbanks, North Liberty, and Quincy. Of these, only North Liberty is a good match to the model. The other sites show significantly stronger semidiurnal signals than anticipated. As mentioned previously, these may result from real, non-tidal sources with diurnal periods. No signals were expected or seen at Goddard and Pietown. Once again, the deep-ocean site, Kokee Park, deviates significantly from the model.

TESTING

The Penticton, Albert Head, and Kokee Park baselines were also used for a validity test. An alternate version of the program was created to search for a 12.25 hour signal. This period was chosen to be near to, but different from known tidal frequencies. When the model values were coherently accumulated using this characteristic period, a null-detection, i.e. a flat line was generated. In turn, no signal with this period should be seen in the GPS data if these techniques are valid. When reprocessed in this manner, no signals were evident from Penticton, Albert Head or Kokee Park. These tests also provide information about the noise limits of this processing. The RMS scatter of the hourly estimates from this reprocessing is 0.23 cm, 0.37 cm, and 0.86 cm for Penticton, Albert Head, and Kokee Park respectively. Given the typical baseline lengths of this project, OLT signals at the 0.4 cm level should be detectable. An additional test was made using a control baseline; the 36.3 km baseline between Goddard and the NOAA Gaithersburg, MD tracking site. These sites should move in unison because of their close proximity and no relative OLT signals should be seen. Upon processing, no signal was evident at the 1 sigma, 0.39 cm level.

CONCLUSIONS

The initial attempt to measure subdaily variations in height caused by ocean-loading appears successful. Semidiurnal lunar tidal signals were detected on nine of fourteen baselines. Null detections on two of the remaining lines were anticipated because of the small amplitudes predicted by the model. Solar semidiurnal signals were detected on five of the baselines. The solar signal should be weaker than the lunar in general. therefore, several of the null detections were anticipated. Unanticipated were the weak tidal signals for the two deep-ocean sites: Bermuda and especially Kokee Park for which the model indicated the largest signal of the sites included in this study. Further investigation of the results for these two sites is indicated.

Given this success, combined network solutions will be attempted in the near future. A priori information will permit realistic constraints to be placed on the tidal signals at a few sites resulting in absolute estimates of OLT at unconstrained sites. Expansion of this study seems worthwhile. For example, the estimation of OLT corrections could be incorporated into the routine site stability studies which NOAA will conduct on the U.S. Coast Guard sites and the results distributed as part of each site's descriptive information.

Another likely application is improved positions for coastal sites used to constrain altimetric tidal models.

Acknowledgements The authors wish to thank Michael Abell and Linda Nussear for the preparation of the data used in this study. Also thanks to Richard Ray for providing the software used to generate the OLT model mentioned throughout this manuscript.

REFERENCES

- Altamimi, Z. and Boucher, C., ITRF93 Coordinates for the 13 Fixed/Constrained Stations, *IGS Electronic Mail 819*, December 26, 1994.
- Neil, A. E., A New Approach for the Hydrostatic Mapping Function, in *Proc. Intern. Workshop for Reference Frame Establishment and Technical Development in Space Geodesy, Communications Research Laboratory, Tokyo*, pp. 61-68.
- Ray, R. and Sanchez, B., Radial Deformation of the Earth by Oceanic Tidal Loading, *NASA technical memo 100743, 1989*, p. 49.
- Schenewerk, M., Kass, W., Mader, G., and Spofford, P., *IGS Analysis Center Questionnaire, 1994*.
- Schrama, E. and Ray, R. A Preliminary Tidal Analysis of TOPEX/POSEIDON Altimetry, *JGR, 1994*, pp 24799-24808.

EMR Clock Estimation

P. Tétreault, J. Kouba, R. Ferland and J. Popelar

**Geomatics Canada
Natural Resources Canada
Ottawa, Canada
internet:pierre@geod.emr.ca**

Abstract

Precise clock corrections have been included in all EMR's ephemerides files (SP3 format) submitted to the IGS since August 1992 and since January 1995 in the EMR weekly Analysis Report to the IGS. EMR's clock corrections are estimated simultaneously with the orbital, EOP and station parameters using phase and pseudo-range observations in 24 hour arcs without data overlaps. The ALGO station, which is equipped with a hydrogen maser, has served with few exceptions as the EMR reference clock. Since a single reference station clock is used, a strong network geometry is required to ensure that precise clock solutions are obtained for all GPS satellites over the 24 hour arcs. Anti-Spoofing (AS) as decreased the EMR's clock corrections precision from 0.5ns to 1.0ns because C 1 and cross-correlated P2 observations must be used instead of the more precise P-code pseudo-range observations. Furthermore, calibration of pseudo-range biases is required whenever AS is in effect, EMR is currently enhancing its processing strategy to eliminate discontinuities, typically less than 1 ns, both during a day and between consecutive days. Nonetheless, EMR clock corrections can presently be used to help time transfer applications at the nanosecond level and, in combination with precise ephemerides, to perform point positioning at the cm level.

Overview

- introduction
- processing strategy
- anti-spoofing
- network geometry
- results
- future work

Introduction

Point Positioning

Precise clocks and orbits can be used to obtain station position at the 10m to the cm level depending on GPS receiver type and observing strategy

Time Transfer

Current GPS clock corrections allow time transfer at the nanosecond level

Processing Strategy

- JPL's GIPSY-OASIS II software with undifferenced carrier phase and pseudo-range observations
- 24 hour arc with no data overlaps
- clocks estimated simultaneously with other parameters
- clock offsets estimated with respect to ALGO which is fixed in the adjustment and uses an hydrogen maser frequency standard
- clocks estimated at 7.5 minute interval using a white noise stochastic model
- satellite clocks initialized using "broadcast" clock correction information but not constrained in the adjustment

Anti-Spoofing (AS)

Impact of AS on clock estimation is twofold

----> quality of pseudo-range observations is degraded if cross-correlated pseudo-ranges used

cross-correlated pseudo-ranges (April 9-15, 1995) 58 cm rms
P-code pseudo-ranges (April 21-26, 1995) 34 cm rms

----> cross-correlated pseudo-range observations are biased with respect to P-code observations and must be corrected before combining both types of observation

**Mean Bias Corrections for Ionospheric Free
Combination of C1 and P2
(January 31, 1995)**

Station	Average Bias/RMS (m)	Receiver	Software
ALBH	0.591/0.148	ROGUE SNR-8000	Turbo 3.0.32.2
ALGO	1.259/0.179	ROWE SNR-8000	Turbo 3.0.32.2
AREQ	0.031/0.179	ROGUE SNR-8000	Turbo 2.8.32
DAVI	2.332/0.114	ROGUE SNA-8100	Turbo 2.8.1.1
DRAO	-1.303/0.139	ROGUE SNR-8000	SFG2 (beta v. 3.0)
FAIR	25.906/0.216	ROGUE SNR-8	Meenix 7.8
FORT	-0.635/0.171	ROGUE SNR-8000	Turbo 2.8
mom	21.090/0.304	ROGUE SNR-8	Meenix 7.8 (DSN)
HART	19.516/0.310	ROGUE SNR-8	Meenix 7.8
KIT3	0.798/0.916	ROGUE SNR-8000	Turbo 2.8.32
KOKB	22.026/0.215	ROGUE SNR-8	Meenix 7.8
KOSG	24.11510.227	ROGUE SNR-8	Meenix 7.8
MADR	24.37410.252	ROGUE SNR-8	Meenix 7.8 (DSN)
MCM4	-0.204/0.167	ROGUE SNR-8000	Turbo 3.0
RCH5	0.40510.173	ROGUE SNR-8000	Turbo 3.0.32.2
SANT	31.19710.181	ROGUE SNR-8	Meenix 7.8
STJO	-0.654/0.221	ROGUE SNR-8000	Turbo 2.8
TATW	-1.014/0.146	SNR-8000	???
Tlob	19.47410.250	ROWE SNR-8	Meenix 7.8 (DSN)
TSKB	-0.61410.191	ROGUE SNR-8000	Turbo 2.8
WETT	11.42310.272	ROWE mm-a	Meenix 7.8
YAR1	19.150/0.227	ROGUE SNR-8	Meenix 7.8
YELL	0.91510.148	ROGUE SNR-8000	Turbo 2.8.32.1

Impact of Anti-Spoofing on EMR results

GPS Week	Pseudo-Range R63s (cm)	EMR Clock RMS IGS combination (nanosecond)	EMR Orbit 3743S IGS combination (cm)
732-733 (pro-AS)	17	0.5	10
736-737 (early AS)	60	10	15
780-781	45	1	12

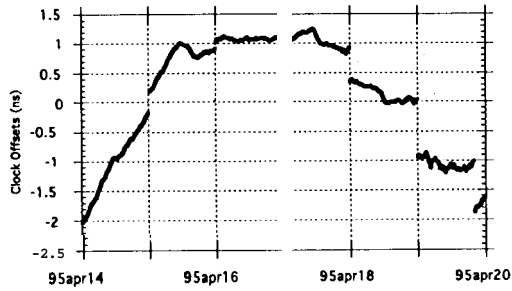
Network Geometry

- **network geometry** must ensure that clock offsets with respect to the reference are obtained for all satellites for the full 24 hour arc
- “holes” in the network results at times in satellites not being linked to the reference clock
- the current 26 station network used by EMR gives nearly 100% satellite clock recovery

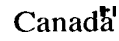
Results

- the reference clock **signature** contributes to all **stations** and **satellites** clock offsets
- **discontinuities** between consecutive days are usually less than 1 nanosecond and represent the bias of daily independent solutions
- **discontinuities** during a day are sometimes present due to a variety of factors including GPS receiver reset and pseudo-range bias changes
- ionosphere affects the quality of data and clock corrections

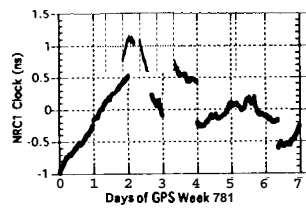
NRC1 Hydrogen Maser Clock Offsets with respect to ALGO
Obtained from EMR Daily Solutions



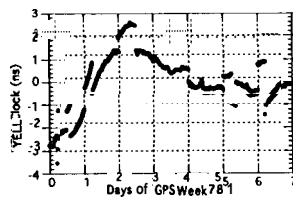
(initial offset: 1400.6ns; drift 13.0 ns/day)



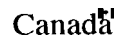
Hydrogen Maser Clock Offsets with respect to
ALGO obtained from EMR Daily Solutions



NRC1



YELL



TYPE TWO ASSOCIATE ANALYSIS AT NEWCASTLE-UPON-TYNE

Philip Davies (p. b.h.davies@ncl.ac.uk)
Geoffrey Blewitt (geoffrey.blewitt@ncl.ac.uk)

Department of Surveying, University of Newcastle upon Tyne,
Newcastle NE1 7RU, United Kingdom

Presented to the IGS Workshop, Potsdam, Germany, 15-18 May 1995

ABSTRACT

Since mid-1994, the distributed data processing approach to construction of the IGS Polyhedron has taken shape. One aspect of this is the creation of new Type Two Associate Analysis Centres (**T2 AACS**) for the monitoring and combination of global and regional networks which are components of the Polyhedron. The Department of Surveying at the University of Newcastle is preparing to function as a Type Two Centre, and is pursuing research into various aspects of the task. A new format known as **Sinex** (Solution Independent EXchange format) has been developed by an IGS working group to promote efficient inter-agency solution exchange. With , initial operations about to begin, this paper discusses aspects of the **T2** analysis function and describes its implementation at Newcastle.

1 INTRODUCTION

Since the adoption of the distributed data processing plan for IGS expansion (*Blewitt et al.* [1993, 1994, 1995]), the Department of Surveying at the University of Newcastle upon Tyne, England, has been preparing to function as a new IGS Type Two Associate Analysis Centre (**T2 AAC**). As part of the global network densification (*Zumberge et al.* [1994]), it will be responsible for comparing and combining network solutions from ACS and **T1** (regional) AACS, and hence constructing a reliable and consistent IGS Polyhedron, in addition to monitoring discrepancies and relative accuracies between the various input solutions.

Blewitt et al. [1994] discuss the following components of the **T2** activities:

- i) Detection of inter-agency (AC and **T1**) discrepancies, e.g. in **eccentricity** vectors.
- ii) Monitoring of solution consistencies (inter-agency, and **w.r.t. ITRF**).
- iii) Weekly publication of a combined global solution

- iv) Weekly publication of an IGS Polyhedron solution
- v) Periodic publication of kinematic solutions

Figure 1 illustrates regular T2 operation from an arbitrary GPS week i .

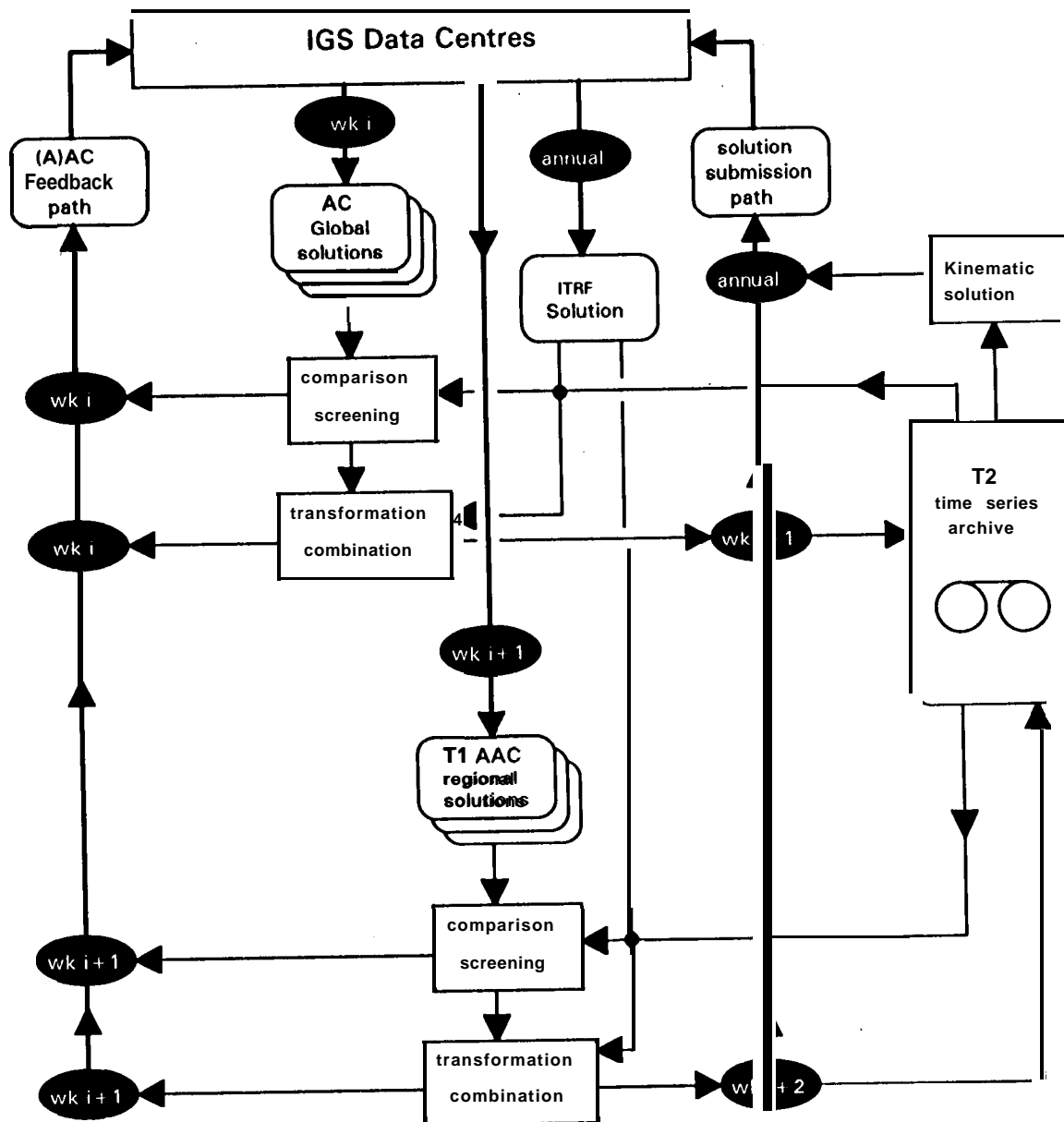


Fig. 1- Schematic representation of the T2 process

The **combined** solution is submitted to an **IGS data centre** one week after the individual solutions appear there, at the time the IGS orbits become available. The Polyhedron

solution is submitted one week later. An annual kinematic report on the Polyhedron is also produced.

In designing an operational **T2 centre**, three areas of particular research interest can be identified. The **T2 role** is relational - that is, it establishes and utilises commonality between two or more parameter solutions created by independent agencies for differing purposes. Therefore, communication, specification and standardisation issues are very important to **T2** design. Secondly, the transformational aspects of the task (that is, the particular information operations to be performed to most effectively accomplish the functions listed above) are currently being developed - this area will be studied more thoroughly when **trial** solutions are submitted. Thirdly, a highly automated system is essential to the establishment of regular analysis - this entails a high degree of formalism in the input, output, decision-making and reporting specifications, and a flexible and robust system design. These considerations are associated with the development of the **Sinex** transfer format, which uses a relational data structure to attribute time and place information to parameter estimates, and contains a history of solution input information which functions as the 'audit trail' of a processing sequence.

2 LOGICAL STRUCTURE OF SINEX

The Sinex format has been designed as a general-purpose solution exchange format for space geodesy, a primary application being the distributed data processing of the IGS. The block structure is reminiscent of a set of relational database tables, and the logical structure can be described in the same terms, with a series of attribute tables attached to each other by means of key fields. This modular design makes the format suitable for **specialised** purposes, such as the **T2 Sinex process catalogue**, described in section 5 below. A subset of the format has been adopted for the IERS Annual Report submissions. The syntax and usage recommendations of **Sinex** will not be detailed here.

The logical starting point of a Sinex document is the SOLUTION/EPOCHS block, which invokes the stations involved in the solution. Here we use the term *station* as usual in surveying, to mean a geometric representation in 'network space' of a physical monument. A single physical monument may have multiple stations attached to it, with different epochal, geometric or descriptive attributes. Also, we distinguish between a *site*, which is a descriptive location (analogous to a postal address) and a *point*, which is a geodetic monument at the site - one site may have multiple points. Each line of the SOLUTION/EPOCHS block, then, invokes a station by giving a site code (which is the familiar four-character ID), a point code (A, B, C, etc., being different monuments at the site) and an integer solution number, used to code multiple estimates of a single monument. For each station is given the data span used in the estimate, and the measurement **technique**. At present, the site codes are considered standardised and unique, while the point and solution codes are agency-assigned and arbitrary.

In the SITE/ID block, each monument (i.e. site code plus point code) named in the station list is associated with a unique ITRF DOMES code and some descriptive information.

The SOLUTION/ESTIMATE block gives parameter values and standard deviations, each line referenced to a station in SOLUTION/EPOCHS (except **erps**, if present) and having a parameter type (e.g. coordinate or velocity; x, y or z). The index numbers in this block are used in **SOLUTION/MATRIX_ESTIMATE** to attach a correlation element to **each** pair of parameters. Two blocks similar to these give *a priori* parameter and **variance-covariance** information.

The SITE/ blocks RECEIVER, ANTENNA and ECCENTRICITY give information about each station, to make clear any differences in station attribute data between submitted solutions. Each line includes a time span, so multiple lines in each of these blocks may refer to the same station, if any details change during the data time span given in SOLUTION/EPOCHS. Clearly, the time spans given in the SITE/ blocks must be within the corresponding station overall data span. The block SITE/GPS_PHASE_CENTER attaches a phase **centre** offset vector to each antenna, referenced by antenna type and serial number.

The solution history is detailed in the INPUT/ blocks HISTORY, FILES and ACKNOWLEDGMENTS and block **SITE/DATA**. Each solution in INPUT/HISTORY is referenced by an agency code (explained in INPUT/ACKNOWLEDGMENTS) and a time stamp. The file location of each solution is given in INPUT/FILES. The lines of INPUT/HISTORY are the header lines of Sinex files earlier in the processing path. Each has an operation code to indicate what role it played in the process. The last line of this block is the same as the header line of the document. Block **SITE/DATA** indicates from which input solutions information on each station in SOLUTION/EPOCHS was drawn. This gives the site, point and solution codes of the station in the current solution (which refer to SOLUTION/EPOCHS), and the equivalent information in the input solution, which may be different, since point and solution codes are not standardised. This allows each parameter in a solution to be **traced** back through several processing steps and Sinex files to its sources.

Using all this information, it should be possible to identify and locate the various source data of any solution, and perform historical searches, auditing and checking in a Sinex archive. The update of these blocks when operating on Sinex solutions is discussed in section 5 below.

Reading Sinex to initialise internal data structures is a basic function of **T2** analysis. The requirements for this to be done unsupervised without ambiguity, and for it to be difficult for analysis agencies to create meaningless Sinex by syntactic or logical mistakes, have been designs goal of the format.

3 COMPARING SOLUTIONS

The new **T2** analysis **centres** are in an **ideal** position to carry out a range of solution comparisons. The results of these will range from the immediate notification of gross discrepancies in ‘standard’ information, to making subtle long-term judgments of the relative performance of the analysis **centres**, and testing scientific hypotheses. The aims of comparison are:

- i) to promote efficient communication and standardisation between analysis agencies,
- ii) to detect errors apparent as discrepancies between solutions,
- iii) to judge the relative quality of solutions and performance of agencies,
- iv) to bring about the consistency necessary to routinely construct eclectic polyhedra,
- v) to carry out the data-screening and relational steps in the polyhedron-building task.

The advantages gained by routine comparison of IGS orbits (*Goad* [1993], *Beutler et al.* [1993]) **are** equally applicable to coordinate solutions, and the experiences of orbit comparison and combination are invaluable in planning the **T2 operations** on coordinate sets. This section discusses solution comparison issues in the context of an automated analysis process.

3.1 BASES OF COMPARISON

Input solutions will be compared:

- (i) with each other,
- (ii) with **ITRF**,
- (iii) with cumulative time series.

Any method of comparison is founded on assumptions about *one* or more factors in the system. Consider, for instance, a number of **ACs** regularly **analysing** a **globally-distributed** common subset of stations. Some example comparisons are:

c omparison over time

We may expect that the stations’ relative motion should have a continuous derivative function, or that station motion between epochs should be small, or whatever. Time series of a combined solution or of solutions from a single agency may be examined. The time series need not be long to be useful - extended time series can test precise kinematic hypotheses, but even a two-epoch series might identify a blunder or station problem introduced (or **removed!**) after the first epoch. Parameters can be individually screened, examined as vectors or combined in a test statistic.

comparison by (A)AC

Probably the most useful type of **comparison** in the early stages will be between analysis agencies estimating a substantial common subset of stations. Given a reasonable number of agencies and a good degree of consistency, a combined solution can be **used** as a standard to compare with **each component** solution. The pairwise comparison technique found useful in orbit assessment, in which all permutations of solution pairs are compared, is another method **being** tested. These assessments may be single or multi-epoch, and examine a range of functions - baseline lengths, **Helmert** parameters and residuals, **geocentre** vectors, kinematic functions, etc., as well as station coordinates and vectors. Individual stations can be examined, or general test statistics constructed.

comparison by station

To supplement comparisons by epoch and by analysis **centre**, other hypotheses are imaginable. For instance, a tectonic assumption that the stations in a particular area should be stable with respect to each other allows a comparison by station. Care must be taken when making possibly unsafe assumptions in the attempt to discover inconsistencies in the measurement system. In the limit, of course, any assumption used to screen data for errors may mask a systematic physical effect.

3.2 CONTENTS OF COMPARISON REPORTS

A question which must be addressed by the **T2** AAC in discussion with the ACS and T1 AACs submitting solutions is the form of the weekly reports on solution comparison. The following comments are intended to stimulate discussion of this subject among participating **Centres**.

The reports should be rapidly produced - the submitting agency should have the initial report on each submission in time to resubmit before the end of the processing week, **if necessary**. This rapid report should be short and easy to digest, **giving** prominent details on any problems the **T2** suspects on the basis of the comparison, especially if these require a resubmission. The first **section** of the report, then, could be a solution **health** check, with perhaps a single line indicating any problems on each of the following headings. A more detailed section of the report will follow on each heading.

- i) **Sinex syntax and structure**: if the submitted Sinex contains syntactic or logical flaws which cannot be easily corrected, or cause ambiguity or meaninglessness, resubmission will be **requested**.
- ii) **Information completeness and integrity**: resubmission will also be requested if information essential to the process is missing, or if the submission is self-contradictory.

- iii) Information discrepancies and Parameter matching This section concerns the compatibility of the submission with others. Anomalies in ‘standard’ (*e.g. site*) information and standardised codes will be notified - it is hoped that a period of this feedback will lead to increased consistency of standard data between analysis groups.
- iv) Station subsets and frame transformations; The common subsets between the submitted solution and other Polyhedron components is the basis of estimating transformation parameters and integrating the solutions. Therefore, the report should tabulate the sizes of these subsets, and the transformation parameters derived from them. If geometric analysis is conducted to quantify the network strength of station subsets, this will be **included**.
- v) Residual analysis: residuals from the comparisons by epoch and (A) AC, as outlined above in **3.1**, will be presented in graphical and statistical form. The format and contents of this presentation are not yet **finalised**, because the types of comparison operation are still **being** studied. T2s therefore need comments from submitting agencies on what information they would like to see in the report, and useful summary statistics.

3.3 RELATING SOLUTIONS

Consider two input solutions received by the **T2 centre**. They each give coordinates for a set of stations, and there is a subset of stations common to both, which is the basis of relating the solutions. Establishing this common subset by a process of **station-matching** (identifying two or more stations estimates as common parameters) is therefore a task antecedent to other **T2** parameter operations. A series of criteria are applied in the station-matching task:

(i) Common physical monument

When stations in the two solutions have the same DOMES code, a tentative match is made. Since multiple stations in a single solution can have the same DOMES, this may not be a unique match. Monument matching without DOMES codes is possible if the four-character site code is **recognised** and there is no point code ambiguity, although this is to be considered inferior to unique monument reference. Standardised DOMES and site codes should be used whenever possible.

(ii) Common epoch

Each station in the solution has an overall data span attached to it - these are used to apply various epoch rules, depending on the situation. In the context of a regular (say weekly) processing cycle, all data spans might be **expected** to fall within the week being processed. A station with a data span in the previous week might then be

separately **parameterised**. Alternatively, an epoch rule based on overlapping data spans, or proximity of mean epochs could be applied. This criterion is therefore context-dependent. It becomes critical when a solution contains multiple estimates for a single monument at different epochs, and it is **required** to match these to estimates in another solution.

(iii) **Local eccentricity**

If two solutions have **analysed** the same data for a station (as is the case with IGS ACS) they should have **used** the same eccentricity data - that is, local tie and phase **centre** offset vectors. **Sinex** therefore requires detailed information on this in the SITE blocks, allowing for changes during the data span. Discrepancies in eccentricity vectors may or may not be simple to compensate for - the '12 will inform the agencies concerned. Making vector correction an automatic procedure at the **T2** is a dangerous approach - in doubtful cases a discrepancy should in the first instance cause the station match to fail.

(iv) **Attribute information**

Of less importance than the spatial and temporal data is the attribute and descriptive information that may be given in the **Sinex** document. This includes the receiver, antenna, agency and site descriptions. Differences in these will be reported on by the T2, but they will not prevent a station match being made.

By applying these criteria, the common station subset of a group of submitted solutions can be constructed. The size of this subset is highly variable - in the case of relating several global AC solutions, the common subset may be a large proportion of the stations **analysed**, whereas when relating a **T1 local** network to a global solution, as few as three common anchor stations may be present.

3.4 EXAMPLE OF SOLUTION RELATION

Consider two submittal **Sinex** documents. They have passed the syntax and logical checking stages, and it is now required to establish the common station subset between them. Consider just the information relating to site HERS (**Herstmonceux** Observatory, UK). We start with the SOLUTION/EPOCHS block:

```
* FROM SUBMISSION 1
+SOLUTION/EPOCHS
* CODE PT SOLN T DATA START_ DATA END MEAN EPOCH_
...
HERS A 1 P 95:001:00000 95:007:86399 95:004:43200
HERS B 1 P 95:001:00000 95:014:86399 95:008:00000
...
-SOLUTION/EPOCHS

* FROM SUBMISSION 2
+SOLUTION/EPOCHS
* CODE PT SOLN T DATA START_ DATA END MEAN EPOCH_
...
HERS A 1 P 95:001:00000 95:007:86399 95:004:43200
```



```
HERS A 2 P 95:008:00000 95:014:86399 95:011:43200
...
~SOLUTION/EPOCHS
```

Submission 1 estimates two monuments at **Herstmonceux: A** in the first week of 1995, and **B** for the first two weeks. Submission 2 estimates just one monument, **A**, separately for the first and second weeks. According to the technique codes, all observations are by GPS.

To establish common physical monuments, we look up the sites referred to in the SITE/ID block:

```
* FROM SUBMISSION 1
+SITE/ID
*CODE PT DOMES T DESCRIPTION LONGITUDE_ LATITUDE _HGHT_
...
HERS A 13212M007 P Herstmonceux GPS mark 000 33 00.0 50 87 00.0 100.0
HERS B 13212S012 P Herst. Rogue SNR-8A 000 33 00.0 50 87 00.0 100.0
...
~SITE/ID

*FROM SUBMISSION 2
+SITE/ID
*CODE PT DOMES_ T DESCRIPTION LONGITUDE_ LATITUDE _HGHT_
...
HERS A 13212S012 P Herstmonceux 000 33 00.0 50 87 00.0 100.0
...
~SITE/ID
```

The common **DOMES** code matches submission one HERS B to submission two HERS A. Submission one HERS A has no match in submission two, so common parameterisation is ruled out. The description and approximate position fields are attributes ignored in station matching.

Next, we examine the epochs of the common monument estimates. Note that the submission one estimate of 13212S012 is for a two-week data span, whereas submission two estimates the two weeks separately. The matching here is, as discussed in 3.3(ii), context-dependent. If the current process is a combined solution for week two, for instance, we might exclude (or separately parameterise) submission two estimate one, and match the week two estimate to submission one. Or, submission two could be excluded for estimating an illegal data span for the weekly process, and the agency requested to resubmit a separate estimate for each week. Other options are imaginable.

Suppose that the epoch match is successful between submission one HERS B 1 and submission two HERS A 2. We now check eccentricity data by relating the SITE/ANTENNA, SITE/ECCENTRICITY and SITE/GPS_PHASE_CENTER blocks.

```
*SUBMISSION 1
+SITE/ANTENNA
* CODE PT SOLN T DATA START DATA END DESCRIPTION S/N
HERS B 1 P 95: 001:00000 95:014:86399 Antenna 1 12375
~SITE/ANTENNA
```

```

*
+SITE/GPS_PHASE_CENTER
*DESCRIPTION S/N L1-ARP(m) L2-ARP(m) Az El
Antenna 1 12345 .0100 .0200 .0300 .0100 .0200 .0300
-SITE/GPS_PHASE_CENTER
*
+SITE/ECCENTRICITY
*CODE PT SOLN T DATA_START DATA END TYP ARP_to_benchmark_(m)
HERS B 1 P 95:001:00000 95:014:86399 XYZ 01.0000 02.0000 03.0000
-SITE/ECCENTRICITY

*SUBMISSION 2
+SITE/ANTENNA
*CODE PT SOLN T DATA_START DATA END DESCRIPTION S/N
HERS A 1 P 95:001:00000 95:007:86399 Antenna 1 12345
HERS A 2 P 95:008:00000 95:014:86399 Antenna 2 67890
-SITE/ANTENNA
*
+SITE/GPS_PHASE_CENTER
*DESCRIPTION S/N L1-ARP(m) L2-ARP(m) Az El
Antenna 1 12345 .0100 .0200 .0300 .0100 .0200 .0300
Antenna 2 67890 -.0300 -.0200 -.0100 -.0300 -.0200 -.0100
-SITE/GPS_PHASE_CENTER
*
+SITE/ECCENTRICITY
*CODE PT SOLN T DATA_START DATA END TYP ARP_to_benchmark_(m)
HERS A 1 P 95:001:00000 95:007:86399 XYZ 01.0000 02.0000 03.0000
HERS A 2 P 95:008:00000 95:014:86399 XYZ 01.0000 02.0000 03.0000
-SITE/ECCENTRICITY

```

The reference point-to-benchmark information given in SITE/ECCENTRICITY is the **same in each case**, but we see that submission two is aware of an antenna **change at the end of week one** which does not occur in submission one- perhaps this is why there are two estimates for this monument in submission two. Without performing a vector correction, we can now only match submission two solution one to submission two, which conflicts with the epoch-match criterion. It might be decided in this case to report on the discrepancy in antenna data to the agencies concerned, and make no station match - this is the safest course. The action taken depends on the situation and the **type of processing** being undertaken.

This example will be **curtailed** here- matching proceeds through several more **stages** of attribute comparison **before** an unambiguous common parameterisation is decided on. Any discrepancies discovered, whether or not they prevent a station match being made, are reported to the analysis groups concerned. In practice, this operation is carried out with reference to a **Sinex Catalogue** file maintained by the **T2** centre - this is discussed in section 5 below.

4 COMBINING SOLUTIONS

Regular solution combination will begin when routine solution comparison shows that the global network estimates of the different ACS have an appropriate degree of consistency. The solution combination function of the **T2** will be developed gradually, in the following stages:

- i) Experimental production of a combined global subset, consisting of all stations **analysed** by at least three ACS,
- ii) The inclusion of all AC stations in the combined estimate,
- iii) Adding regional networks (with global Anchor Stations) to the Polyhedron.

Submitted solutions will be rotated to a common frame using estimated **Helmert** transformations and **combined** by a weighted least squares estimation, using loose datum constraints. It is expected that the constraints of submitted solutions will vary widely, therefore it is important that full a priori data be supplied in the Sinex submission. We now look at some statistical tools and solution weighting techniques and consider their appropriateness for our analysis.

4.1 STATISTICAL TESTS

Quality control

In performing a **Helmert** transformation between pairs of solutions, the quality of input coordinates can be controlled by statistical tests for **outliers** and other model errors (*Kosters and Kok* [1989]).

For **detecting outliers**, *Baarda's* “w-statistic” can be used (often called “data snooping”), as developed by *Baarda* [1967, 1968]. An iterative version of data snooping tests the alternative hypothesis that there are multiple **outliers** [e.g., *Kok*, 1984].

For detecting functional model problems, we can test the alternative hypothesis that the input data are not normally distributed. Non-parametric tests can be more powerful than **chi-square** tests for this purpose (*Conover, 1980*). A possible candidate is the **Lilliefors** test, which is a test of the Kolmogorov type, in which the test statistic is maximum discrepancy between observed and computed cumulative distributions, This would be applicable to intercomparisons of solutions, and *King et al. [1995]* has **applied** this to GPS time-series analysis.

For detecting stochastic model problems, we think the unit variance test is of limited value since it is well-known that GPS computed errors are optimistic. Rather than test the unit variance, it might be more realistic to use a comparison of free-network solutions to provide a unit variance which can then be used as an overall scaling factor. An extension of this approach is the application of variance component estimation (see section 4.1).

Reliability and Marginal Detectable Error

Following *Baarda's* concepts, “internal reliability” is the size of errors in the input data that can be detected using a **specified** probability in the **outlier** test. We can more

generally think of “internal reliability” as a **hyperellipsoid** in a space spanned by the data. The “marginal detectable error” (**m.d.e.**) in a particular direction is the radius of this **hyperellipsoid** in that direction. Supposing an observation error of magnitude **m.d.e.** passed through the analysis undetected, we could compute the bias that would result in any of the estimated parameters. This bias is called the “external reliability.” We could compute the external reliability for **each** observation, and find the maximum value. This would indicate the sensitivity of our transformation parameters to our inability to detect **outliers**.

As is the usual problem of hypothesis testing, there is no objective guidance as to choosing an appropriate level of significance. Ultimately, test parameters tend to be chosen to suit the user’s needs, and are based on experience with samples of real data.

Kosters and Kok [1989] discuss the **discernability** between hypotheses using reliability theory, and suggest ways to assess whether all 7 parameters are required in a similarity transformation. For fiducial-free GPS solutions, an example would be to test whether the geocentre or scale parameters deviate more than the calculated external reliability. If they do not, then we **could** accept the null hypothesis and leave those parameters out of the **Helmert** transformation (and combination process). If a transformation parameter does deviate significantly, we should first look for functional and stochastic model errors (e.g., normality of residuals), and either reject a solution, or include the additional estimated transformation parameters. This **procedure** could be applied to time-series of solutions from the same analysis **centre**, or to solutions from different analysis centres at the same epoch.

4.2 VARIANCE COMPONENT ESTIMATION

An interesting and currently unresolved issue in solution combination is the method of assigning weight matrix scale factors (**blockwise** variance components) to the input solutions. This affects both **Helmert** parameter estimation for frame transformation and weighted least squares combination. Various approaches are possible, with varying degrees of statistical rigour and intuitiveness. As usual in such situations, robustness, simplicity and intuitive appeal are at least as important as statistical justification in choosing a technique! In orbit combination, methods **based** on **RMS** values of **Helmert** residuals estimated pairwise between solutions or between each solution and a combined estimate have been proposed. Derivations justifying such approaches are based on assumptions of no correlation between solutions.

The more general methods of variance component estimation, a good geodetic development of which is by **Grafarend and Schaffrin [1979]**, are more statistically powerful, being able to handle a variety of second-order designs (i.e. a variety of **covariance** matrix block structures and parameters) and inter-block **covariances**. In general, a number **n** of observation blocks exist, where solution **i** consists of a vector of values **l_i** and an associated **variance-covariance** matrix denoted **Q_{ii}** . This includes a

variety of situations, e.g. the blocks may be successive-epoch solutions for a set of stations, or a variety of overlapping networks, etc.

These solutions are to be combined in a least squares estimation, where the overall second-order design matrix Σ (the **variance-covariance** matrix of the observations) has the form:

$$\Sigma = \begin{bmatrix} \sigma_1^2 Q_{11} & 0 & \dots & 0 \\ 0 & \sigma_2^2 Q_{22} & \dots & 0 \\ \vdots & \vdots & \ddots & \vdots \\ 0 & 0 & 0 & \sigma_i^2 Q_{ii} \end{bmatrix}$$

that is, the network solutions are **uncorrelated** and the **variance components** σ_i^2 are to be estimated (which are relative scaling factors between the network solutions). If, alternatively, correlation is suspected, it is necessary to specify design matrices Q_{ij} ($i \neq j$) giving the form of the correlation, and the **covariance components** σ_{ij} may also be estimated. More complex **second-order** designs may be proposed and investigated, such as additive variance components of the form $\Sigma_{ii} = \sigma_{i1}^2 I + \sigma_{i2}^2 Q_{ii}$ (two estimated components for each block), and others.

In this case, the **Helmert** blocking technique (one solution per block) would be used for the least squares estimation, iterated such that the first **LS** estimate \hat{x} yields the first Σ , which gives the second \hat{x} , etc. The σ_i^2 ($i = 1, \dots, n$) converge from initial values of unity. At each iteration, the quadratic form of the **LS** error matrix (the weighted sum of squares of observation residuals) is **equated** to its expectation, assuming no blunders and no first or second order model errors, to yield at convergence a best invariant quadratic unbiased estimate of variance components, identical with the **MINQUE** estimate (*Koch [1987]*) and with the Maximum Likelihood estimate (*Ziqiang [1989]*).

Various **expedient** modifications have been proposed to the full theory for simplicity and computational efficiency (*Ziqiang [1989]*, *Koch [1986]*). A significant objection to such an approach is that the resulting variance components are not statistically significant with small samples - it might not be useful until a reasonable time-series of results has amassed. Another objection is that any **outliers occurring** in the data at this stage may be rendered undetectable (e.g. by data snooping) if variance component estimation is being applied.

The **T2 centre** will initially assign unity weight scale factors to all analysis **centres**. A research priority when solution comparisons begin will be parallel experiments on the various methods of relative solution weighting, the assessment of which will determine the approach adopted.

5 SINEX MAINTENANCE USING CATALOGUES

The **T2** software being **developed** at Newcastle is based around the use of a Sinex **catalogue file**, which is a specialised Sinex document used to govern the process of station matching. For a particular operation on a set of submitted Sinex documents, a **catalogue** file is prepared, containing a subset of Sinex blocks, most importantly SITE/ and SOLUTION/ blocks. The purpose of this file is to inform the software of stations to be **expected** in the incoming Sinex solutions, and give the **expected** attributes of those stations (eccentricity vectors, antenna details, etc., etc.). After syntax and logic checking, each solution is matched to this document, discrepancies are logged, and internal data structures are created.

A 'standard' **catalogue** file containing all regularly processed stations will be developed, and updated with information changes as the **Centre** becomes aware of them. Since the **catalogue** has the multiple solution numbers facility of Sinex, it is also used to control multiple parameterisations for points involved in tectonic events, and for other multi-epoch investigations. The a priori data blocks are used to hold the 'standard' nominal parameter values and constraints, so these **can** also be compared to the input solutions, and the appropriate matrix operations carried out if **necessary**. A further software module **can** create a **catalogue** file from one or more Sinex submissions - this allows solution intercomparison without external reference (to detect changes in submitted data from an AC over time, for instance). Sinex **catalogues** with INPUT/ blocks will be used as indices to archived solutions and to cross-check submitted solution histories.

Some **T2** operations output parameter estimates (e.g. **Helmert** transformations and **LS** combinations) which will be written as Sinex output. The **catalogue** file is again useful here, providing the attribute information in the output estimate. The software keeps track of the data operations performed to enable the automatic update of the INPUT/HISTORY and INPUT/FILES blocks, creating a process audit **trail**. Operations producing other types of output (test statistic values, for instance) have less well-developed formats at present. If distribution of these data is deemed advantageous as the distributed system matures, new Sinex block types could be defined for the purpose. At present, the **FILE/COMMENTS** free-format block is provided for users to exchange miscellaneous information by mutual arrangement.

6 IMPLEMENTATION

The schedule for implementation of the IGS distributed processing scheme allocated a period of one month between the submission of a trial Sinex solution (for a particular week) by each AC, and the commencement of routine operations by **T2 centres**. This period is required to report to ACS, request resubmission where necessary, correct design faults and misunderstandings, prepare for operational processing, etc. Although

the implementation is now behind schedule, it is still intended to carry out the pilot stage when a set of trial submissions becomes available. This will be followed by routine solution comparison, in the early days of which it is anticipated that many inconsistencies will be identified by feedback within the distributed system. Removing these problems will allow routine combined solutions and **polyhedron** solutions to be **produced**. Since the points made in this paper are based largely on anticipation of the way the system and the **Sinex** communication will work, and precede real data processing experiments, this material is to be considered partly speculative and as a prompt for discussion of the issues raised.

ACKNOWLEDGEMENTS

The **Sinex** format was developed by the **Sinex** Working Group, an IGS ad hoc committee (G. **Blewitt**, Y. Bock, C. **Boucher**, G. **Gendt**, W. **Gurtner**, and J. **Kouba**). We would also like to thank Z. **Altamimi**, J. **Freymueller**, M. **Heflin**, and T. **Herring**, for their valuable suggestions which were incorporated into **Sinex**.

REFERENCES

- Baarda, W. [1967] Statistical concepts in geodesy, *NGS-publications on geodesy, New series, Vol. 2, No. 4, Delft*.
- Baarda, W. [1968] A testing procedure for use in geodetic networks, *NGC-publications on geodesy, Vol. 2, No. 5, Del ft*.
- Beutler G., J. **Kouba**, T. Springer [1993], Combining the orbits of the IGS processing centres, Position paper in *Proceedings of the IGS Workshop*, Ottawa, Canada, October 1993.
- Blewitt** G., Y. Bock, G. **Gendt** [1993], Regional clusters and distributed processing, Position paper in *Proceedings of the IGS Workshop*, Ottawa, Canada, October 1993
- Blewitt** G., Y. Bock, J. **Kouba** [1994], Constructing the IGS polyhedron by distributed processing, Position paper in *Proceedings of the IGS Workshop*, Pasadena, California, December 1994
- Blewitt** G., Y. Bock, and G. **Gendt** [1995], Global GPS network densification: a distributed processing approach, *Manuscript Geodaetica* (in press)
- Conover W. J. [1980] *Practical Nonparametric Statistics*, Second Edition, John Wiley and Sons.

Goad C. [1993], IGS orbit comparisons, *Proceedings of the IGS Workshop*, Bern, Switzerland, March 1993

Grafarend E. & B. Schaffrin [1979], **Variance-covariance-component** estimation of **Helmert** type, *Surveying and Mapping*, vXXXIX n3 pp225-234.

King N.E., J. L. Svarc, E. B. Fogleman, W. K. Gross, K. W. Clark, G. D. Hamilton, C. H. Stiffler, and J. M. Sutton, [1995] Continuous GPS observations across the Hayward fault, California, 1991-1993 (in press).

Koch K. [1986], Maximum likelihood estimate of **variance-covariance** components, *Bulletin Geodesique* v60 pp330-338.

Koch K. [1987], *Parameter estimation and hypothesis testing in linear models*, Springer-Verlag, Berlin.

Kok J. [1984], On data snooping and multiple **outlier** testing, NOAA Technical Report NOS NGS 30, **Rockville**, Maryland.

Kosters A. and J. Kok [1989], Statistical testing and quality analysis of observations and transformation parameters in combining 3-dimensional networks, Paper presented at the IAG Congress, Edinburgh, August 1989.

Ziqiang O. [1989], Estimation of **variance-covariance** components, *Bulletin Geodesique* v63 pp139-148.

Zumberge J., R. **Neilan**, I. Mueller [1994], **Densification** of the IGS global network, Position paper in *Proceedings of the IGS Workshop*, Pasadena, California, **December** 1994

ITRF and IGS Regional Densifications

C. BOUCHER

IERS Central Bureau/IGN Paris, France

1) THE ITRF WORKSHOP

1.1) Report of the Workshop

A Workshop has been organized by the IERS Terrestrial reference Frame Section (ITFS) of the IERS Central Bureau in order to discuss with representatives of the Analysis centers as well as other interested people. It was held in Paris on May 8 and 9 1995 and gathered 30 attendees.

Nine contributing papers were presented to stimulate discussion. Proceedings will be published and available at the IERS/CB.

The following contributions were given:

Boucher C. The ITRF. Proposals for an improved strategy

Ma C. VLBI analysis issues with respect to the TRF

Montag H. Some comments on the ITRF solution

Beutler G. The contribution of the IGS to the establishment of the ITRF

Willis P. DORIS and IERS Terrestrial Reference Frame: open questions and comments

Andersen P. H. Simultaneous analysis of GPS and VLBI data

Wooden W. Comparisons between WGS84 and the ITRF

The recommendations were established and presented at the IERS Workshop held just after on May 10 to 12 in Paris.

It was also decided to present them during this meeting. The main findings can be summarized now:

a) Necessity to improve the method of combination

This implies in particular:

- to use the full covariance matrix of individual solutions
- to ask for minimal constraints or free solutions
- to use the SINEX/ISEF1 format

b) Concerning the ITRF datum

An international agreement is needed. The baseline proposal will be:

-to fix the origin by a weighted mean of SLR, GPS and DORIS results

-to fix the scale by a weighted mean of SLR, VLBI, GPS and DORIS results

-to fix the orientation by a best alignment to past BIH/IERS orientation at 1988.0

- to fix the time evolution by a NNR condition close to geophysical models

c) Concerning the IERS Network,

It was stressed the following issues:

-the growing need to take actions concerning the design of this network, and not only to consider what has been done by the various contributors

-to try to improve the existence and quality of the local survey information

-to adopt and apply a classification of stations belonging to the IERS network

d) Multiplicity of ITRF

An important aspect is the clarification of concepts and vocabulary. In particular, ITRF should be used for any frame published with an IERS label and which is a realization of the International Terrestrial Reference System (ITRS).

In this scope, various types of ITRF can be considered:

- complete means that all available data received by IERS are used. It implies that the set of station coordinates is maximum, but requires a classification which indicates the various levels of quality

- primary means that the solution is resulting from highest level standards concerning models, input data, station selection, datum...

- individual means a realization done by an individual Analysis Center but explicitly referred to ITRS

-time series means that station positions are time series (daily, weekly, monthly, yearly ..)

e) Links with WGS84

It was clearly recommended to investigate closely the connection between ITRS/ITRF and WGS84, and then widely publish the related information. The recent work done by DMA on these issues should be used for that purpose.

1.2) Recommendations of the ITRF Workshop

The Workshop proposed some Recommendations which are issued from the presentations and discussions:

Recommendation 1

To adopt a protocole for the production of ITRF by establishing and accepting a set of documents and take care of their premanent updating:

A: Interfaces between the IERS Terrestrial Frame Section (ITFS) and Analysis Centers

B: Description of the ITRF datum

C: Procedures applied to realize a Primary Frame

D: Procedures applied to realize a Complete Frame

E: Procedures applied to realize a Time Series Frame

F: User's guide on the access to ITFS results (reports, mails, WWW...)

Recommendation 2

To adopt a conventional definition on the ITRF datum without constraints coming from EOP and to utilize it in order to obtain stable sets of coordinates for the various ITRF solutions.

Recommendation 3

To investigate the interest to adopt a reference ITRF in the same way one can adopt reference values for fundamental constants, by opposition with best estimates.

Recommendation 4

To update the new IERS Standards in accordance with the recommendations of this Workshop, in particular concerning WGS84.

Recommendation 5

To establish a Committee on IERS Network Design and Implementation (CINDI) which should take care particularly of the following tasks:

- to select new sites by stimulating relevant national agencies to settle proper instruments

- to improve the number or the geographical repartition of collocations either by settlement of new instruments at existing sites or by the use of multiple systems such as the TIGO system under development by Germany

- to stimulate the improvement of the local eccentricity data set either by adding new local surveys or evaluating their actual quality

- to define a classification of stations and develop quality control, in particular to check the class assesment of each station as performed by the ITFS of IERS

2) The ITRF94 solution

The ITRF94 solution which is under development at the ITFS will follow these characteristics:

- a) combination of the solutions which will provide positions and velocities with full covariance matrix. A new software (GEOMIX) is planned to be used.

- b) the datum will be selected as described in the previous chapter

- c) the received solution will be divided into two classes. Class I solutions will consist of position and velocities with full covariance matrix in the SINEX format and with acceptable quality by comparison with ITRF93.

- d)The analysis will consist of successive combinations within each technique and then globally. One of the issues will be to

determine a convenient scaling factor for each a priori covariance matrix. The result will be the ITRF94 solution.

e) a first attempt to classify the resulting station coordinates should be done

f)The other received solutions (class II) will be compared with the ITRF94 solution

3)A pilot experiment for a monthly ITRF (ITRF-TM1)

The ITFS plans to undertake a pilot experiment to compute a monthly time series: ITRF-TM1.

A call for proposal will be issued among the analysis centers in order to select those which would accept to provide each month their contribution.

This test has been considered mainly thanks to the IGS pilot experiment for weekly GPS solutions. Clearly the monthly GPS solutions will be derived from these weekly solutions without reprocessing from GPS analysis centers.

For the other techniques, it would be desirable to have at least one or preferably two monthly solutions (VLBI, SLR or DORIS). It is understood that LLR may not be suitable for this test but only for global contributions.

DETERMINATION OF ANTENNA PHASE CENTER VARIATIONS USING GPS DATA

Markus Rothacher, Stefan Schaer, Leoš Mervart, Gerhard Beutler
Astronomical Institute, University of Berne
CH-3012 Bern, Switzerland

ABSTRACT

When processing GPS data without using a correction model for elevation-dependent *phase center variations (PCV)* of GPS antennas two error types have to be considered: (1) a bias in the (relative) station height (up to 10 cm) if different antenna types are mixed, (2) a scale factor in the baseline length (up to 0.015 ppm) which is essential on long baselines even if antennas of the same type are used.

Both effects are of importance in the context of the *International GPS Service for Geodynamics (IGS)* — for global solutions as well as for regional densification of the IGS network with a mixture of different receiver and antenna types. The elevation-dependent PCV also have an impact on the estimation of tropospheric zenith delays and ionosphere parameters (both effects relying on a correct mapping).

Two independent methods are available to obtain antenna phase center calibrations: the *anechoic chamber tests*, where the phase pattern of a single GPS antenna is measured, and the *estimation of phase center corrections from the GPS data* taken on short baselines. We focus on the parameterization and estimation of the PCV from GPS measurements. The consistency of the estimates of the coefficients of a spherical harmonics development is shown for two cases, elevation-dependent corrections only and for the azimuth- and elevation-dependent corrections. The solutions are compared to the results obtained from anechoic chamber tests.

There is hope that residual problems concerning the interpretation of *absolute* calibrations can be sorted out in the near future by a close and fruitful collaboration of the groups performing chamber tests and those deriving corrections from GPS data processing.

INTRODUCTION

In early tests and studies concerning the combination of different antenna types the emphasis was put on the calibration of the *vertical* and possibly *horizontal offsets* between the phase centers of various antennas. In preparation for the EUREF-89 Campaign (Seeger et al., 1992), one of the first major campaigns to involve most of the geodetic GPS receivers and antennas available at that time (Minimac 2816, TI-4100, Trimble 4000SLD, and WM-102), an antenna calibration campaign was organized at Wettzell to determine the relative phase

center offsets. The analysis showed (Gurtner et al., 1989) that discrepancies up to about 4 cm could be detected between the nominal values published by the receiver manufacturers and the GPS estimates. At that time it was thought, that by using these calibration values the antenna combination errors could be reduced to below the 1 cm level. In these early studies only L1 and L2 solutions were checked, neither the use of the ionosphere-free linear combination (called L3 below) nor the estimation of troposphere parameters were considered for very short baselines. In 1992, few months after the start of the IGS Test Campaign (Beutler et al., 1994), we detected a bias of about 10 cm in height for Zimmerwald in our daily solutions with respect to the ITRF (i. e. SLR) results. ‘The GPS results essentially stemmed from the baseline Wetzell – Zimmerwald, a mixed Rogue (Dome Margolin B antenna) – Trimble 4000SSE (4000ST L1/L2 GEOD antenna) baseline. After checking the local ties between the SLR/VLBI and GPS points and after installing an Ashtech Z-12 next to the Trimble receiver in Zimmerwald it became clear that the 10 cm height error was due to the different antenna phase patterns of the Rogue and Trimble antennas. This observation was confirmed by (Rocken et al., 1992): if troposphere parameters were estimated in an L3 solution the elevation-dependence of the phase center was mis-interpreted by the parameter estimation program as tropospheric refraction creating the large bias in height.

Comparable to the effect of relative and absolute troposphere biases (Beutler et al., 1988) there are two major impacts of the elevation-dependent PCV on geodetic GPS results:

- (i) If different antenna types with different elevation-dependences of the phase center location are mixed, mainly the relative station height is affected. As pointed out above this bias may reach values up to 10 cm — *independent* of the baseline length.
- (ii) If only antennas of the same type are used, the main effect is a scale factor in the network of up to about 0.015 ppm due to the fact that for long distances the antennas “see” the same satellite under different elevation angles; an error pattern similar to a incorrect mapping function in the troposphere delay model is the result.

It is clear that azimuth-dependent variations may exist, too, which would cause biases in the horizontal position. In addition, there might be considerable differences between antenna units of the same type. VLBI, pointing its antennas towards the celestial radio sources, does not suffer from this type of PCV.

For the IGS as well as for many other GPS applications, these antenna phase center variations are one of the major error sources today. Already now the IGS global network is equipped with different receiver and antenna types. For the **densification** of the network the problem of receiver/antenna mixing will even become more pronounced. Any change of an antenna at one of the permanent IGS sites may cause an apparent jump in its coordinate time series and thus may affect the velocity estimates. *Unmodeled* PCV will also produce systematic biases in the determination of troposphere and ionosphere models, both IGS products to be established in the near future (see (Rocken et al., 1995) and (Schaer et al., 1995)). Even the change of the elevation cut-off angle (e.g. for the processing of AS data) may produce systematic changes in the GPS solutions.

To correct the biases caused by the PCV all GPS antennas used in a network have to be calibrated, i.e. elevation-dependent or elevation- and azimuth-dependent corrections have

to be determined for each antenna type or even each individual antenna. The two methods available to determine such corrections are described in more details below.

TWO INDEPENDENT ANTENNA CALIBRATION METHODS

Two independent methods are in use today to determine the PCV of geodetic GPS antennas: the anechoic chamber measurements and the determination of phase center corrections from processing GPS data. It is important to have both methods available to detect problems in either of the two approaches. For comparisons and a clear understanding it is important to be aware of the degrees of freedom inherent in the two calibrations techniques.

Degrees of Freedom **in** the Calibration Values

Elevation- and azimuth-dependent calibration values determined by both methods have some inherent degrees of freedom one should be aware of to fully understand what chamber measurements are referring to and what parameters may be estimated from the GPS data. An original set of phase center corrections consisting of a phase center offset vector \mathbf{r}_0 (usually the “mean” phase center location) and an azimuth/zenith-dependent function $\Delta\phi(\alpha, z)$ may be transformed in the following way into a new set \mathbf{r}'_0 and $\Delta\phi'(\alpha, z)$ that will give exactly the same results as the original set when applied in GPS data processing:

$$\mathbf{r}'_0 = \mathbf{r}_0 + \Delta\mathbf{r} \quad (1a)$$

$$\Delta\phi'(\alpha, z) = \Delta\phi(\alpha, z) - \Delta\mathbf{r} \cdot \mathbf{e} + \Delta\phi_0 \quad (1b)$$

where $\Delta\phi_0$ and the offset vector $\Delta\mathbf{r}$ may be chosen arbitrarily, and \mathbf{e} denotes the unit vector in the direction antenna – satellite defined by the zenith distance z and the azimuth α .

The constant $\Delta\phi_0$ is an arbitrary phase offset, constant for all directions, and $\Delta\mathbf{r}$ allows for an arbitrary location of the “mean” phase center in three dimensions (i.e. in vertical *and* horizontal direction).

As an example the elevation-dependent PCV transformed with $\Delta\mathbf{r} = (\mathbf{0}, \mathbf{0}, Ah)$ and $\Delta\phi_0 = -Ah$ for four different values of Ah are shown in Figure 1. All these values give identical results when introduced into the GPS data processing together with the corresponding phase center offsets Ah in height.

The constant $\Delta\phi_0$ is often uniquely defined by asking for

$$\Delta\phi(\alpha, 0) = 0 \quad (2)$$

and the vector \mathbf{r} may be defined as a “mean” phase center location over the zenith interval $[0, z_0]$ using e.g. the condition

$$\int_{\alpha=0}^{2\pi} \int_{z=0}^{z_0} \Delta\phi(\alpha, z) \sin z \, dz \, d\alpha = \min. \quad (3)$$

It is obvious that this “mean” phase center r_0 depends on the zenith angle cutoff z_0 and that the two components r_0 and $\Delta\phi(\alpha, z)$ of a calibration set have to be consistent with each other.

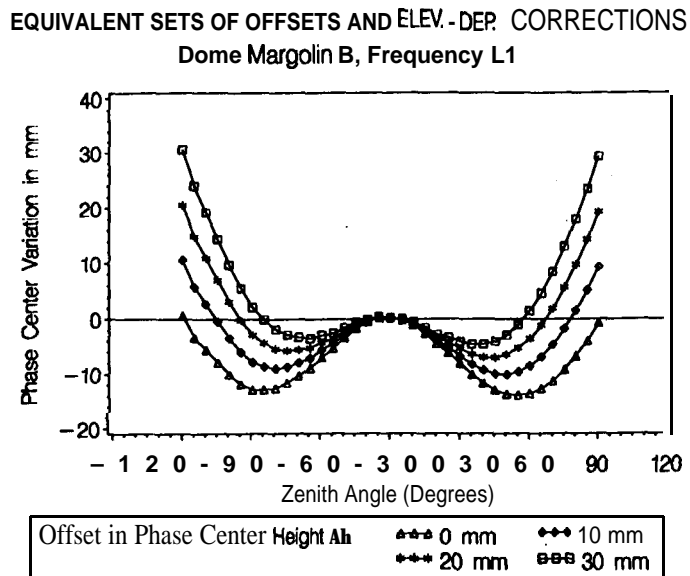


Figure 1. Elevation-Dependent PCV Transformed According to Eqns. (1a) and (1b) with $\Delta r = (0, 0, Ah)$ and $c = -Ah$

Because GPS is an interferometric technique we have the additional problem that from data collected on short baselines only the differences between the PCV of the two antennas may be estimated.

Anechoic Chamber Tests

The measurements are performed in an anechoic test chamber where one specific antenna is mounted on a positioner, that may rotate the antenna around two independent axes and shift it in three directions. The transmitting antenna is kept fixed while the receiving antenna (to be tested) is rotated through zenith angles from -90 to $+90$ degrees for various azimuth values. To rotate the test antenna as precisely as possible around the “mean” phase center for the actual measurements, the antenna is first shifted with respect to the center of rotation until the phase center variations with elevation are minimal and as symmetrical as possible for zenith angles corresponding to $-z$ and $+z$ degrees. Apart from the recording of the antenna phase values using a stripchart recorder, the signal amplitude and axial ratio pattern are common measurements in chamber tests. These recordings have to be performed for both GPS carrier frequencies. Finally the location of the center of rotation with respect to a physical point on the test antenna, e.g. the *antenna reference points (ARP)* as defined by the IGS, has to be determined. For more details on chamber measurements we refer to (Schupler et al., 1991), (Schupler et al., 1994), and (Wohlleben et al., 1988).

As an example Figure 2 shows the elevation-dependent PCV in L1 for some geodetic GPS antennas as measured and made available by Schupler (downloaded by anonymous ftp in May 1995).

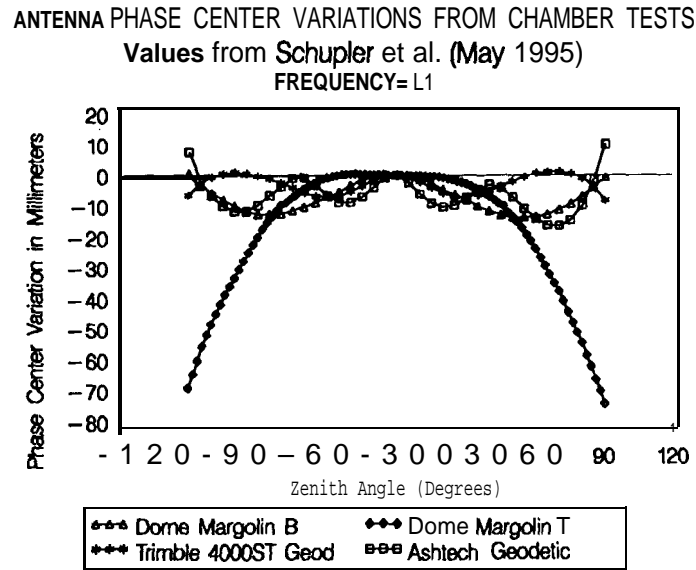


Figure 2. Elevation-Dependent PCV in 1,1 from Chamber Measurements

From Figure 2 we clearly see the various degrees of freedom as discussed in the previous section:

- (i) Only the change in the phase with elevation can be measured, i.e. an unknown (and irrelevant) phase offset remains undetermined (constant $\Delta\phi_0$ in eqn. (1 b)). In the case considered here the phase values were set to zero for zenith angle $z = 0$ according to eqn. (2).
- (ii) In principle the center of rotation for the antenna tests may be arbitrarily chosen corresponding to the vectors r_0 or r'_0 in eqns. (1a) and (1b). Obviously the phase pattern of most of the antennas in Figure 2 was minimized using a condition similar to that in eqn. (3). For the Dome Margolin T antenna, however, no such minimization was performed.

It is one of the advantages of chamber measurements that a single antenna may be calibrated. To collect the chamber measurements, however, a considerable effort is required as compared to the setup of a GPS calibration campaign.

Phase Center Estimation from GPS Data

The first phase center corrections obtained from GPS were simple vertical (and horizontal) offsets between different antennas determined on short baselines with known point coordinates (see e.g. (Gurtner et al., 1989), (Mireault et al., 1993), and many others). We mention in

particular the GPS group at UNAVCO which periodically performed receiver and antenna tests for receiver evaluations (Braun et al., 1994).

In 1994 a few groups started estimating elevation-dependent correction models from GPS data, among them (Mader et al., 1994), who determined elevation-dependent corrections from the GPS post-fit residuals and (Breuer et al., 1995) setting up the coefficients of low-degree polynomials as parameters.

We at AIUB modified the Bernese GPS Software (Rothacher et al., 1993) in order to be able to estimate the parameters of two different models for elevation- or elevation- and azimuth-dependent PCV:

- (i) Coefficients of piece-wise linear functions in elevation (and azimuth): polygonal approach.
- (ii) Coefficients of a series of spherical harmonic functions of maximum degree n_{\max} and maximum order $m_{\max} \leq n_{\max}$:

$$\Delta\phi(\alpha, z) = \sum_{n=0}^{n_{\max}} \sum_{m=0}^n \tilde{P}_{nm}(\cos z) \cdot (a_{nm} \cos m\alpha + b_{nm} \sin m\alpha) \quad (4)$$

where $\Delta\phi(\alpha, z)$ is the phase center correction (or range correction) in the direction with zenith angle z and azimuth α . \tilde{P}_{nm} are *normalized* associated Legendre polynomials of degree n and order m ; a_{nm} and b_{nm} are the unknown coefficients to be estimated. The normalization used is given in (Schaer et al., 1995), eqn. (6).

To prevent the normal equation system from becoming Singular a loose a priori constraint has to be put on each parameter in case (i) because of the arbitrary constant $\Delta\phi_0$ in eqn. (1b) whereas in case (ii) the zero-degree coefficient a_{00} cannot be estimated. The results from case (i) may be introduced more easily into other software packages (linear interpolation between tabular values) whereas the representation (ii) is physically more meaningful, in particular for the azimuth-dependent variations.

It is also clear from eqns. (1a) and (1 b) that the station heights have to be fixed on known ground truth values, if elevation-dependent corrections are estimated and that all three components of the station coordinates have to be fixed if elevation- and azimuth-dependent variations are determined. This requirement is not necessary if **the antennas were rotated during the test campaign. When estimating the PCV**, one and the same set of coefficients may be estimated from several antennas of the same type (grouping of antennas).

The advantage of the ‘‘GPS approach’’ compared to chamber tests is certainly the smaller effort needed to obtain calibrations for a large number of antennas in a short time period. A small network with known point coordinates within 1 mm (at least the heights of the points) has to be available, however. Unfortunately, as mentioned in the introduction, only the differences between the PCV of different antennas may be obtained with GPS and, therefore, the PCV from chamber measurements for at least one reference antenna have to be introduced as known.

ANTENNA CALIBRATION CAMPAIGNS

GPS data from three campaigns were used to estimate PCV and to check these estimates.

Thun 1994 Antenna Calibration Campaign

In this campaign taking place on a test range of the Swiss Federal Office of Topography in Thun, Switzerland, two sessions (days 248 and 249 of year 1994) of 24 hours each were measured with (for antenna names and antenna sketches see the files ANTENNA.GRA and RCVR.ANT.TAB at the IGS Central Bureau Information System described in (Gurtner et al., 1995)):

- 2 Ashtech Z-12 with GEODETIC L1/L2 P antennas
- 2 Leica SR299E with EXTERNAL antennas, with and without ground plane
- 2 Trimble 4000SSE with 4000ST L1/L2 GEOD antennas
- 2 Trimble 4000SSE with TR GEOD L1/L2 antennas, with and without groundplane
- 2 Turborogues with Dome Margolin T antennas

The 10 monuments of the test network in Thun are separated by about 10 m; the ground truth is known to within 1 mm. Between the sessions the antennas were exchanged.

The institutions involved were:

- Federal Office of Topography, Wabern, Switzerland (Organization; Trimble receivers)
- Institut Géographique National, Paris, France (Ashtech receivers)
- Institut für Angewandte Geodäsie, Wettzell, Germany (Operator)
- Technical University, Munich, Germany (Turborogue)
- Bavarian Academy of Sciences, Munich, Germany (Turborogue)

Observations from Graz

A few days of data from August 1994 and November 1994 were also available from Peter Pesec at the Graz Observatory, Austria, including Rogue, Turborogue and Trimble receivers on baselines of a few meters. This data was mainly included in this study to detect any significant biases between Dome Margolin B and T antennas.

Baseline Onsala-Zimmerwald from **IGS**

The long mixed baseline Onsala – Zimmerwald of about 1200 km with a Rogue (Dome Margolin B) and a Trimble 4000SSE (4000ST L1/L2 GEOD) receiver was processed for 46 days (DOY 070-115, 1995) to test the various PCV available from chamber tests and from the estimation from GPS data.

RESULTS

Antenna Offsets

Before starting to estimate any PCV the coordinates of the points were estimated to obtain the “mean” phase center offsets for the various antenna types involved in the campaign of Thun by comparing the results to the ground truth. An elevation cutoff angle of 20 degrees was used. The resulting phase center offsets are summarized in Table 1.

Day	Receiver	Antenna Type	No.	L1 Offset (mm)			L2 Offset (mm)		
				N	E	U	N	E	U
248	TRIMBLE TR	GEOD L1/L2 W/O	1	2.7	-4.6	15.1	4.5	-0.1	13.1
249	TRIMBLE TR	GEOD L1/L2 W/O	1	2.7	-4.7	15.1	5.4	0.5	14.6
248	TRIMBLE TR	GEOD L1/L2 W/O	2	2.8	-5.5	13.6	5.9	0.1	10.4
249	TRIMBLE TR	GEOD L1/L2 GP	2	2.7	-5.3	-0.6	3.8	0.1	-3.5
248	TRIMBLE	4000ST L1/L2 GEOD	1	0.0	0.2	1.3	0.3	0.1	1.7
249	TRIMBLE	4000ST L1/L2 GEOD	1	-0.1	0.1	0.9	-0.2	0.1	1.0
248	TRIMBLE	4000ST L1/L2 GEOD	2	0.0	-0.2	-1.3	-0.3	-0.1	-1.7
249	TRIMFILE	4000ST L1/L2 GEOD	2	0.1	-0.1	-0.9	0.2	-0.1	-1.0
248	ASHTECH	GEODETIC L1/L2 P	1	-2.2	-2.3	2.2	-1.1	-3.6	5.0
249	ASHTECH	GEODETIC L1/L2 P	1	-1.7	-1.4	5.0	-0.9	-3.5	7.5
248	ASHTECH	GEODETIC L1/L2 P	2	4.8	-5.7	4.8	7.9	0.1	7.6
249	ASHTECH	GEODETIC L1/L2 P	2	4.5	-6.8	0.2	7.2	-0.7	3.7
248	SR299E	EXTERNAL WITHOUT	1	2.2	-2.7	20.5	3.0	0.6	9.9
249	SR299E	EXTERNAL WITH	1	4.7	-4.2	-2.5	6.8	3.2	-5.1
248	SR299E	EXTERNAL WITHOUT	2	1.6	-2.7	22.4	4.9	1.2	9.9
249	SR299E	EXTERNAL WITH	2	5.0	-4.7	-0.6	6.3	2.7	-1.9
249	TURBOR.	DORNE MARGOLIN T		0.0	-2.7	-14.7	3.6	-2.0	-8.4

Table 1. Phase Center Offset Differences with Respect to the IGS Values. Mean Offset of the 4000ST L1/L2 GEOD Antennas was set to the IGS Value. Antenna Types Containing “W/O” and “WITHOUT” Were Used *Without* Groundplane (GP)

All phase center offsets in Table 1 are corrections to the IGS values available at the IGS Central Bureau Information System (CBIS, see (Gurtner et al., 1995), file RCVR.ANT. TAB) and were computed fixing the *mean* offset of the two 4000ST L1/L2 GEOD antennas to the IGS value. Table 1 shows that the horizontal offsets are of the order of a few millimeters, in some cases even between two antennas of the same type. In general the vertical offsets are not larger, but the use of an antenna *without groundplane* systematically changes the vertical offset by about 1 to 2 cm. This effect will even be more pronounced when using a lower elevation cut-off angle. The Dome Margolin T antenna has an offset of about 1.5 cm when compared to most other antennas.

Elevation-Dependent Corrections from GPS

Both estimation models, the piece-wise linear and the spherical harmonics functions, were tested and revealed no significant differences. Therefore only the spherical harmonics results will be presented here. A maximum degree of $n_{max} = 10$ and an order of $m_{max} = 0$ (elevation-dependence only) were used (see eqn. (4)). All the PCV were computed relative to the Trimble 4000ST L1/L2 GEOD antenna no. 1. The IGS offset values were introduced as “mean” phase center offsets for all antenna types.

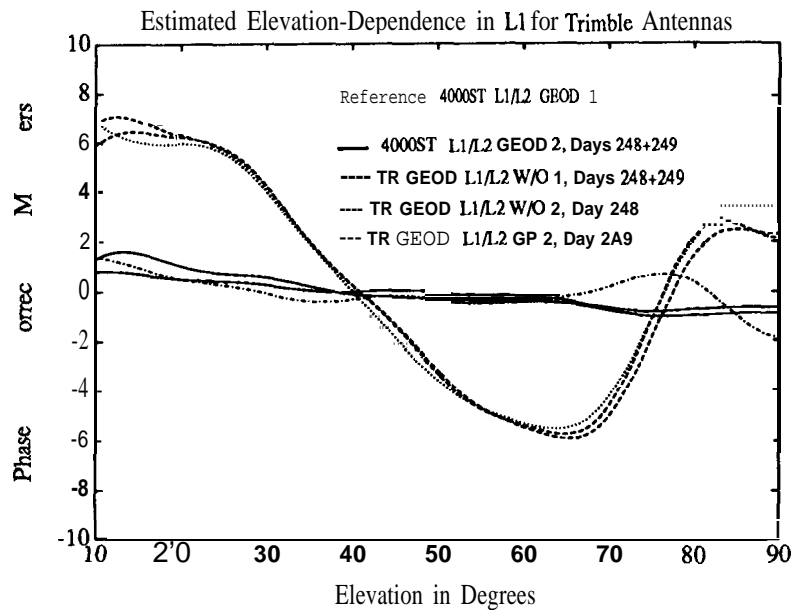


Figure 3. Trimble Antennas: Spherical Harmonics Development of Degree 10 Estimated from GPS Data

Figure 3 shows the results for the two Trimble antenna types for both 24-hour sessions (days 248 and 249, see also Table 1) in Thun:

- The estimates for the same antenna are very similar for both sessions
- The estimates for different antennas of the same type are also very consistent.
- The compact Trimble antenna TR GEOD L1/L2 W/O GP (without groundplane) exhibits a very different behaviour with elevation. If the groundplane is attached to this antenna, however, it behaves almost like a 4000ST L1/L2 GEOD antenna. The groundplane changes the phase pattern of the antenna significantly. The same effect shows up for the SR299 EXTERNAL antenna (see Table 1).

In Figure 4 the PCV for the Ashtech antennas are plotted. Again the antenna pattern is repeatable within 1 to 2 mm, except for the low elevations (< 15 degrees), where multipath is most probably the critical influence.

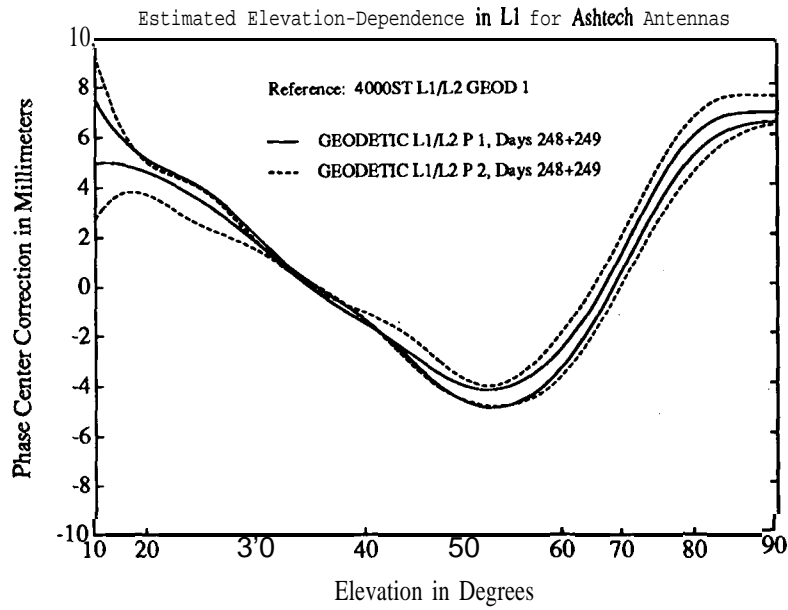


Figure 4. Ashtech Antennas: Spherical Harmonics Development of Degree 10 Estimated from GPS Data

The reason for the large bias of about 10 cm in the height for a mixed Rogue - Trimble baseline when using the ionosphere-free linear combination L3 (and estimating troposphere delays) becomes apparent in Figure 5.

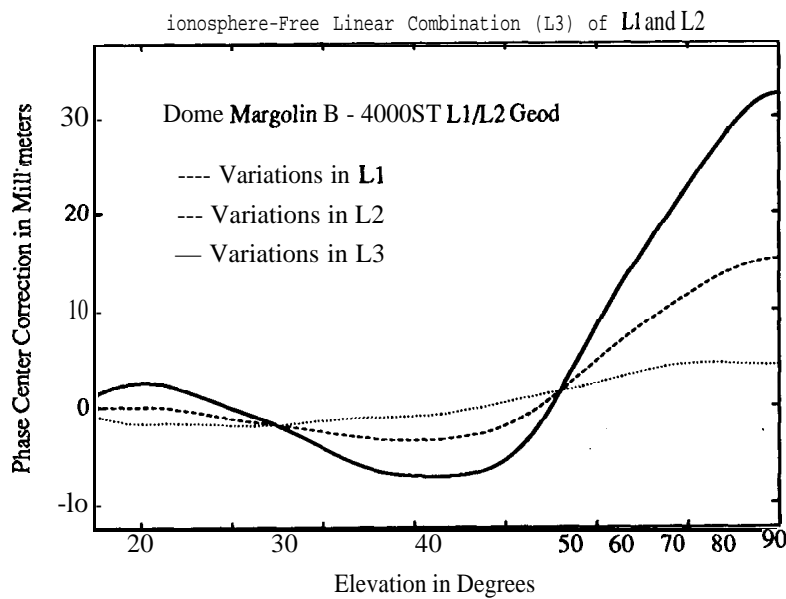


Figure 5. Magnification Effect of the Phase Center Variations in the Ionosphere-Free Linear Combination. Spherical Harmonics Development of Degree 10 for the Dome Margolin B Estimated from GPS Data

The variations in L3 are much larger than those in L1 and L2. The results in Figure 5 were computed using the Graz GPS data.

Azimuth-Dependent Correction from GPS

As an example for the estimation of azimuth-dependent PCV Figures 6 and 7 depict the differences between the phase patterns of the Dome Margolin B and the Trimble 4000ST L1/L2 GEOD antenna for the L1 and the L2 frequency. The Graz data set was used for the estimation. The two areas inside the dashed lines enclose the region — we call it the “northern hole” — where no GPS satellites are ever visible and therefore no corrections can be estimated. This hole in the data might be removed by rotating the antennas systematically (by e.g. 180 degrees for a second session).

The consistency of the estimated azimuth-dependent variations from day to day and between antennas of the same type is similar to the consistency of the elevation-dependent variations given in the last section.

The PCV of the Dome Margolin B (Rogue) and Dome Margolin T (Turborogue) antennas are almost identical (within about 2 mm over all the azimuth and elevation angles down to 15 degrees).

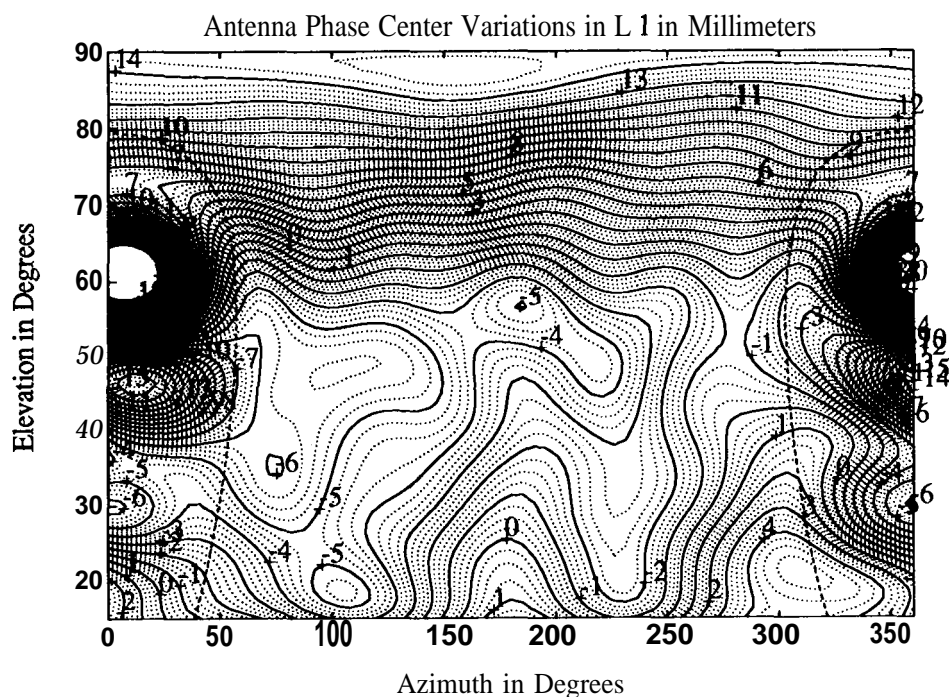


Figure 6. Spherical Harmonics Development of Degree 10 and Order 5 Estimated for the Difference Between Dome Margolin B and 4000ST L1/L2 GEOD Antenna

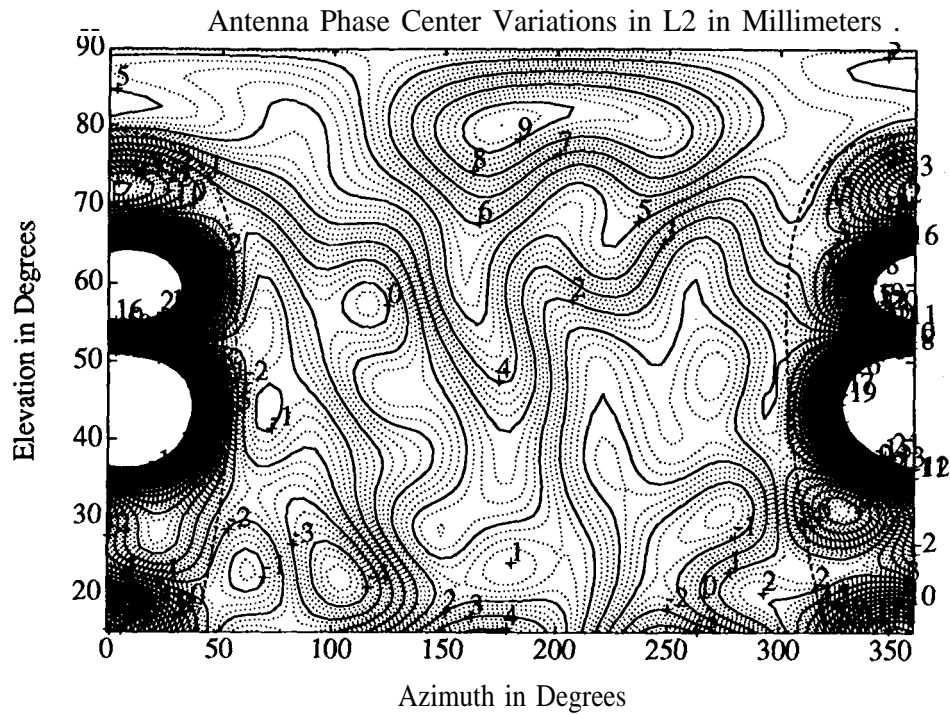


Figure 7. Spherical Harmonics Development of Degree 10 and Order 5 Estimated for the Difference Between Dome Margolin I? and 4000ST L1/L2 GEOD Antenna

Multipath effects are clearly visible in the azimuth-dependent phase corrections for elevation angles below 20 degrees. They limit the applicability of corrections determined at one location to another location with a different multipath environment. This an important issue to be studied in future.

Comparison with Chamber Test Results

The elevation-dependent variations established with GPS were compared to the chamber test results in the case of the Dome Margolin B and 4000ST L1/L2 GEOD antenna (i.e. only the difference can be compared). The good agreement between the two independent methods may be seen from Figures 8 and 9 for L1 and L2 respectively. The plots also indicate that there is *no* significant difference between the Dome Margolin B' and T antennas, The comparison has to be interpreted with care, because it only shows that the *difference* between the antenna types are reasonably consistent and that obviously the difference of the adopted "mean" phase centers was about the same. The consistency of offsets and elevation-dependent variations requested in eqns. (1a) and (1b) could not be safely established for the chamber measurements and there might still be problems in the absolute calibrations (see next section).

No attempt was made so far to compare the azimuth-dependence of the phase patterns.

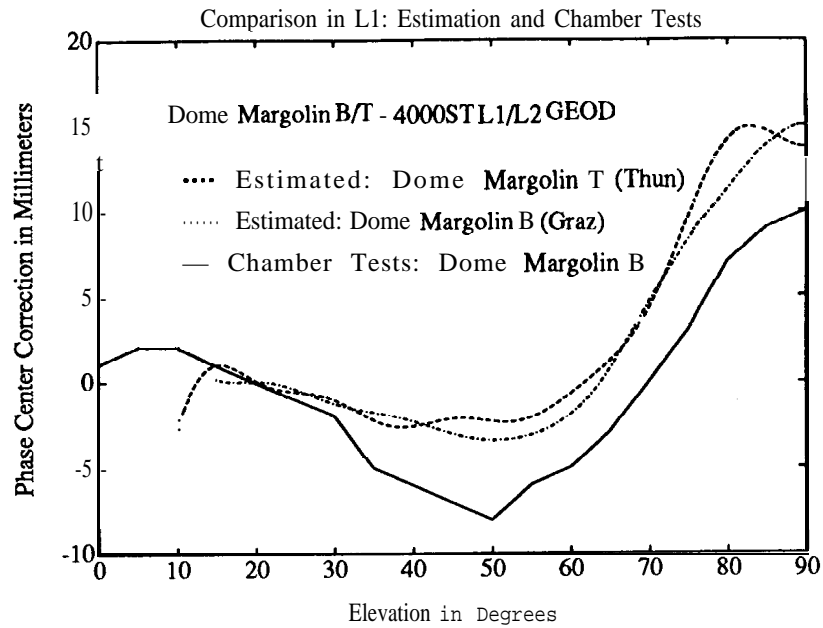


Figure 8. Comparison Between Chamber Measurements from Schupler (May 1995) and Values Estimated from GPS Data

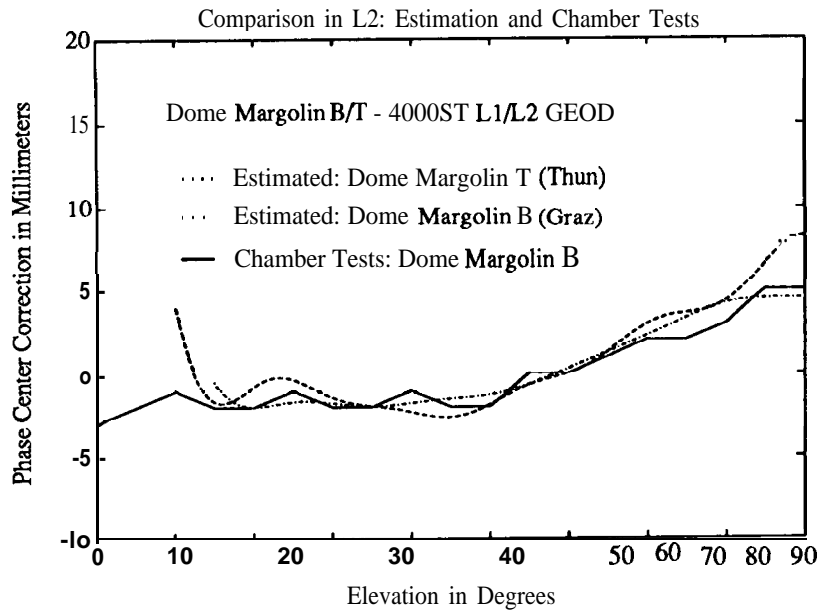


Figure 9. Comparison Between Chamber Measurements from Schupler (May 1995) and Values Estimated from GPS Data

Checking of Phase Center Corrections on a Long Baseline

The long mixed baseline Onsala – Zimmerwald (baseline length 1200 km) was used to check the relative and in particular the *absolute* values of the antenna calibrations. Only chamber measurements can provide the *absolute* phase center corrections. The baseline components and the baseline length were compared to ITRF93 values (from SLR and GPS, see (Boucher et al., 1994)) for 46 days using different sets of antenna phase center corrections. The results of the daily ionosphere-free (L3) solutions with troposphere estimation are given in Figure 10.

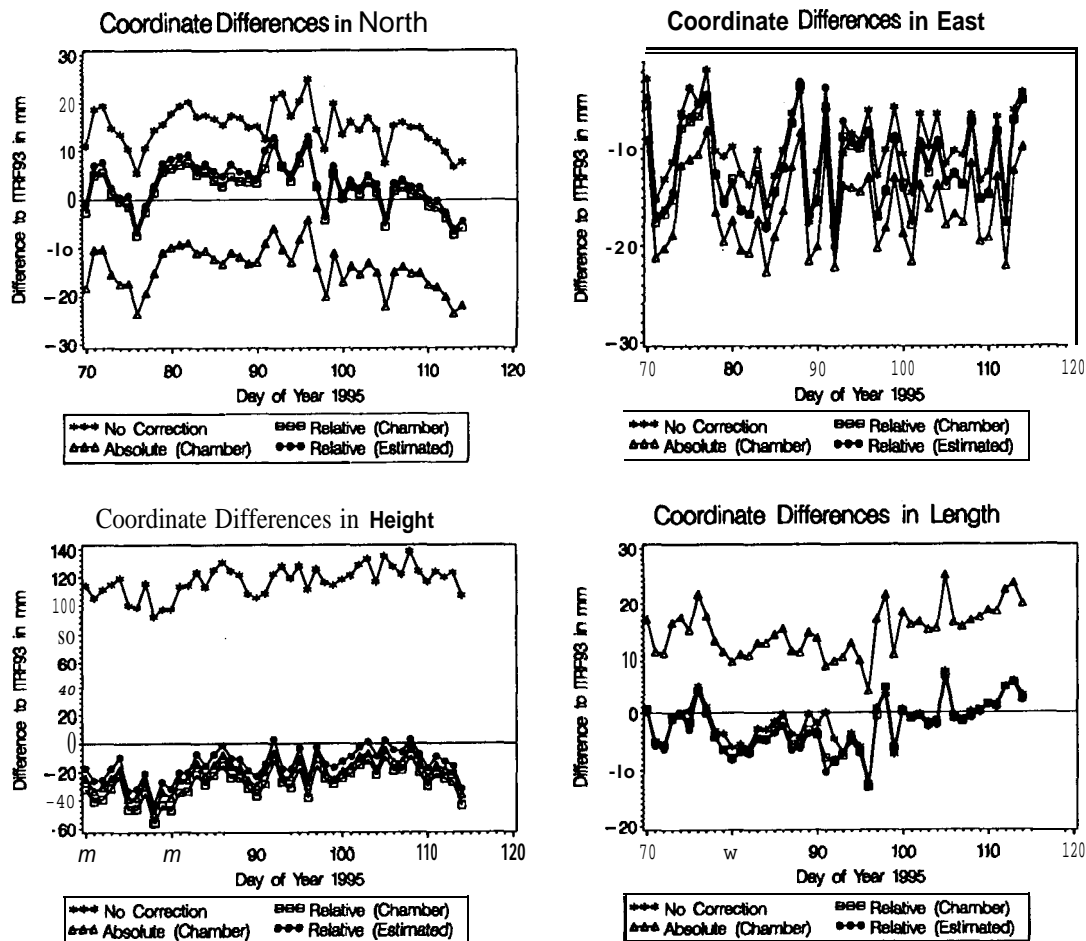


Figure 10. Results for the Baseline Onsala - Zimmerwald (Dome Margolin B - 4000ST L1/L2GEOD) Using Different Sets of Elevation-Dependent Phase Center Corrections Compared to ITRF93. “Relative” Corrections: Only Difference Between Antennas Introduced. Chamber Measurements from Schupler (May 1995).

The following tests were performed: (a) no corrections applied, (b) chamber measurements from Schupler for both antenna types (absolute correction) applied, (c) the difference

between antenna types from chamber measurements, and (d) our differential estimates assuming the *absolute* PCV for the Dome Margolin B antenna to be zero. The largest effect, the bias of about 11 cm in the height, clearly shows up if *no* corrections are applied. If chamber values are introduced for both antennas, there is a significant bias of about **1.5 cm (or 0.012 ppm)** in the baseline length not present for the other phase center corrections showing that there are still problems with the *absolute* calibration. A bias is also present in the north component for “no correction” and “absolute correction”. Although the ITRF93 coordinates may also be in error (in particular because the CODE GPS solution using model (c) was part of the ITRF combination), the scaling of the baseline for absolute corrections is clearly too large to be attributed to the ITRF93. The corrections estimated from GPS look very promising, although the underlying assumption that the Dome Margolin B antenna shows no significant elevation-dependence is questionable.

CONCLUSIONS AND OUTLOOK

From the results shown in this paper it is evident that the estimation of phase center corrections in elevation (and azimuth) from GPS data give important contributions to the problem of phase center variations and the combination of different antenna types. The determined corrections for antennas of the same type and for different days are very consistent.

Multipath is certainly the most critical error source for the estimation of PCV from GPS data, especially for the azimuth-dependence. This problem as well as the problem of the “northern hole” might be reduced by rotating the antenna between the sessions. An experiment with such rotations has been performed by the Institut für Angewandte Geodäsie in Wettzell. We will gain more insight into the multipath problems from analysing these data.

Comparisons of our estimates with chamber test results look promising. The problem of the *absolute* calibration is not solved yet, however. We hope that with the cooperation of exponents using the two techniques — anechoic chamber measurements and GPS — the remaining problems will be solved and a consistent set of antenna offsets and elevation-dependent variations will result which is urgently needed by the GPS community. It seems unavoidable that new GPS calibration campaigns — making full use of the experiences gained in tests reported above — have to be performed in the near future.

REFERENCES

- Beutler, G., I. Bauersima, W. Gurtner, M. Rothacher, T. Schildknecht, 1988, Atmospheric Refraction and Other Important Biases in GPS Carrier Phase Observations.. *Monograph 12*, School of Surveying, University of New South Wales, Australia.
- Beutler, G., I. 1. Mueller, R. Neilan, 1994, The International GPS Service for Geodynamics (IGS): Development and Start of Official Service on 1 January 1994. *Bulletin Géodésique*, Vol. 68, No. 1, pp. 43-51.
- Boucher, C., Z. Altamimi, L. Duhem, 1994, Results and Analysis of the ITRF93. *IERS Technical Note 18*, Observatoire de Paris, October 1994.

- Braun, J., C. Rocken, J. Johnson, 1994, Consistency of High Precision GPS Antennas, *EOS Transactions*, AGU 1994 Fall Meeting, Vol. 75, No. 44, p. 173.
- Breuer, B., J. Campbell, B. Görres, J. Hawig, R. Wohlleben, 1995, Kalibrierung von GPS-Antennen für hochgenaue geodätische Anwendungen, Paper accepted for publication in *Zeitschrift für satellitengestützte Positionierung, Navigation und Kommunikation*, April 1995.
- Gurtner, W., G. Beutler, M. Rothacher, 1989, Combination of GPS Observations Made with Different Receiver Types, *Proceedings of the 5th International Geodetic Symposium on Satellite Positioning*, Las Cruces, New Mexico, March 13–17, Vol. 1, pp. 362-374.
- Gurtner, W., R. Liu, 1995, The Central Bureau Information System, *International GPS Service for Geodynamics, Annual Report 1994*, ed. J. Z. Zumberge, R. Liu, and R. Neilan, JPL, California, in preparation.
- Mader, G.L., J.R. MacKay, 1994, *Calibration of GPS Antennas*, draft publication.
- Mireault, Y., F. Lahaye, 1993, Evaluation of Inter-receiver Biases Between Ashtech, Leica, Rogue, and Trimble GPS Receivers, *EOS Transactions*, AGU 1993 Fall Meeting, Vol. 74, No. 43, p. 197.
- Rocken, C., 1992, *GPS Antenna Mixing Problems*, UNAVCO Memo, November 12, 1992, Boulder, Colorado.
- Rocken, C., F.S. Solheim, R.H. Ware, M. Exner, D. Martin, M. Rothacher, 1995, Application of IGS Data to GPS Sensing of the Atmosphere for Weather and Climate Research, *Proceedings of the IGS Workshop*, Potsdam, Germany, May 15-17, 1995, this volume.
- Rothacher, M., G. Beutler, W. Gurtner, E. Brockmann, L. Mervart, 1993, *The Bernese GPS Software Version 3.4: Documentation*, Astronomical Institute, University of Berne, Switzerland.
- Schaer, S., G. Beutler, L. Mervart, M. Rothacher, U. Wild, 1995, Global and Regional Ionosphere Models Using the GPS Double Difference Phase Observable, *Proceedings of the IGS Workshop*, Potsdam, Germany, May 15-17, 1995, this volume.
- Schupler, B. R., T.A. Clark, 1991, How different Antennas Affect the GPS-Observable, *GPS-World*, Nov./Dec. 1991, pp. 32-36.
- Schupler, B.R., R.L. Allshouse, T.A. Clark, 1994, Signal Characteristics of GPS User Antennas, Preprint accepted for publication in *Navigation* in late 1994.
- Seeger, H., W. Augath, R. Bordley, C. Boucher, B. Engen, W. Gurtner, 1992, Status-Report on the EUREF-GPS-Campaign 1989 to the IAG EUREF-Subcommission, *Veröffentlichungen der Bayerischen Kommission für die Internationale Erdmessung*, Astronomisch-Geodatische Arbeiten, München, Heft Nr. 52, pp. 26-34.
- Wohlleben, R., H. Mattes, O. Lochner, 1988, The “dynamics” of the MPIfR anechoic chamber between 300 and 2 mm wavelength, *Proceedings of the 11th ESTEC Antenna Workshop on Antenna Measurements*, Onsala, Sweden, pp. 225-235.

AUSTRALIAN, ANTARCTICA, PACIFIC, AND INDIAN PLATE VELOCITIES USING THE IGS NETWORK

Kristine M. Larson

Department of Aerospace Engineering Sciences, University of Colorado
Boulder, CO 80309 USA

Jeffrey T. Freymueller

Geophysics Institute, University of Alaska
Fairbanks, AK 99775 USA

ABSTRACT

GPS measurements spanning four years have been used to determine velocities for 10 sites on the Australian, Pacific, Antarctica, and Indian plates. Except for sites on the Pacific plate, velocities are in good agreement with the NNR-NUVEL1 -A model (DeMets et al., 1994; Argus and Gordon, 1991). The Pacific plate velocities are slightly faster than model predictions, which agrees with previous geodetic analysis (Robbins et al., 1993). Wellington, New Zealand, located in the Australian-Pacific plate boundary zone, moves with a velocity midway between the predicted velocities of the two plates. Sites in southern India and Nepal both move at predicted Indian plate velocities. The GPS site velocities have also been used to derive Euler vectors for the relative motions of the four plates. Relative Euler vectors for Australia-Antarctica and Australia-India agree within one standard deviation with the NUVEL- 1 A predictions,

INTRODUCTION

Space geodetic data collected over the last two decades have made it possible to measure plate motions over the time scale of years rather than millions of years (e.g. Robbins et al., 1993). Prior to the development of the Global Positioning System (GPS), the cost of space geodetic methods restricted their use to a small number of sites. On a global scale the existing VLBI and SLR data were generally too sparse to allow a complete treatment. Most of the existing work in this regard has been limited to a comparison of site velocities with NUVEL1 predictions. The expansion of the IGS network in the early 1990's provides an ideal data set to make a more complete study of global plate motions. In this paper we will use the IGS network to estimate the motions of the Pacific, Australia, Antarctica, and India plates.

MEASUREMENTS AND ANALYSIS

The sites we will discuss in this paper are listed in Table 1. There are four sites (Yaragadee, Hobart, Canberra, and Townsville) on the stable Australian plate and two sites (Kokee Park and Pamatai) on the Pacific plate. All these sites have participated in the IGS

Table 1. Data

site	start	stop	Epochs
Australia			
Hobart	Mar. 1993	Mar, 1995	69
Canberra	Jan. 1991	Mar. 1995	140
Yaragadee	Jan. 1991	Mar. 1995	144
Townsville	Jan. 1991	Nov. 1992	51
Wellington	Jan. 1991	Feb. 1995	60
Pacific			
Kokee Park	Jan. 1991	Mar. 1995	125
Pamatai	Feb. 1992	Mar. 1995	-74
Antarctica			
McMurdo	Jan. 1991	Mar. 1995	114
India			
Bangalore	Jan. 1991	Mar, 1995	15
Kathmandu	Jan. 1991	Apr. 1994	7

network. We also have one site, Wellington, New Zealand, which is located in the Australia-Pacific plate boundary zone. On the Indian plate, we have a site in southern India (**Bangalore**) and a site in Kathmandu, Nepal. Of these 10 sites, 8 were first observed during the GIG '91 experiment conducted in January-February 1991 (**Heflin et al., 1992**). We have subsequent y used data from these sites, when available, approximate y once per week for the period from February 1992 through March 1995. An analysis of a subset of **these** data through 1993 were previous] y presented by Larson and **Frey Mueller (1995)**. The sites on the Indian plate were primarily measured as part of regional campaigns. **Bangalore** recently became an IGS site, and multiple epochs are available from 1994 and 1995. The number of observations at each site ranges from a high of 144 for Yaragadee to 7 at Kathmandu. The temporal distribution of this study can be seen in the time evolution of coordinates for **Yaragadee** (Figure 1). In addition to the sites we are using to study the Australia-Antarctica-Pacific-India plate motions, we also used a large number of IGS network sites for precise orbit determination and reference frame definition. Figure 2 shows the location of the 30 sites we used over the period 1991-1995. The GPS constellation grew from 15 satellites in 1991 to its completed status at the present time. The precision of the individual measurements in Figure 1 improve with time, which reflects both the expansion of the GPS constellation and the IGS network.

The GPS data were analyzed with the **Gipsy 2.0** software developed by the Jet Propulsion Laboratory of the California Institute of Technology. Each position .estimate is based on 24 hours of precise pseudorange (when available) and phase data decimated to 6 minute points. We generally followed the strategy described by **Heflin et al. (1992)**. The coordinates of 6 globally distributed sites were constrained to agree with **VLBI/SLR** coordinates with an *a priori* uncertainty of 10 meters, while the remaining sites were unconstrained. These loose constraints are sufficient to avoid singularities in the GPS solutions, but are not sufficient to specify the reference frame. We used standard estimation

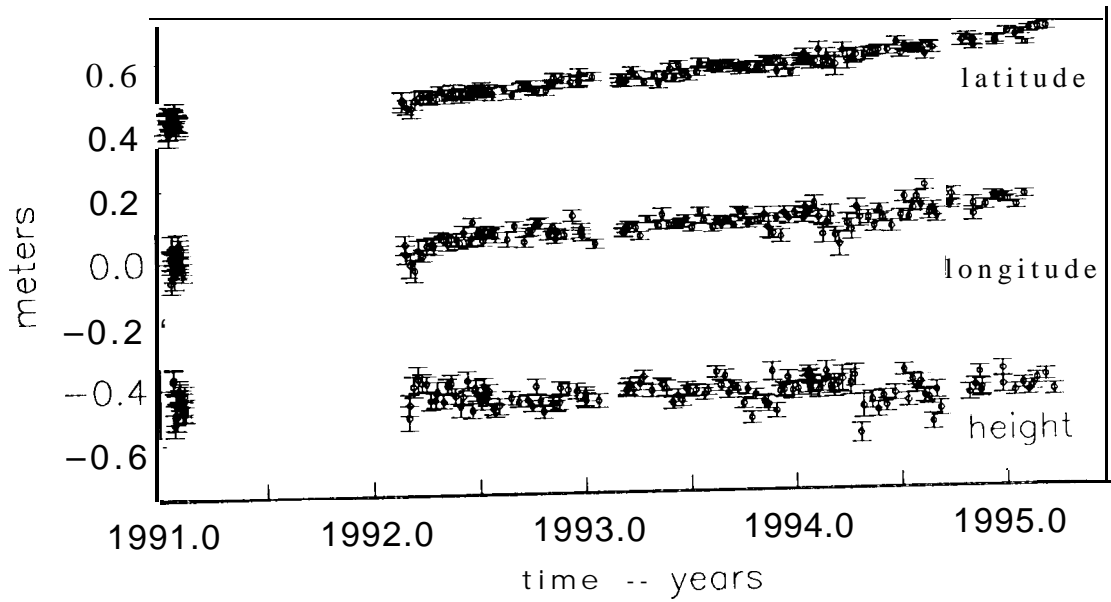


Fig. 1. Time series for **Yaragadee**, Australia. Error bars are one standard deviation. The weighted RMS about the best-fit line is 12, 21, and 32 mm for latitude, longitude, and height. The time series begins during GIG '91 (January 1991), restarts in February 1992, and continues until March 1995.

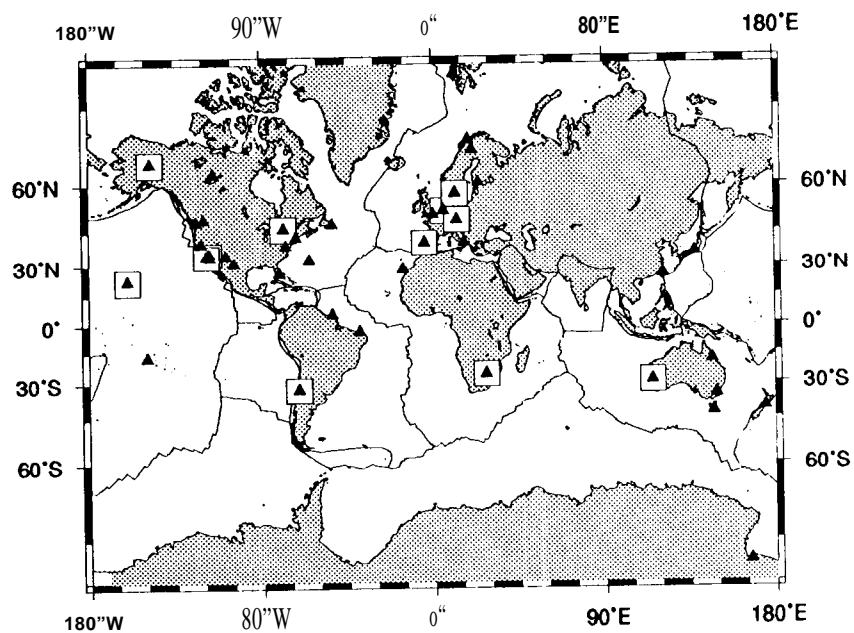


Fig. 2. Triangles represent IGS network sites used in this study. Open squares represent stations used to define the reference frame.

techniques for satellite state vectors, phase biases, tropospheric delays, and clocks. Antenna phase center corrections from Schupler and Clark (1991) were also applied.

There is a reference frame ambiguity in each GPS solution because both the station coordinates and satellite orbits were estimated with very loose constraints. We apply *a posteriori* reference frame constraints by translating, rotating and scaling the station coordinates from each GPS solution to agree on average with the ITRF92 reference frame (Boucher et al., 1993). The reader is directed to Blewitt et al. (1992) for details of the transformation. The fit is weighted by the formal errors of the GPS solution, scaled by 2.5, and by the formal errors for the ITRF92 station coordinates. The scale factor was chosen to reduce the chi square per degrees of freedom to 1.

We selected a subset of 12 sites from the ITRF92 model as reference sites to define this transformation. The choice of reference sites was dictated by the quality of each site's position and velocity, and by the geometry of the reference network. We sought reference sites which were observed consistently throughout 1991-1995 so that our realization of the reference frame would be consistent over time. The reference sites we have used are highlighted in Figure 2. This method of specifying the reference frame does not constrain the position or velocity of any one position; instead it constrains the weighted average of all the reference sites.

GEODETIC RESULTS

Position estimates and covariances were then used to determine Cartesian station velocities. We assumed linear motion with time, estimating both horizontal and vertical site velocities. Table 2 tabulates the results of this analysis, Figure 3 shows the horizontal velocities at the Australian-Pacific-Antarctic sites, along with the NUVEL1-A absolute plate motion predictions, hereafter referred to as NNR-A (Argus and Gordon, 1991). The velocities of the sites on the Australian and Antarctica plates are in excellent agreement with the

Table 2. Station Velocities and Standard Deviations - mm/yr

Station	North	GPS		NNR-A		
		East	u p	North	East	u p
Bangalore	35.4*4.1	35.7*5.8	7.1*12.2	41.4	40.1	0.0
Canberra	54.6±1.0	19.6*1.5	2.7±2.6	53.7	17.7	0.0
Hobart	53.1*1.9	17.9±3.8	15.4±8.0	54.4	12.8	0.0
Kathmandu	39.2*3.5	37.7±6.5	9.2±13.4	42.3	36.7	0.0
Kokee Park	36.6±1.0	-61.7*2.7	-0.8±3.0	32.3	-58.3	0.0
McMurdo	-13.1*2.5	9.4±2.9	-10.0*6.8	-11.7	7.5	0.0
Pamatai	34.3*1.6	-76.8±5.0	-3.4*7.5	31.5	-62.9	0.0
Townsville	56.7±2.0	30.9*3.9	19.3*8.5	54.7	30.0	0.0
Wellington	34.1*1.2	-15.1±2.0	13.9*3.6	37.1	-0.6	0.0
Yaragadce	58.8*1.1	36.2*1.9	5.6*2.9	59.1	39.0	0.0

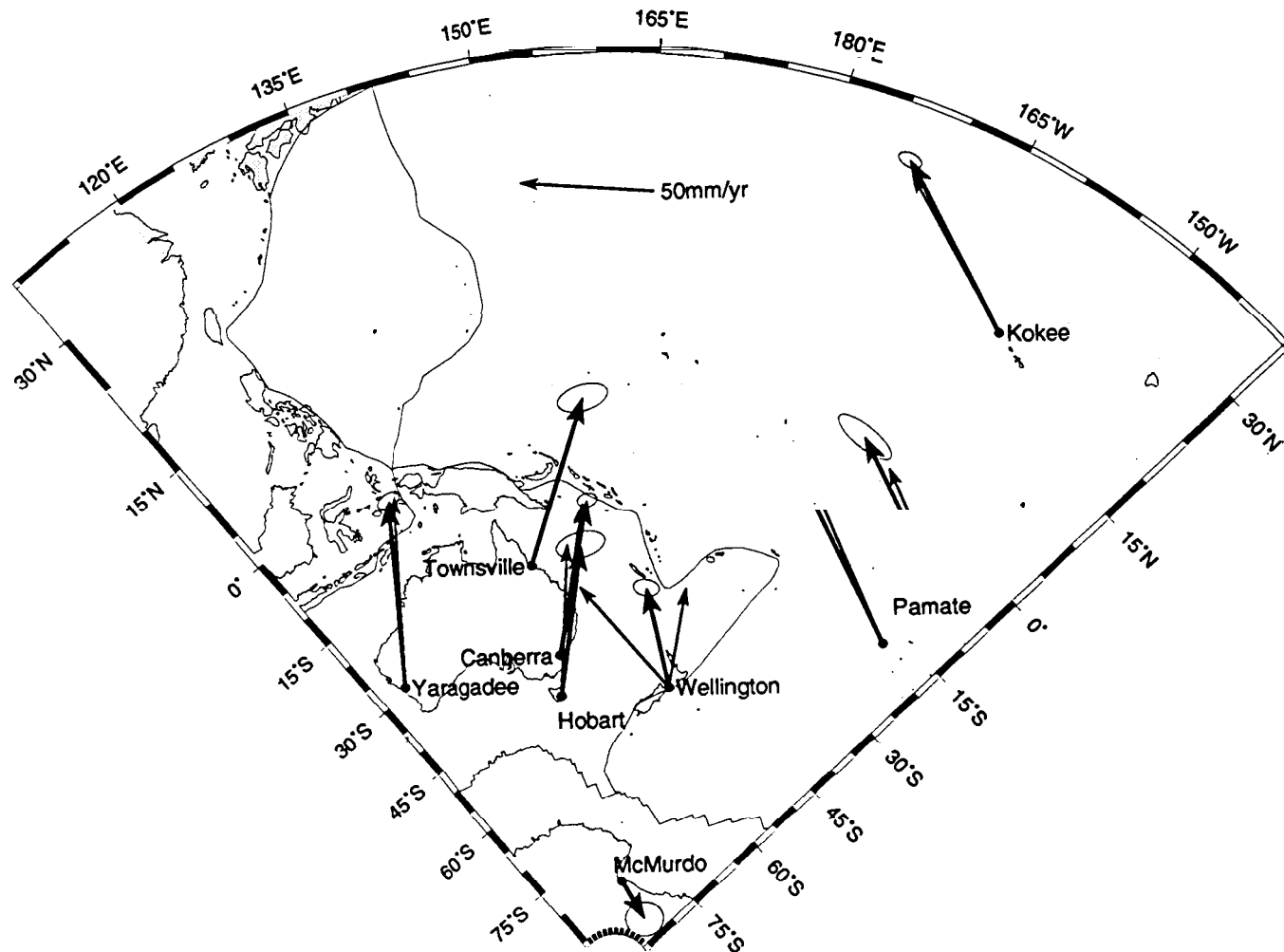


Fig. 3. Velocities for sites on the Antarctic, Pacific, and Australian plates, with 95% confidence ellipses. NNR-NUVEL1-A predictions are thin arrows. Predictions for both the Australian and Pacific plates are shown for Wellington.

predictions of the NNR-A model. Clearly Wellington does not agree well with the Australian plate prediction. Instead, it exhibits motion which is between the two plate predictions.

The GPS rate for Pamatai, Polynesia is 86 ± 5 mm/yr. Robbins et al. (1993) report 87 ± 3 mm/yr for another Polynesian site (Huahine) based on SLR data. The GPS and SLR rates agree far better with each other than with plate model predictions: NNR (73.5 mm/yr) or NNR-A (69.7 mm/yr). The discrepancy could be caused by an inconsistency in reference frame between the geodetic velocities and NUVEL1, or it could result from a real difference in the motion of the Pacific plate. In order to determine which is the cause, we will need more data from additional sites on the Pacific plate. The velocity of Kokee Park also disagrees with the NNR-A prediction, although the agreement is slightly better with the ITRF92 velocity for Kokee Park (33.5 mm/yr North, -61.5 mm/yr East).

Velocities for the Indian plate are shown in Figure 4. The GPS velocity estimates for both Bangalore and Kathmandu agree with NNR-A predictions to better than two standard deviations. The result for Kathmandu is particularly interesting. Given that Kathmandu is well within the Himalayas convergence zone, one would expect its velocity to reflect that compression. Kathmandu's velocity has important implications for the spatial distribution of strain across this plate boundary zone.

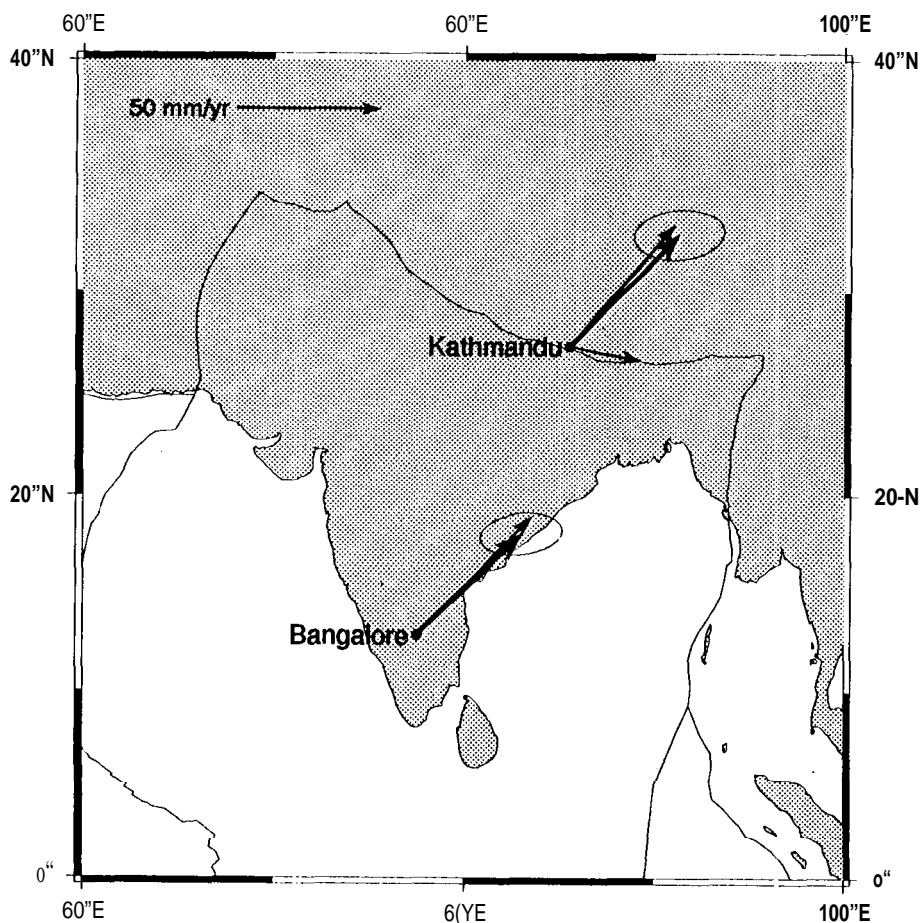


Fig. 4. Geodetic velocities for Bangalore, India and Kathmandu, Nepal, with 95% confidence ellipses. Also shown are the NUVEL1-A predictions. For Kathmandu, both the Eurasian and Indian predictions are shown.

PLATE KINEMATIC MODELS

The velocity of any geodetic site on any plate can be written as $\mathbf{v} = \boldsymbol{\omega} \times \mathbf{r}$ where $\boldsymbol{\omega}$ is the Euler vector of the plate, and \mathbf{r} is the position of the site. The plate tectonic model assumes that station velocity is horizontal ($\mathbf{v} \cdot \mathbf{r} = 0$) because $(\boldsymbol{\omega} \times \mathbf{r}) \cdot \mathbf{r} = 0$ for all \mathbf{r} and $\boldsymbol{\omega}$. The vertical component of the site velocity thus contributes nothing to the estimation of the Euler vector, so there are in reality only two data per station, and three parameters per Euler vector. To be completely correct, we would need to project our three-dimensional velocities into the local horizontal plane (and use two data per site), or estimate a vertical velocity at each site in addition to the plate velocity. In either case, a single site is not sufficient to uniquely determine the Euler vector of the plate it lies on. The relative Euler vector for a plate pair is simply the difference of the two Euler vectors.

We used the estimated site velocities and their covariances to simultaneously estimate Euler vectors for the Australia, Antarctica, Pacific, and India plates. Of these plates, only the Antarctica Euler vector is not uniquely determined by the geodetic data. Since there is **only** one site on the Antarctica plate, we are required to **apply** an **a priori** constraint to avoid a singularity in inverting the system. Because McMurdo is near the spin axis, the z component of the Antarctica Euler vector is poorly determined by the data. Thus, we have constrained the z component of the Antarctica Euler vector to its NNR-A value with an **a priori** uncertainty of 0.05 degrees/million year. Results for this inversion are summarized in Table 3. Given that we don't have good agreement for the Pacific plate sites with NNR-A, it is not surprising that the Euler vector for the Australian-Pacific plate pair does not agree well with NUVEL1 -A. The Australia-Antarctica and Australia-India Euler vectors agree with NUVEL1-A predictions to better than one standard deviation.

We have also calculated the Euler vector for Australia, assuming that **Bangalore** and **Kathmandu** are located on the Australian plate. The **GPS** velocities can be fit to better than one standard deviation when you assume they are located on the Indian plate, whereas the fit degrades to three standard deviations when you assume the Australian plate.

Table 3. Relative Euler Vectors and Standard Deviations
degrees/million years

	X	Y	Z
Australia-Antarctica			
GPS	0.498±0.030	0.408±0.024	0.141*0.052
NUVEL-1A	0.496*0.007	0.391*0.010	0.148*0.008
Australia-Pacific			
GPS	0.441*0.054	-0.037±0.026	1.010*0.028
NUVEL-1A	0.536±0.014	0.016*0.014	0.931*0.014
Australia-India			
GPS	0.091±0.036	0.265±0.142	-0.048*0.066
NUVEL-1A	0.067±0.036	0.291±0.070	-0.029*0.017

CONCLUSIONS

With a four year time span of GPS observations, we were able to estimate coordinate velocities for 10 sites on the Australia, Antarctica, India, and Pacific plates. Except for sites on the Pacific plate, we find good agreement between the NNR-A predictions and the GPS estimates. We have additionally estimated Euler vectors for the four tectonic plates. Relative Euler vectors for Australia-Antarctica and Australia-India plate pairs agree within one standard deviation with NUVEL-1 A. The site at Wellington is moving with a velocity intermediate between the Australian and Pacific plates, consistent with its location in the plate boundary zone. Sites in Nepal and India both exhibit velocities consistent with location on the Indian plate.

Acknowledgments. We thank the Geodetic Survey of Canada (Pierre Heroux), Scripps Institution of Oceanography (Yehuda Bock and Keith Stark), Jet Propulsion Laboratory (Dave Starr), and Goddard Space Flight Software (Carey Nell) for archival support. Martin Hendy and John Beavan provided helpful information and various data from Wellington and McMurdo. The data from India and Nepal were collected in a collaborative effort. We thank R. Bilham, M. Jackson (CU), J. Paul, V. Gaur, S. Jade, V. Kumar, (Bangalore), R. Burgmann (UC Davis), and C. Reigber (GFZ). The technical staff of the Jet Propulsion Laboratory has always been helpful, in particular Will y Bertiger, Geoff Blewitt, Ken Hurst, Mike Heflin, Steve Lichten, Ron Muellerschoen, Yvonne Vigue, Frank Webb, and Jim Zumberge. Yehuda Bock made useful suggestions on an earlier analysis of these data. KML thanks Dave Smith of the Goddard Space Flight Center for a visiting scientist fellowship and Robert B. Miller for helpful discussions. This research was funded by NSF EAR-9209385 and NASA NAGS-1908. This study would not have been possible without the development of the IGS and the IGS products.

REFERENCES

- Argus, D., and R. Gordon, No-net rotation model of current plate velocities incorporating plate motion model NUVEL-1, *Geophys. Res. Lett.*, **18**,2039-2042, 1991.
- Blewitt, G., M. Heflin, W. Bertiger, F. Webb, U. Lindqwister, and R. Malla, Global Coordinates with Centimeter Accuracy in the International Terrestrial Reference Frame using the Global Positioning System, *Geophys. Res. Lett.*, **19**, 853-856, 1992.
- Boucher, C., Z. Altamimi, and L. Duhem, ITRF 92 and its associated velocity field, *IERS Technical Note 15*, IERS Central Bureau, Observatoire de Paris, 1993.
- DeMets, C., R. Gordon, D. Argus, and S. Stein, Current plate motions, *Geophys. J. Int.*, **101**, 425-478, 1990.
- DeMets, C., R. Gordon, D. Argus, and S. Stein, Effect of recent revisions to the geomagnetic reversal time scale on estimates of current plate motions, *Geophys. Res. Lett.*, Vol. 21, No. 20,2191-2194, 1994.
- Heflin, M., W. Bertiger, G. Blewitt, A. Freedman, K. Hurst, S. Lichten, U. Lindqwister, Y. Vigue, F. Webb, T. Yunck, and J. Zumberge, Global Geodesy using GPS without fiducial sites, *Geophys. Res. Lett.*, **19**, 131-134, 1992.
- Larson, K.M. and J. Freymueller, Relative motions of the Australian, Pacific, and Antarctic plates using the Global Positioning System, *Geophys. Res. Lett.*, **22**, No. 1, 37-40, 1995.
- Robbins, J. W., D. E. Smith, and C. Ma, Horizontal crustal deformation and large scale plate motions inferred from space geodetic techniques, in *Contrib. of Space Geodesy to Geodynamics: Crustal Dynamics*, AGU Geodynamics Series, Vol. 23,21-36, 1993.

- Robaudo, S., and C. G. A. Harrison, Plate tectonics from SLR and VLBI global data, in *Contrib. of Space Geodesy to Geodynamics: Crustal Dynamics, AGU Geodynamics Series*, Vol. 23, 51-71, 1993.
- Schupler, B. and T. Clark, How Different Antennas Affect the GPS Observable, *GPS World*, Nov. -Dec., 1991.
- Smith, D. E. *et al.*, Tectonic motion and deformation from Satellite Laser Ranging to LAGEOS, *J. Geophys. Res.*, 95, 22,013-22,041, 1990.

THE FINNISH PERMANENT GPS ARRAY FinnNet: CURRENT STATUS

J. Kakkuri, H. Koivula, M. Ollikainen,
M. Paunonen, M. Poutanen, and M. Vermeer
Finnish Geodetic Institute
Geodeetinrinne 2, FIN-02430 Masala, Finland

ABSTRACT

The Finnish Geodetic Institute started in 1993 the planning and construction of the national permanent GPS array, FinnNet, eventually to comprise of 12 sites. The reference basis of the network, the GPS receiver at the **Metsähovi** Geodetic Observatory, has been in continuous operation since 1991. It also works with the International GPS Service for **Geodynamics (IGS)**. Five stations of the network **will be** used in the nation-wide differential GPS service. In this report the status of the FinnNet and the **Metsähovi** permanent GPS station is briefly reviewed.

INTRODUCTION

The Fennoscandian Regional Permanent GPS network was established by the Nordic Geodetic Commission in response to the initiative of the directors of the Nordic Mapping Institutes. The general purpose of this network is to contribute to geodetic control **surveys, but it can also play** an important role in geodynamic investigations. The Finnish part of the permanent network, comprising of 12 sites, will be fully operational in the first half of the year 1996. The net is designed in such a way that the maximum land uplift differences and horizontal motions inside the country can be detected. The sites will be established on the bedrock and they are located close to the precise **levelling** net. Also absolute gravity at the stations can be measured.

Space geodetic operations at the **Metsähovi** Geodetic Observatory of the Finnish Geodetic Institute (**FGI**) (latitude 60.22° N, longitude 24.390 E) were begun in 1978 using a ruby satellite laser. Other relevant activities since then have been Doppler satellite observations, founding of a mobile VLBI point in 1989 at **Sjökulla** (a site about 3 km north of the observatory), where also a DORIS (Doppler **Orbitography** and Radiopositioning Integrated by Satellite) **orbitography** beacon started in 1990. Permanent GPS observations were launched in 1991. The **VLBI** point has also been used in several

international and national GPS campaigns since 1989. Thus **Metsähovi** forms a solid reference basis for the FinnNet.

PERMANENT GPS STATION AT METSÄHOVI

A permanent GPS receiver has been in continuous operation at the **Metsähovi** Geodetic Observatory since May 1, 1991, when it started supplying data to the **CIGNET** (Cooperative International GPS Network) net. Initially an Ashtech GPS receiver was used. After procurement of a MiniRogue **SNR-8C** GPS receiver the antenna was transferred to a new 20-m high tower (**Paunonen**, 1993a). The antenna is anchored to the bedrock with a 20-m long invar bar. The electrically isolated, vertically floating mount keeps the height of the antenna constant within one millimetre (**Paunonen**, 1993b). Direct sunlight creates some changes in the horizontal position of the antenna due to the uneven illumination of the guy wires. For monitoring this effect a 20-m long plumb line inside a tube was installed permanently in the tower in September 1993. The observed movements have been less than three millimetres from the mean position. A 5-MHz external frequency from a hydrogen maser feeds the receiver. Statens Kartverk, Norway, retrieves the data directly from the receiver via modem every day. An archive copy of the data is kept at the institute. This receiver was connected to the IGS (International GPS Service for Geodynamics) network from the very beginning in June 1992. On April 30, 1995 the MiniRogue receiver was replaced by a TurboRogue SNR-8 100 receiver, but the old Dorne-Margolin B antenna was kept.

FINNISH PERMANENT GPS ARRAY

The Finnish part of the Fennoscandian permanent GPS network, FinnNet, is progressing further towards completion. Six stations in addition to **Metsähovi** are operational: **Tuorla**, **Virolahti**, **Vaasa**, **Sodankylä**, **Joensuu** and **Olkiluoto**, the latter one operating on behalf of the power company **Teollisuuden Voima Oy** (as will be also **Konginkangas** and **Kuhmo**). **Oulu** is to follow in summer 1995, and the others in the first half of 1996. See Figure 1 for details.

The stations are equipped with 2.5-m tall steel grid towers on concrete pedestals, being **thermally** stable to within 1 mm. Only in **Olkiluoto** a squat, armed concrete pillar was erected with a lower thermal expansion tolerance, 0.1 mm, in order to serve as a reference for local crustal deformation measurements by GPS (**Chen** and **Kakkuri**, 1994). Wooden huts were chosen for housing the instruments, The huts contain a mechanically insulated pillar for use by the **FGI's** absolute laser gravimeter (**JILAg-5**). At **Sodankylä** and **Tuorla** existing housings were used instead, as will be the case at **Oulu**, where a 8.5-m high existing mast will be converted for the GPS use by utilizing a similar height stabilization system as that at **Metsähovi**. The modems are all of type **Telebit Worldblaser**.

From the initiative of the FGI a permanent GPS station is in the building stage at Suurupi in Estonia through an ongoing joint project between the Estonian National Land Board and the FGI (Ellmann and Rudja, 1995). The GPS antenna will be mounted on top of a 20-m high lighthouse. Suurupi is planned to be in active connection with the FinnNet. As scheduled, the station will be operational in 1996.

During the August 15-27 DOSE'94 (Dynamics Of the Solid Earth) campaign, Tuorla, Virolahti and Sodankylä were again permanently operating. Vaasa, Oulu, Joensuu, Sjökökulla and Riga in Latvia were occupied temporarily by portable TurboRogues on loan from Jet Propulsion Laboratory (NASA). This campaign was primarily aimed at connecting a number of tide gauges in Finland and Sweden to the permanent network.

The connection of six GPS array sites to the GPS Finland 1992 net, consisting of 22 GPS sites at the first-order triangulation stations (Ollikainen, 1994), was established in 1994. In this campaign the EUREF-89 points Sjökökulla, Nisula and Kaunispää were included in order to get a direct connection to the EUREF-89 system (Jokela, 1995). Data from Metsähovi, Onsala and Tromsø IGS stations were also included to get a connection to the ITRF system. None of the FinnNet array sites are EUREF-89 GPS sites, but the site from Sjökökulla to Metsähovi is reasonably short, 2.8 km.

Initially the employment of TurboRogue GPS receivers was planned and four units were bought in 1994, but after some period of use and the launch of differential GPS operations Ashtech Z-12 receivers were finally selected. These have 12 channels, which are necessary to support all visible satellites accessible to a user in the field. The TurboRogue type choke ring antennas are retained for compatibility and also because they have superior multi-path properties for high precision work (Rocken et al., 1994)

USE OF THE FinnNet FOR DIFFERENTIAL POSITIONING

The FGI made an agreement with the Finnish Broadcasting Company, YLE, to produce corrections for differential GPS positioning from five stations. The corrections will be sent by YLE in FM-RDS radio data transmissions according to the RTCM standard (RTCM, 1994). The stations which will be connected to the YLE network are Metsähovi, Vaasa, Joensuu, Oulu and Sodankylä, see Fig. 1. At Metsähovi eventually only one antenna will be used to feed both the TurboRogue and Ashtech Z-12 receivers. Until today the corrections have been delivered only from Metsähovi, but all five stations will start continuous transmissions via YLE in the beginning of 1996.

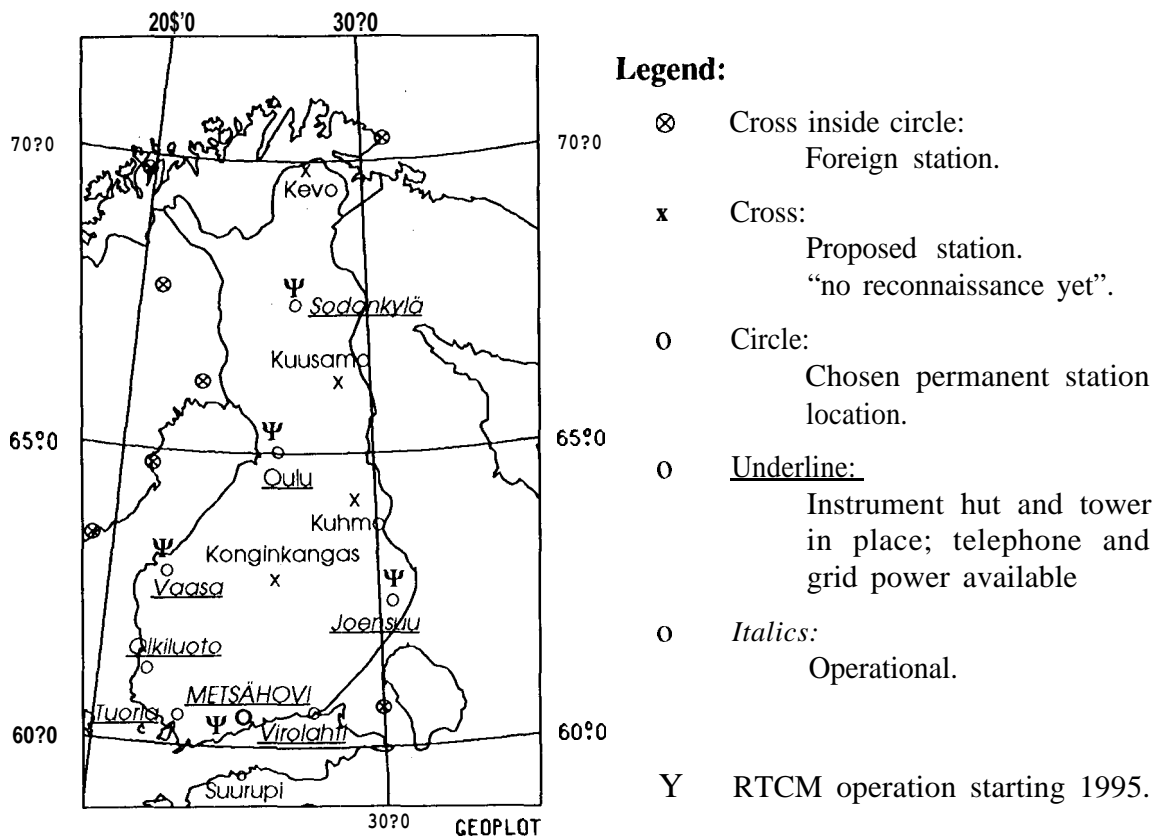


Fig. 1. Finnish Permanent GPS Array - FinnNet, as of June 1995.

REFERENCES

- Chen, R. and J. Kakkuri (1994), Feasibility study and technical proposal for long-term observations of bedrock stability with GPS. Report YJT-94-02, Nuclear Waste Commission of Finnish Power Companies, Helsinki, 33 pp.
- Ellman, A. and A. Rudja (1995), National Report of Estonia, a paper presented at the *Helsinki Symposium of the IAG Subcommittee for the EUREF*, Kirkkonummi, Finland, May 3-6, 1995.
- Jokela, J. (1995), The realization of the EUREF Network in Finland, a paper presented at the *Helsinki Symposium of the IAG Subcommittee for the EUREF*. Kirkkonummi, Finland, May 3-6, 1995.
- Ollikainen, M. (1994), Results of the Finnish GPS Campaign 1992. In *12th NKG General Assembly*, Ullensvang, Norway, 30.5.-3.6.1994, 11 pp.
- Paunonen, M. (1993a), Comparison of globally and locally determined site tics for the Metsähovi GPS station, *Proc. of the 1993 IGS Workshop* (Eds. G. Beutler and E.

- Brockmann), IAG, IUGG, International GPS Service for Geodynamics (IGS), 25-26 March 1993, Astronomical Institute, University of Bern, Switzerland, pp. 310-317.
- Paunonen, M. (1993b), Height-stabilised 20-metre antenna mounting system of the CIGNET GPS station at Metsähovi, Newsletter of *Space Geodetic Measurements Sites Subcommission (SGMS)*, IAG, IUGG, International Coordination of Space Techniques for Geodesy and Geodynamics (CSTG), Vol. 4, No. 1, May 1993, pp. 7-10.
- Rocken, C., J. Johnson, J. Braun, C. Meertens, S. Perry (1994), UNAVCO facility GPS receiver tests. Draft 7/21/94, July 1994.
- RTCM (1994), Radio Technical Commission for Maritime Services, *RTCM Recommended Standards for Differential Navstar GPS Service*. Version 2.1. Developed by RTCM Special Committee No. 104. Washington, D.C.

THE CENTRAL EUROPE REGIONAL GEODYNAMIC PROJECT AND ITS RELATION TO IGS

Peter Pesec

**Institute for Space Research, Dept. Satellite Geodesy,
Austrian Academy of Sciences, Graz, Austria**

ABSTRACT

The Central Europe Regional Geodynamic Project (CERGOP) was accepted by Section C of the Central European Initiative (CEI) 1993. At present 11 countries are participating in this project which will provide a stable reference frame **CEGRN** for subregional investigations and deformation studies in the Central European region. A set of precise coordinate is produced every year, special attention is paid to a “seamless” connection with globally defined reference frames. Several study groups have been formed for utilizing the results in a scientific way. The paper summarizes the scientific **objectives**, the **organisational** structure and the possible relations of CERGOP to global projects like **IGS**.

INTRODUCTION

Within the frame of the Central European Initiative (CEI) the Committee of Earth Sciences was established in 1990. Following the recommended rules for collaborative international projects in this area, the Central Europe Regional **Geodynamics** Project (**CERGOP**) was proposed by Hungarian and Polish scientists. It was originally based on earlier proposals of section C (Geodesy) of CEI and can be considered as a logical continuation of earlier **geodynamic activities** in the Central European area, now based on modern space techniques and on a flexible and reliable **organisational** scheme. CERGOP was approved by the CEI Section C conference in Ksiaz Castle, Poland in May 1993.

The basis of CERGOP is the **Central European Regional GPS Geodynamic Reference Network (CEGRN)**, which acts as a common reference for **all geodynamic** investigations in the CEI area and should tie the already existing national (local) reference frames by defining a clear common set of coordinates and their probable velocities by GPS methods. As some of the **CEGRN** stations are already operating for or will be included in continental and global networks (**IERS, IGS, EUREF**) CERGOP will accept the standards and recommendations of IGS, will give valuable input for global and continental solutions and **will** support e.g. **EUREF** by operating an increasing number of permanently recording reference stations. In the following

the main objectives of CERGOP, the current status of its **realization**, its impact on **geodynamic** research in Europe and its relation to IGS, as well as future developments are summarized.

THE MAIN OBJECTIVES OF CERGOP

The main objectives of CERGOP are described in detail in the proceedings of the 1st **CEI CERGOP** Working Conference, pages 7 - 24. . In a nutshell they can be summarized as **follows**:

To collect satellite, geodetic, astronomical and **gravimetric** data sufficient for exhaustive analysis and interpretation of the **geodynamic** interactions in the region of Central **Europe**;

To investigate various geodynamic **processes** and **geotectonic** features in the Central European region, in particular the Teisseyre-Tomquist zone and the **Carpathian** and Subalpine Orogeny;

To provide a precise geodetic frame for monitoring all features which can be observed by geodetic means (environmental **monitoring**, **technogen** deformation, earthquake **engineering**, etc.);

To establish precise baselines indispensable for the **geodynamical** investigations to be carried out in the frame of other European **geodynamical** projects;

To collect materials for providing a **geoid-map** with centimeter accuracy for the Central Europe territory.

CONCEPT AND REALIZATION

The scientific concept of CERGOP is based on the merging of actually on-going national activities in the field of **geodynamic** research which are supplemented by border crossing projects. Specifically this means that most of the financial burden has to be carried by the national institutions. At present the following 11 countries have joined **CERGOP**: Austria, Croatia, Czech Republic, Germany, Hungary, Italy, Poland, Romania, Slovakia, **Slovenia**, Ukraine. Each country is represented by a National Investigator (**N.I.**), which form the International Project Working Group **IPWG**. As can be seen in the following Fig. 1 the IPWG is headed by the CERGOP Management Group formed by the **N.I.** of Germany, Hungary, Italy, and Poland.

Establishment of an International Project Working Group

The overall project tasks of IPWG include the organisation of observation **campaigns**, the supervising of the study groups **activities**, the performance control of the data center and the processing **centers**, and the liaison with overlapping international projects. Besides the overall project **tasks**, the members of IPWG disseminate **informations**, keep and establish contacts with existing international projects and organisations (e.g. IGS, **EUREF**, **WEGENER**, **IDNDR**, **EUROPROBE**, Baltic Sea

Level **Project**, Extended SAGET, and others). IPWG is chaired by the **NI** of Hungary and co-chaired by the **NI** of Poland.

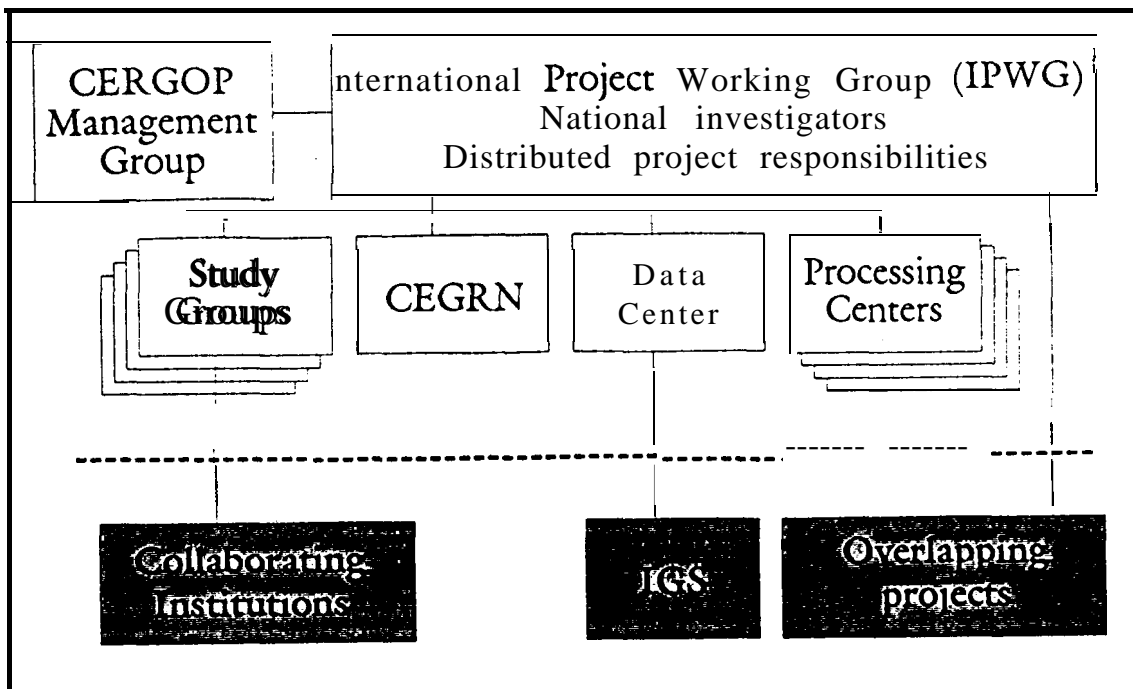


Fig. 1: Organizational structure of CERGOP

Maintenance of a Precise Reference Network

One of the first important steps was the establishment of a Central European GPS **Geodynamic Reference Network**, which serves as the common basis for all scientific projects. It consists not only of the mere sites but also of the complete infrastructure which enables a proper operation (instrumentation, **maintenance**, communication, observing **personell**). Financial support for covering part of the **maintenance** of **CEGRN** during the next 3 years was given by the European Community.

Establishment of Study Groups

During the last year all-together 11 CERGOP study groups (**CSG**) were proposed by the national representatives. They are formed by the collaboration of scientists from two or more member countries and are designed for carrying out research in a particular field. This field may cover objectives directly related to CERGOP (core research) or only linked to CERGOP (associated research). Some **CSG** have started their work recently, some are just in the stage of being developed. In the following the titles and the responsible chairmen are listed:

CSG 1: Investigation of tropospheric delays (P. **Pesec**, Austria);

CSG 2: CERGOP site quality monitoring (I. **Busics**, Hungary);
CSG 3: CERGOP reference frame (J. **Rogowski**, Poland);
CSG 4: Standardisation of data- and processing centers (G. **Stangl**, Austria);
CSG 5: Permanent and epoch GPS CERGOP stations (J. **Sledzinski**, Poland)
CSG 6: CEGRN and precise levelling (J. **Simek**, Czech Rep.)
CSG 7: CERGOP gravity network (M. **Barlik**, Poland);
CSG 8: Geotectonic analysis of the region of Central Europe (P. **Vyskocil**, Czech Rep.)
CSG 9: Geoid in Central Europe (proposed);
CSG 10: Monitoring of recent crustal movements in the Eastern Alps with GPS (C. **Marchesini**, Italy);
CSG 11: Three dimensional plate kinematics in Romania (D. **Ghitau**, Romania).

Semiannual Reports and Consultations

The CERGOP working group meets twice a year at different places of the member countries. Detailed summaries of the national activities are supplemented by the reports of the data center, the processing centers, and the individual study groups. All reports are compiled and published (presently in the “Reports on Geodesy” of the Warsaw University of Technology).

CENTRAL EUROPEAN GPS GEODYNAMIC REFERENCE NETWORK

Station Distribution

In order to keep the number of sites at a reasonable level **IPWG** decided to appoint - after consultation - to each member country a restricted number of stations which are served within CERGOP - even if they are upgraded to a permanent station. At present, **CEGRN** comprises 31 sites, the station distribution is shown in **Fig.2**.

Data Center

Graz, Austria took over the annoying task of acting as the official data center of **CERGOP**. It is responsible for archiving all incoming data (permanent stations, epoch-campaigns), checking and distributing the data to other organisations and providing continuous access to the data-sets stored. The data center is organized similar to the IGS data centers and can be interrogated via anonymous **FTP** and dial-up modem. Up to 3 **GByte** disc memory is at disposal for data storage, older data are stored on magneto-optical discs.

Processing Centers

By now 4 processing centers are in operation:

--- Institute of Geodesy and Geodetic Astronomy, Warsaw, Poland;

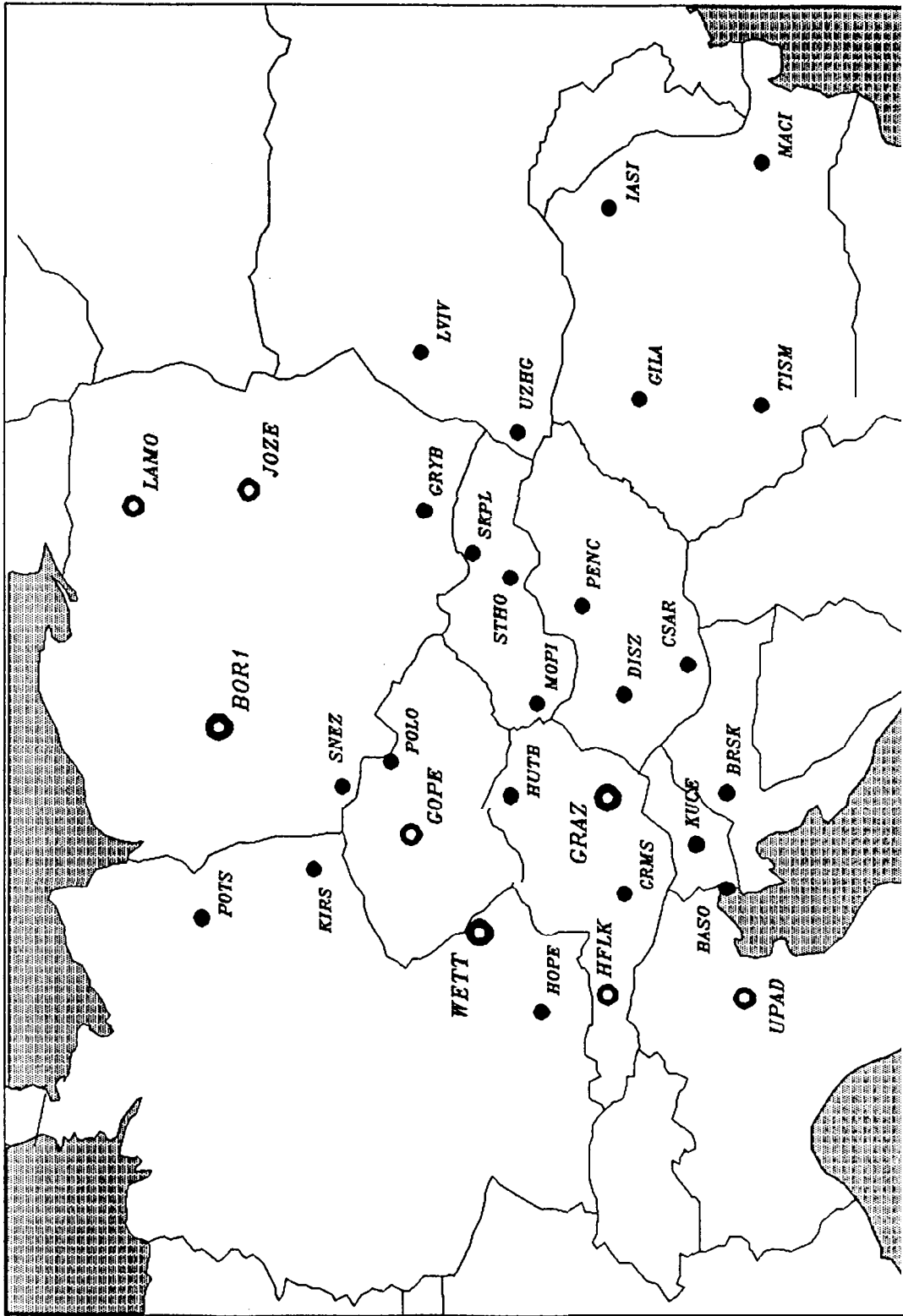


Fig.2: Station distribution of the CEGRN stations (Status May 1995).

- Institute for Space Research, **Graz**, Austria;
- Research Institute of Geodesy, **Zdiby**, Czech Republic;
- **FÖMI** Satellite Geodetic Observatory, **Pent**, Hungary.

IFAG Frankfurt indicated its interest to act as an additional processing center in the future.

The main task of the processing centers is to compute an annual set of coordinates for all **CEGRN** stations. All processing centers are currently using the **Bernese** software package, **CSG 4** determines and recommends the official set of coordinates. In addition, the determination of daily coordinate sets for the permanently recording stations is on the schedule.

Available Products

The products placed at disposal by the data center for further use are station descriptions (including receiver **types**, **eccentricities**, . . .). relevant sets of coordinate and the respective **covariance matrices**, and in future, specific data of the station environment like 4-D meteorological data and **multipass** information.

POSSIBLE RELATIONS OF CERGOP TO IGS

CEGRN can be regarded as a regional reference frame, which was established according to the guidelines of **IGS**. A considerable part of the reference stations was observed during the **IGS Epoch'92** campaign giving a first link to the global **IGS** frame. **CEGRN** contains the **VLBI/SLR/GPS** fundamental station **Wetzell (FRG)** and the **SLR/GPS** stations **Graz** (Austria) and **Borowiec** (Poland) operating as European core stations of **IGS** as well. In addition, the permanently operating stations **Jozefoslaw** and **Lamkowko** (Poland), **Pecny** (Czech Republic), **Padova** (Italy) and **Hafelekar** (Innsbruck, Austria) make their data available - via Internet or Modem - to the **CERGOP** data center at **Graz**, which transfers all collected data to the regional **IGS** data center at IFAG Frankfurt on a daily basis. At present, all-together eight stations of the **CEGRN** network monitor the **CERGOP** reference frame on a permanent **basis**, their data are included in the daily solution of the **IGS** orbit determination center **CODE** at the University of **Berne**.

It should be stressed that, according to the present **plannings**, some more stations will receive a permanent status in the near future (after solving some communication problems). **Daily** solutions computed at the **CERGOP** processing centers and referred to **ITRF** will be routinely available. All **CEGRN** stations (31 at present) are obliged to take part in the official **CEGRN GPS campaign**, which (following the **IGS** concept of sporadic epoch-like campaigns) is being carried out in May/June every year. Therefore, at least one complete set of coordinates per year is at disposal for all **CEGRN** stations which can be incorporated into regional and global solutions.

CONCLUSIONS

The Central Europe Regional Geodynamic **Project** takes most of the national **geodynamic** investigations of 11 countries under a common umbrella. Mutual assistance promotes the use of modern space techniques for attaining accuracies of coordinates in the sub-centimeter region which is required for **geodynamic** research. Due to accepted procedures the products can be incorporated in continental and global solutions. The activities are controlled by the International Project Working Group. However, the main tasks have to be fulfilled and financed by the underlying national organizations. Some financial support has been given by the European Community within "Copernicus" for the next 3 years.

REFERENCES

Fejes I., A. Kenyeres: The Central Europe Regional **Geodynamic** Project (**CERGOP**); Presented at the 1st Turkish Int. Symp. on Deformations Istanbul, Sept. 5-8,1994.

J. Sledzinski et al.: Proceedings of the 1st **CEI CERGOP** Working Conference Warsaw, Poland, February 1994; Reports on Geodesy No. 2(10), 1994, Special Issue.

J. Sledzinski et al.: Proceedings of the 2nd **CERGOP** Working Conference Pent/Budapest, Hungary, November 1994; Reports on Geodesy No. 5(13), 1994, Special Issue.

J. Sledzinski et al.: Proceedings of the 3rd **CERGOP** Working Conference in Sz6dliged/Pent, Hungary, May 1995; Reports *on Geodesy*, in print.

Experience with Data Flow in the CORS Network

W. Strange, N. Weston
NOAA, SSMC3, 1315 East-West Highway,
Silver Spring, MD 20910
301-713-3222; e-mail: nweston@ngs.noaa.gov

M. Schenewerk
NOAA, SSMC4, 1305 East-West Highway
Silver Spring, MD 20910
301-713-2854; e-mail: mark@tony.grdl.noaa.gov

INTRODUCTION

The CORS network is a group of GPS reference stations which **will** provide code range and carrier phase data to users in support of post processing applications. Governmental, academic, and private users will be supported in performing **after-the-fact** positioning of fixed points and moving platforms. Ultimately, the CORS network is expected to consist of 50 to 100 stations located nationwide.

The GPS data will be recorded at a 5 second sampling rate in the the **RINEX 2** format. The daily data sets can be retrieved over the INTERNET and will available for 21 days. After that period, the data will be archived on CD ROM.

Currently the National Geodetic Survey provides data from twelve sites. Only the **Gaithersburg** data is provided at a 5 second rate. The other stations are providing data at a 30 second sampling rate.

During a 12 month period beginning in December, 1994, the U.S. Coast Guard (**USCG**) will install a 51 station network along U.S. coasts which will include the Great **Lakes**, Alaska, Hawaii, and Puerto Rico to support marine navigation. By agreement, NGS will utilize these stations as part of the CORS network and make the data available for post processing applications. Additional stations will be established over the next two to three years, by the USCG in support of the US Army Corps of Engineers for river navigation (approx. 10 stations) and by the Federal Aviation Administration to support air navigation (**approx.** 29 stations). These sites will be CORS compatible and are expected to become a part of the CORS network. Additional stations are expected to be added where needed to provide complete **areal** coverage.

FILE TRANSFER PROTOCOL (FTP)

FTP is a user interface to the File Transfer Protocol. FTP copies files over a network connection between the **local** "client" host and a remote "server" host. FTP runs on the client host.

The user's system must have access to the INTERNET and support the File Transfer Protocol (**FTP**). Some useful ftp commands are given below.

ascii	set ascii transfer type
binary	set binary transfer type
bye	terminate ftp session and exit
cd	change remote working directory
dir	list contents of remote directory
get	receive one file
help	print local help information
mget	get multiple files
input	send multiple files
prompt	force interactive prompting on multiple commands
put	send one file
quit	terminate ftp session and exit

* Actual commands may vary among operating systems.

TO ACCESS CORS ARCHIVE

To access the CORS public directories, follow the steps below;

Type the "**ftp**" command followed by the INTERNET address proton .ngs.noaa.gov

```
ftp proton. ngsonoaaogov
Login: anonymous
Password: your complete e-mail address
```

You should be at the ftp command level indicated by the prompt ftp > If you are having trouble, type help to print local help information or review the section FILE TRANSFER PROTOCOL for help with additional commands.

All CORS related directories and files are located in the **directory** cors and can be accessed by typing;

```
cd cors
```

The following sub-directories contain additional files and information.

- rinex Rinex data **files**.
- coord NAD 83 and ITRF positional information for the CORS sites.
- station_log** Station information, antenna specifications and site contacts.
- utilities Programs for manipulating the **RINEX** files.

DIRECTORY STRUCTURE

```

ftp --|
      |
      |--- cors ---|
      |             |
      |             |--- rinex ---|
      |             |             |
      |             |             |--- cors1 ---| yyddd --|--- *.94n.Z
      |             |             |             |--- *.940.Z
      |             |             |             |--- *.94s.Z
      |             |             |
      |             |             |--- cors2 ---| yyddd --|--- *.94o.Z
      |             |             |             |--- *.94s.Z
      |             |
      |             |--- itrfr ---|
      |             |             |--- itrfr92*
      |             |             |--- itrfr93*
      |             |             |--- iers_itrfr92*
      |             |             |--- iers_itrfr93*
      |             |
      |             |--- README.txt (this file)
      |             |--- RINEX-2.txt
      |             |--- news.let (newsletter)
      |             |
      |             |--- coord ---|
      |             |             |--- position.*
      |             |             |--- derivation ----| derivation.txt
      |             |
      |             |--- station_log ---|
      |             |             |--- *log
      |             |
      |             |--- utilities ---|
      |             |             |--- inflate.exe
      |             |             |--- join24pc.exe
      |             |             |--- join24.txt
      |             |             |--- decimate.exe
      |             |             |--- decimate.inp
      |             |             |--- decimate.txt
      |             |             |--- gzip.exe
  
```

FILE FORMAT

The RINEX files are stored in the UNIX compress format. These files have the extension “.z” appended. You may retrieve the compressed files as is by using the “get” command and the complete file name or you may **uncompress** the file before retrieving it. To uncompress first, use the “get” command followed by the filename without the “.Z” extension. If you transfer the **file in** compressed mode, be **sure** to set the transfer mode to “binary”. Executable files should be transferred in “binary”

mode while uncompressed **RINEX** files and text files should be transferred in "ascii" mode.

UTILITIES

Several DOS based utility programs are available to manipulate the **RINEX** data files. Versions also exist for other platforms such as Silicon Graphics, Sun Microsystems and Hewlett Packard.

inflate.exe Self-extracting utility program to uncompress files with the ".Z" extension.

gzip.exe Another utility program to compress / uncompress files.

join24pc.exe Utility program to join two or more hourly **RINEX** observation or navigation files.

decimate.exe Utility program to decimate 5 second data to a user specified rate.

ACCESS VIA WWW

NGS has developed a home page on the Internet World Wide Web (**WWW**) for online access to information on its products, services and program activities.

The CORS products and data are available through **NGS's** home page which is **accessible through either** NOAA's home page or by typing in the URL (Uniform Resource Locator) which is

<http://www.ngs.noaa.gov>

when using a browsing tool **such as** Mosaic.

EMAIL

If you would like to be on the CORS e-mail list, please send your request to Don Haw at don@ngs.noaa.gov .

ADDITIONAL INFORMATION OR REQUESTS

For additional information please **contact** the appropriate person below.

Administration:	William E. Strange bstrange@ngs.noaa.gov (301) 713-3222
	Paul R. Spofford pauls@ngs.noaa.gov (301) 713-3205
Information:	Don Haw don@ngs.noaa.gov (301) 713-3208
	Jim Drosdak jimd@ngs.noaa.gov (301) 713-3219
Newsletter:	Neil D. Weston nweston@ngs.noaa.gov (301) 713-3235

CORS
National Geodetic Survey, NOAA
N/CG1 SSMC#3
1315 East-West Hwy,
Silver Spring, MD 20910-3282

AVAILABILITY

RINEX data is available from the following stations,

Site Name	Site ID	Receiver	Antenna	Sample Rate	File Format
Denver, CO	dent	Trimble SSE	Trimble	30 seconds	Daily
Gaithersburg, MD	gait	Trimble SSE	Dome M	5 seconds	Hourly
Haskell, OK	hklo	Trimble SSE	Trimble	30 seconds	Daily
Hillsboro, KS	hbrk	Trimble SSE	Trimble	30 seconds	Daily
Lament, OK	lmno	Trimble SSE	Trimble	30 seconds	Daily
Pietown, NM	piel	Turbo Rogue	Dome M	30 seconds	Daily
Platteville, CO	pltc	Trimble SSE	Trimble	30 seconds	Daily
Richmond, FL	rcm5	Turbo Rogue	Dome M	30 seconds	Daily
Table MT, CO	tmgo	Turbo Rogue	Dome M	30 seconds	Daily
Vici, OK	vcio	Trimble SSE	Trimble	30 seconds	Daily
Westford, MA	wes2	Turbo Rogue	Dome M	30 seconds	Daily
White Sands	wsmn	Trimble SSE	Trimble	30 seconds	Daily

FILE NAMING CONVENTION

The RINEX file naming convention is as follows:

{SSSS}{DDD}{H}.{YY}{T} where SSSS is the four letter site identifier, DDD is the day of year, H is a letter which corresponds to the hourly UTC time block, YY is the year and T is the file type.

Hourly UTC time block identifier (H)

0001020304050607080910111213 14151617181920212223
a b c d e f g h i j k l m n o p q r s t u v w x

File type Ending (T)

Meteorological	m
Observation	o
Navigation	n
Summary	sum or s

COAST GUARD STATIONS

RECEIVERS:

TWO (2) ASHTECH Z12 RECEIVERS AT EACH SITE

SAMPLING RATE:

5 SECOND PLANNED (1 SECOND POSSIBLE)

TRANSMISSION TO CENTRAL FACILITY:

AT&T FTS2000, X.25 PACKET SERVICE

DATA TRANSMITTED AFTER EACH SAMPLE - NO ON SITE STORAGE

AMOUNT OF DATA TRANSFERRED:

-5 Mbytes/DAY/STATION

CORS STANDARDS ACTIVITIES

- **CORS STATION STANDARDS**

- **TO BE ISSUED JUNE/JULY 1995**
- **REQUIRED AND DESIRABLE ACTIVITIES**

- **RINEX VERSION 2 STANDARDS**

- **OPTIONAL FIELDS REQUIRED FOR INCLUSION**
- **IN COLLABORATION WITH USERS AND HARDWARE VENDORS**
- **TO BE ISSUED JUNE/JULY 1995**

- **REQUIRED ANTENNA PHASE CENTER MODELING**

- **WORKING WITH HARDWARE VENDORS ON STANDARD NAMES**

- **METEOROLOGICAL SENSORS**

- **NOAA FORECAST SYSTEMS LABORATORY IS DEVELOPING SPECIFICATIONS**

CORS STATION TYPES

- **TYPE A**

- **MULTIPLE RECEIVERS AT STATION**
- **99 PERCENT RELIABILITY**
- **5 SECOND SAMPLE RATE**
- **IMMEDIATE DATA ACCESS VIA TELEPHONE PACKET SERVICE (X.25)**
- **HOURLY DATA FILES**

- **TYPE B**

- **SINGLE RECEIVER AT STATION**
- **30 SECOND SAMPLE RATE**
- **DAILY DATA ACCESS VIA INTERNET**
- **DAILY DATA FILES**

AUGMENTATION STUDY RECOMMENDATIONS

- **WIDE AREA (FAA) AND LOCAL AREA (COAST GUARD) DGPS SHOULD BE IMPLEMENTED**
- **LOCAL AREA DGPS SHOULD BE EXPANDED NATIONWIDE**
- **ALL FEDERAL REFERENCE STATIONS SHOULD COMPLY WITH CORS STANDARDS**
- **DOT, WITH OTHER AGENCIES, SHOULD COORDINATE ALL FEDERAL AUGMENTED GPS SYSTEMS**
- **RINEX FORMAT RECOMMENDED FOR POST-PROCESSING APPLICATIONS**

QUALITY CONTROL

- **QCV3 QUALITY CHECKING**
- **DAILY POSITION ESTIMATES**

COAST GUARD STATIONS

CENTRAL FACILITY:

CURRENTLY HP WORKSTATION WITH 9 Gbytes OF STORAGE
HP WORKSTATION WITH 2 Gbytes OF STORAGE
X.25 LINE
INTERNET

EXPECTED EXPANSION SECOND COMPLETE FACILITY WITH
AUTOMATIC SWITCHING TO REDUNDANT SYSTEM IF PRIMARY GOES
OUT

DATA DISTRIBUTIONS:

HOURLY RINEX FORMAT FILES FOR EACH STATION EACH HOUR.
THREE (3) WEEKS ON-LINE, ON HARD DISK FOR INTERNET ACCESS.

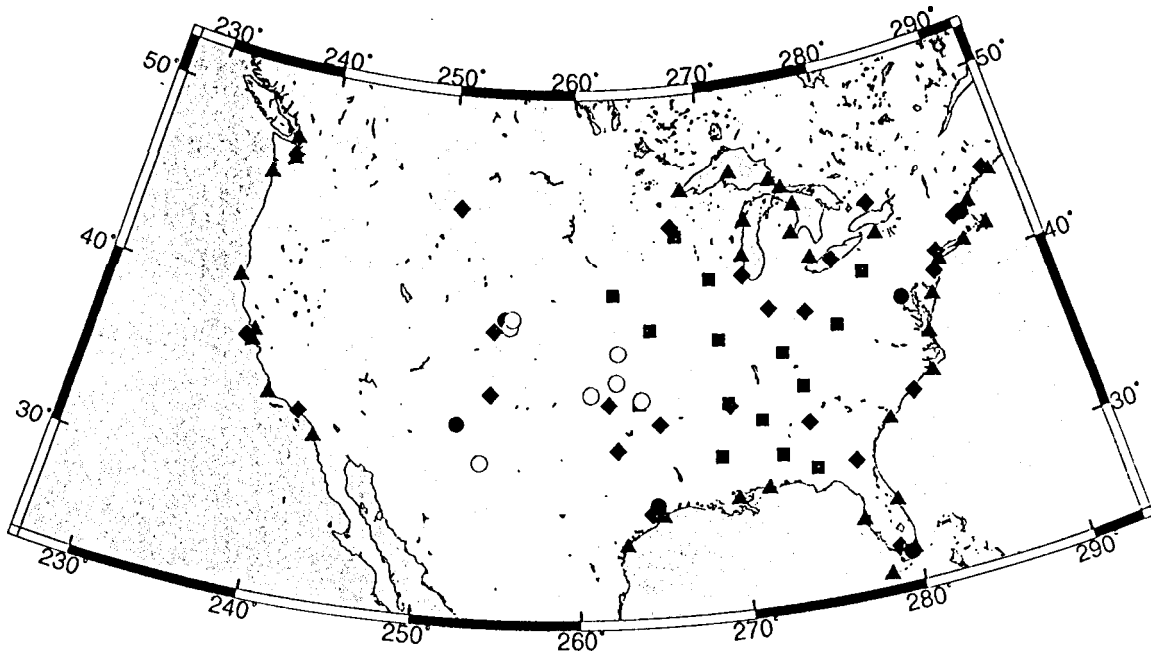
RAW RECEIVER FORMAT FILES ON CD ROM FOR ARCHIVING AND
DISTRIBUTION.

TIME FRAME:

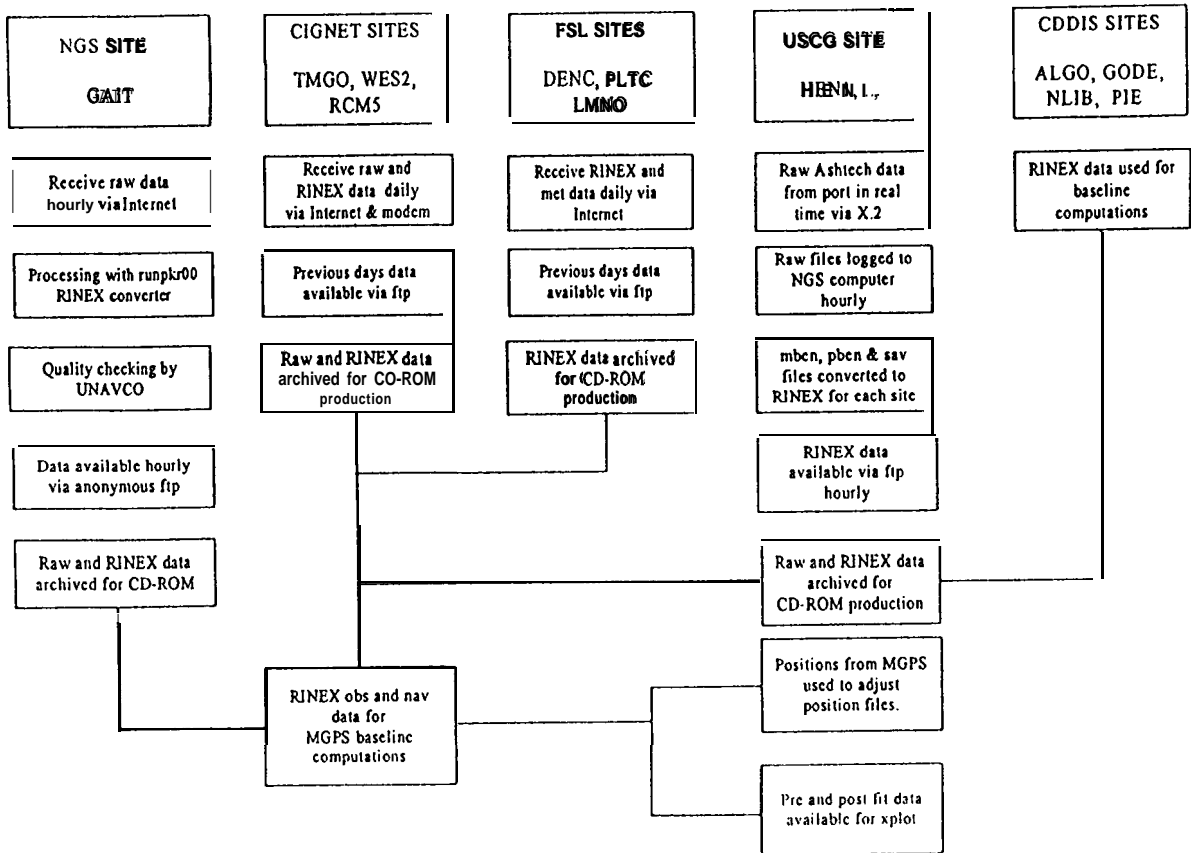
STATIONS BEGAN OPERATING IN MAY, 1995. ALL STATIONS (-50)
EXPECTED TO BE OPERATING BY THE END OF THE 1995 CALENDAR
YEAR.

COAST GUARD STATION CURRENT SCHEDULE

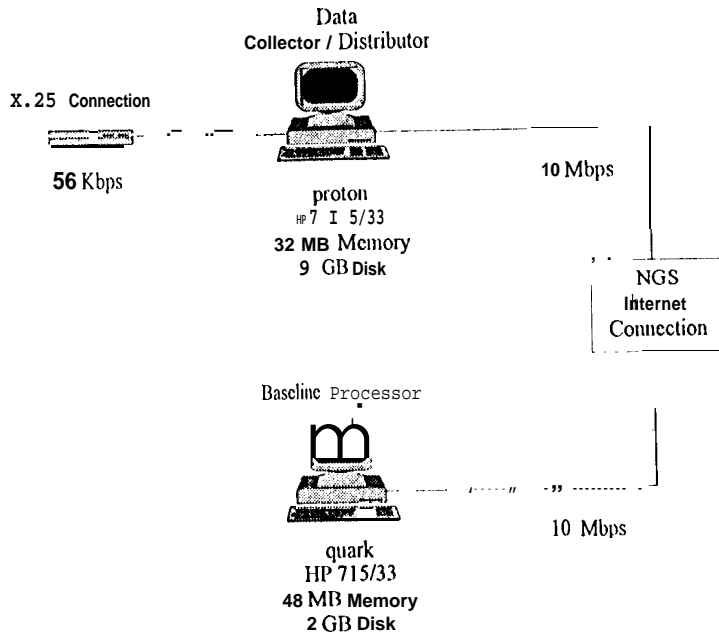
MAY 1995	(5 STATIONS)
	• PORTSMOUTH, NH
	• MONTAUK POINT, NY
	• SANDY HOOK, NJ
	• WHITEFISH POINT, MI
	• NEEBISH ISLAND, MI
JUNE 1995	(4 STATIONS)
JULY 1995	(8 STATIONS)
AUGUST 1995	(10 STATIONS)
SEPTEMBER 1995	(8 STATIONS)
OCTOBER 1995	(4 STATIONS)
NOVEMBER 1995	(5 STATIONS)
DECEMBER 1995	(4 STATIONS)



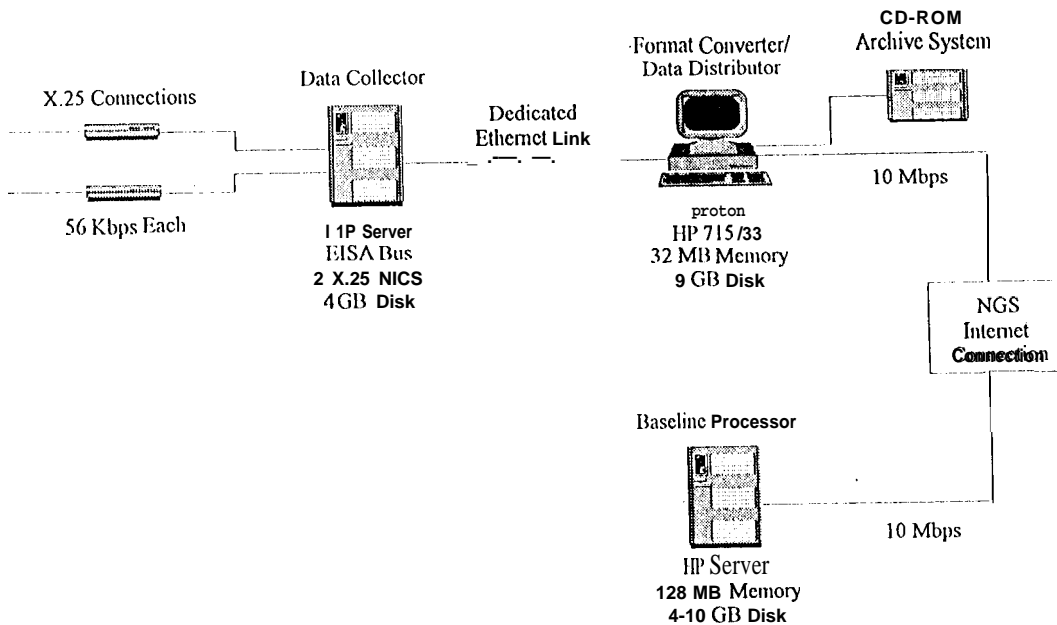
■ USCOE ▲ USCG ◆ FAA ● NOAA ○ WPDN



CORS Data Collection and Distribution (Current Configuration, Phase 0)



CORS Data Collection and Distribution (Proposed Configuration, Phase 1)



CONTROL GPS NETWORKS FOR THE GEOPHYSICAL APPLICATIONS (Russia and CIS)

S. K. Tatevian

Institute of Astronomy, RAS, 48 Pyatnizkaya,
109017 Moscow, Russia.

Internet: statev@inasan.rssi.ru

The great part of Russian territory and adjacent states of the former USSR are located on the Eurasian plate, that undergoes the **intraplate** deformations. Along the south border there are fragments of several smaller plates: **Anatolian**, Lesser Caucasus, Iran, Afghanistan, Indian, several **microplates** of China and Mongolia. In the east this plate is adjacent to the Pacific and North American plates. Belts of active recent deformations and of high **seismicity** are located in the zones of plates interaction.

To study this complicated pattern and for improvement of the regional geodynamic model a development of the 3-level structure of the control GPS network would be efficient and such a project is studied now, namely: 1) a regional network, collocated with several core sites of the global GPS network and having a profile design with the main line along the 54-56 parallel and with 4 meridional lines for monitoring of the interplates movements and, partly, the **intraplate** deformations; 2) subregional networks in the complicated active areas, like the **Caucasus-Caspian**, **Pamir-Tien Shari**, **Ural Mountains**, **Baikal rift zone**, the **Kurils-Kamchatka**, for studies of the fine structure of the field of deformations and for **seismo-** zoning; 3) local networks in the most **seismoactive** areas for discovering of potential earthquake sources and for short time predictions.

Two Federal Programs, approved by the Russian Government for the next 5 years, foreseen an application of the space geodesy technique (mainly **GPS-GLONASS** systems) for the precise positioning and deformations studies:

- Federal System of Seismological Networks and Earthquake Predictions. (Ministry of RF for Civil Defence,... and Elimination of Consequences of Natural Disasters and Russian Academy of Sciences).
- Federal Programm of the Fundamental Geodetical Network Development with the use of space techniques. (Federal Department of Geodesy and Cartography). The Ministry of Science and Technology supports also the Scientific Program of the Crustal Deformation Studies, as a part of the **GLOBAL CHANGES** program.

With a view to expand the IGS Global Network on the **CIS** area the next sites have been installed:

RSNR-8000 receivers, provided by the **GFZ** -Potsdam:

ZWENIGOROD (operates as a core station),

KRASNOYARSK (operates, problems with communications),

PETROPAWLOVSK / Kamchatka (will be installed soon),
KITAB (core station).

T 4000 SSE receiver :

MENDELEEVO (operates permanently at the State Time Standard station).

Proposed future sites are as follows:

Svetloe (collocated with the future **QUASAR station**),

Zelenchukskaya (future **QUASAR station**), **Badary/ Irkutsk**,

Yakutsk (when communication problems will be solved).

The local control GPS networks are developed in several active regions (North Caucasus, Central Asia, Pamir-Tianshan) in cooperation with **GFZ** and **IFAG(Germany)**, **MIT/UNAVCO** (USA) for the deformations studies.

Following the catastrophic earthquake (October 4, 1994) at the Shikotan Island - **Kurils**, a special expedition has been organized by V. N. Strakhov (director of the Institute of Physics of the Earth, RAS) for studying the tectonic consequences of the earthquake. (Information and Analytical Bull. Sp. Is. N1. Ott.1994. FSSN, RF)

In order to reveal possible large scale deformations within the island the GPS measurements have been carried out at the 12 points of the Shikotan geodynamic survey traverse, that exists since 1985. Three receivers - **Trimble 4000 SSE** - have been used in a static 2-frequency regime at 3 sites simultaneously in 2-6 hours sessions. At all 23 lines of 1-7 km long were measured. The results have been compared with the data of regular electronic distance measurements since 1985. Preliminary data analysis have demonstrated that the north-eastern part of the island has sustained minor horizontal deformations and that the most significant consequence of the earthquake is a general submergence of the Shikotan island by 0.6 m. The final conclusion will be made after the **additional data analysis using precise orbital parameters provided by IGS. It is very important now to continue the precise GPS measurements in the Sakhalin-Kamchatka area**, as the region Avacha Bay near **Petropawlovsk** is one of the dangerous regions according to the long term predictions for 1991-1995 (Fedotov at al. in Volcanology and Seismology, 1993, N 6, p 3-12). The Avacha Bay may well be happen to be a site of release of seismic energy, sufficient for one earthquake of 8.5 M accumulated in the Kamchatka region (Fedotov and al. 1994, Bull. FSSN, RF).

The other very important application of the GPS technique could be precise measurements of the horizontal and vertical motions of the **Caspian Sea** area for understanding of the mechanisms of the catastrophic sea level changes. This project is now considering in the frame of the complex international program "**CASPY**".

Remark. On May, 27 very strong earthquake has happened in the north part of Sakhalin island. The town Neftegorsk was absolutely destroyed.